2019 Neutron Scattering User Meeting

Tuesday 04 June 2019 - Wednesday 05 June 2019

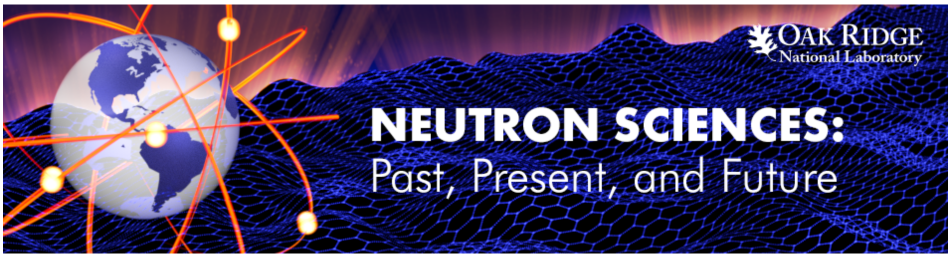

Book of Abstracts

Spallation Neutron Source
Oak Ridge National
Laboratory

SPEAKER ABSTRACTS

Challenges at the Frontiers of Matter and Energy

Dr. Harriet Kung, Associate Director of Science for Basic Energy Sciences,
Department of Energy

Abstract:

Building on over a decade-long of strategic planning, the Basic Energy Sciences program in DOE's Office of Science continues to engage the scientific community in charting new research directions for our program. This presentation will highlight program priorities and potential new funding opportunities in FY 2020. Specifically, research in support of quantum information sciences, microelectronics, data analytics, and computational materials and chemical sciences will be emphasized.

Scattering Neutrons from Cuprate Superconductors: Past, Present, and Future

John Tranquada
Condensed Matter Physics & Materials Science Division
Brookhaven National Laboratory, Upton, NY 11973-5000

The 1986 discovery of superconductivity in $La_{2-x}Ba_xCuO_4$ was tremendously exciting. The observation of antiferromagnetic order in the parent compound La_2CuO_4 by neutron diffraction a year later provided motivation for me to join the Neutron Scattering Group at Brookhaven. The main tool at the time was the triple-axis spectrometer, which allowed exploration of excitations and correlations in the thermal-energy range. The development of time-of-flight spectroscopy at ISIS more than a decade later made it possible to explore the full bandwidth of the antiferromagnetic excitations, which can extend above 300 meV. To take full advantage of this technique, we had to wait for the SNS, where the high flux now makes it practical to obtain four-dimensional data from rotating crystal measurements, often revealing unexpected features. With time, new issues arise. We have done recent transport measurements on a crystal of $La_{2-x}Ba_xCuO_4$ to high magnetic fields at a composition that exhibits stripe order in zero field. The measurements suggest a gradual dimensional reduction of superconducting correlations with field, from 3 to 2 to 1 dimensional above 25 T. Does spin stripe order survive to these fields? We will need the Second Target Station and a dedicated high-field instrument in order to answer this question.

At the Intersection of Neutron Scattering and Nuclear Materials Research

Brent Heuser, Professor and Associate Head for Undergraduate Programs, Department of Nuclear
Plasma, and Radiological Engineering
University of Illinois

Abstract:

Light Water Nuclear Reactor (LWR) technology and the development of advanced nuclear reactors depend on materials innovation and mitigating deleterious environmental effects. The talk will focus on the utility of neutron scattering techniques to interrogate LWR structural materials. Emphasis will be placed on the study of hydrogen precipitation and transport, the ability to ***now*** perform neutron scattering measurements at very low hydrogen concentration, and the use of the newest generation of neutron scattering instruments to interrogate nuclear materials.

Neutron Scattering for Probing Internal Structure of Intelligent Soft Matter

Eugenia Kharlampieva, Associate Professor, Department of Chemistry
University of Alabama at Birmingham

Abstract:

Macromolecular self-assembly and bio-inspired fabrication of polymeric nanostructures are of interest for a broad spectrum of applications in bio nanotechnology. This talk will focus on resolving the architecture of nano-thin polyelectrolyte coatings and hollow particles (capsules) produced by layer-by-layer (LbL) assembly on inorganic templates where interactions between adjacent layers are controlled by either electrostatic or hydrogen-bonding forces. Our study establishes a basis for regulating the organization of self-assembled polymer films, crucial for developing nanostructured responsive materials with controllable functions.

Uncovering the Chemistry of Solids with “*in situ”* Neutron Diffraction

Efrain E. Rodriguez

Chemistry and Biochemistry, University of Maryland, College Park, MD 20742

Historically, neutron powder diffraction has been one of the most powerful means to obtain the structure of crystalline solids. Progress quickly escalated after Hugo Rietveld introduced his method for quantitative analysis of diffraction data from his least squares technique. Since then neutron instrumentation has improved in both flux and resolution; therefore, the community of materials and solid-state chemists now seek to push the boundaries of what neutron diffraction can teach us about the chemical reactivity of solids. In this lecture, I will cover some of the recent progress in chemical studies with “*in situ*” neutron diffraction whereby a crystalline material is measured under sample environments that change the chemical composition of the sample with time. I will cover in particular the areas where the Spallation Neutron Source (SNS) has made advances in four categories: 1) synthesis of intermetallics from molten fluxes, 2) synthesis of metal oxides from salt fluxes, 3) ion exchange reactions in energy storage materials, and 4) chemical looping of metal oxides with natural gas. The first two represent the search for new phases starting from solutions, and the second two how the solid structure evolves driven by either redox chemistry or thermochemistry. The time-of-flight instruments like POWGEN can further help understand the kinetics of these chemical processes. I briefly discuss the implications of this past work for the future of neutron diffraction and the science of synthesis.

TABLE TOPICS WORKING LUNCH ABSTRACTS

Sample Environments: High Magnetic Field and Low Temperature

Saad Elorfi[1], Cory Fletcher[1], Chris Redmon[1], Gary Lynn[1], Todd Sherline[1], Matt Collins[1], Adam Aczel[2],
Matt Stone[2], Daniel Pajerowski[2], Barry Winn[2], Stuart Calder[3], Qiang Zhang[3], Lisa Debeer-Schmitt[4],
Timothy Charlton[4], Victor Fanelli[5], John Caruth[5], Josh Pierce[6], Collin Broholm[7]

[1]Low Temperature & Magnets Team, Sample Environment Group, Neutron Scattering Division, ORNL
[2]Spectroscopy Group, Neutron Scattering Division, ORNL
[3]Diffraction Group, Neutron Scattering Division, ORNL
[4]Large Scale Structures Group, Neutron Scattering Division, ORNL
[5]Beamline Support Group, Neutron Scattering Division, ORNL
[6]Instrument Methods, Projects & Technologies Group, Neutron Technologies Division, ORNL
[7]John Hopkins University (external committee member)

This poster presents an overview of sample environment capabilities at ORNL for high magnetic fields and low temperatures. It also advertises a steering committee consisting of both sample environment staff and instrument staff. This committee regularly meets to discuss the status and needs of this suite of capabilities, and helps to identify and prioritize activities, equipment, innovations and resources to enable such capabilities to be made available in an operationally reliable way in the User Program. Users are encouraged to engage this committee in order to enable and facilitate novel experiments.

The neutron imaging facility at the High Flux Isotope Reactor, Oak Ridge National Laboratory

Yuxuan Zhang [a], Hassina Bilheux [a], Louis Santodonato [b], Jean-Christophe Bilheux [a], Jiao Lin [a],
Paris Cornwell [a], Erik Stringfellow [a], Matthew Pearson [c]

[a] *Neutron Scattering Division, Oak Ridge National Laboratory, Oak Ridge TN, USA 37831*
[b] *Advanced Research Systems, Inc., Macungie, PA, USA*
[c] *Neutron Technologies Division, Oak Ridge National Laboratory, Oak Ridge TN, USA 37831*

The neutron imaging facility (IMAGING) is located at CG-1D, High Flux Isotope Reactor (HFIR). IMAGING uses a polychromatic neutron beam in the cold range for a broad range of scientific applications ranging from energy materials, to plant physiology and additive manufacturing. Apertures (with different diameters D, pinhole geometry) are used at the entrance of the helium-filled flight path to allow variations of the figure of merit L/D, where L is the distance between the aperture and the detector where the image is produced. Recently, techniques such as laminography and monochromatic polarized neutron imaging have been prototyped at CG-1D. An intuitive data acquisition systems (EPICS) and state-of-the-art Python Jupyter Notebooks data processing, reconstruction and analysis have been implemented to allow more efficient use of beam time and increased scientific productivity. Samples sit on a translation/rotation stage for alignment and tomography purposes. The detector field-of-view is approximately 7 cm x 7 cm using the charge-coupled device (CCD). Large samples, sample environment, and equipment can be accommodated at Imaging. Recent technique implementation, upgrades and scientific results are presented in this poster, along with the future developments at this instrument.

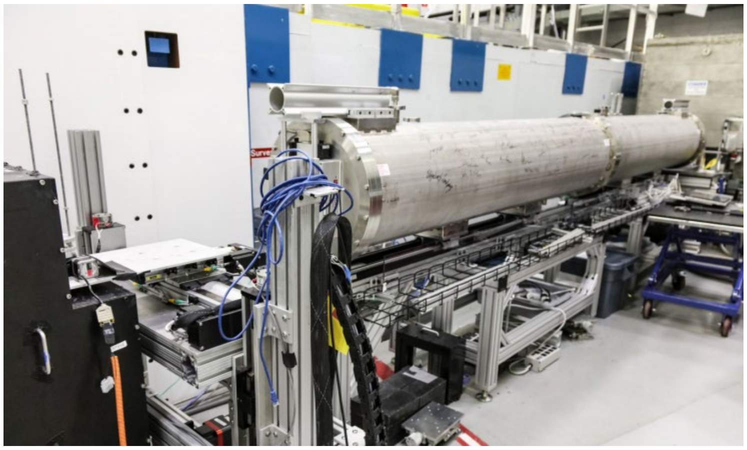

IMAGING at HFIR, ORNL.

Acknowledgments

This research was sponsored by the Scientific User Facilities Division, Office of Basic Energy Sciences, U.S. DOE. This research used resources at the Spallation Neutron Source and the High Flux Isotope Reactor, U.S. Department of Energy (DOE) Office of Science User Facilities operated by the Oak Ridge National Laboratory. Some of this research was sponsored by the Laboratory Directed Research and Development Program of ORNL. Research at the Manufacturing Demonstration Facility (MDF) was sponsored by the U.S. DOE, Office of Energy Efficiency and Renewable Energy, Advanced Manufacturing Office, under contract DE-AC05-00OR22725 with UT-Battelle, LLC.

Levitation Furnaces for Neutron Scattering at Oak Ridge National Laboratory

D.G. Quirinale[1], R.A. Mills[2], G.W. Lynn[2]

[1] Neutron Technology Division, NScD, Oak Ridge National Laboratory

[2] Neutron Scattering Science Division NScD, Oak Ridge National Laboratory

The NScD has invested in the development of several state-of-the-art containerless processing furnaces for ultra-high temperature (1000-3000 °C) experiments. These include the Neutron Aerodynamic Levitator (NAL) as well as the Neutron Electrostatic Levitator (NESL). Presented are the advantages and disadvantages of each system, the underlying levitation mechanisms, and some of their recent scientific successes.

High Temperature Sample Environments for Neutron Scattering at ORNL

R.A. Mills

Neutron Scattering Science Division NScD, Oak Ridge National Laboratory

Oak Ridge National Laboratory boasts two neutron scattering facilities in the Spallation Neutron Source (SNS) and the High Flux Isotope Reactor (HFIR.) Many of the experimentalists require extreme conditions to perform experiments; one such extreme environment is high temperature.
We present the current and future capabilities offered from the high temperature sample environment team including equipment ranging from high temperature closed cycle refrigerators to electrostatic laser heated levitators.

MANTA: a muli-analyzer neutron spectrometer at the High Flux Isotope Reactor

M. Daum and M. Mourigal. A. Aczel, and B. Winn

School of Physics, the Georgia Institute of Technology. Oak Ridge National Laboratory

In the last few decades, condensed matter research has demonstrated that genuinely quantum forms of matter can be stabilized in dense materials. Progress is challenged by our inability to directly measure entanglement in dense matter: quantum phases in materials can only be identified indirectly through their peculiar dynamical response functions. Inelastic neutron scattering is the most powerful, versatile and unambiguous experimental technique to probe quantum coherence and exotic dynamical responses of electronic magnetic moments in materials. However, U.S. instrumentation typically requires large samples and is limited in information rate, and furthermore is threatened by new paradigms for orders of magnitude efficiency increases developed in Europe. To combat this challenge, a novel ultra-high-efficiency inelastic neutron scattering spectrometer called MANTA has been proposed.

MANTA would use a crystal monochromator and focusing optics to provide high incident neutron flux. The existing CTAX analyzer would be complemented by a modern multiplexing analyzer that enables simultaneous measurements over a wide range of scattering angles and multiple final energies. This would allow rapid mapping of excitations in the scattering plane while preserving the ability to measure with high flux in a localized region of Q,ω space, as required for parametric studies. This should allow for inelastic measurements on milligram samples with the flexibility to also use larger samples when available, fully benefiting from the world's highest continuous flux of cold neutrons from the High Flux Isotope Reactor (HFIR) at Oak Ridge National Laboratory (ORNL). Due to its unique geometry, MANTA ideally complements instrumentation at current and future pulse neutron sources at ORNL as a no-compromise instrument for complex sample environments. This implementation comprises three main thrusts: engineering design and procurement of a primary spectrometer that energy filters, polarizes and focuses the neutron beam at the sample position using recent innovations for a 10-fold increase in time-average flux compared to current instrumentation; engineering work and procurement of a secondary spectrometer based on a multi-analyzer concept for an additional 10-fold increase in detection efficiency; procurement of sample environment systems including a 15 T low-temperature-superconductor cryo-magnet and low-temperature inserts.

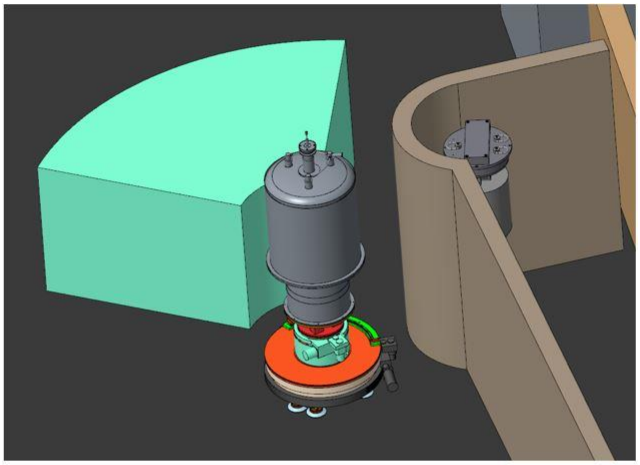

Figure 1. Early engineering view of the MANTA spectrometer on the north side of HFIR's cold neutron guide hall (from Barry Winn).

The Triple Axis Spectrometers at HFIR

Songxue Chi, Tao Hong, Adam Aczel, Wei Tian, Travis Williams, Masaaki Matsuda,
and Jaime Fernandez-Baca

Neutron Scattering Division, Oak Ridge National Laboratory

Triple-axis spectrometry (TAS) is a technique used in inelastic neutron scattering that was first developed by Bertram Brockhouse at the Chalk River Laboratories in Canada. It allows measurement of the scattering function at any point in energy and momentum space physically accessible by the spectrometer. The thermal triple axis instruments at HFIR were originally designed and installed in the 1960's. In 2000 the reactor beam tubes were upgraded, and the monochromator systems redesigned and rebuilt to modern standards, providing the U.S.'s highest thermal triple-axis flux (for a given resolution) onto the sample. The advantages of TAS include its high time-average intensity, versatility in neutron optics, customizable resolution and good signal/noise ratio. The suite of TAS at HFIR include three thermal neutron TAS (HB1A, HB1 and HB3) and one cold neutron TAS, CTAX. The uniqueness of each instrument will be presented.

CHESS: A Look into the Next Generation of Neutron Instruments

Marcus Daum, Oak Ridge National Laboratory

CHESS is the new proposed direct geometry inelastic spectrometer dedicated to the analysis of small samples with modest energy resolution (2.5-5% of Ei). This relatively short instrument will take full advantage of both the increased peak brilliance of the SNS Second Target Station (STS) coupled moderators, and of the recent advances in instrument design and technology, to achieve unprecedented performance for inelastic scattering in the cold energy range. The simulations predict that it will exceed that of CNCS by at least a factor of 200. Two sections of ballistic octagonal guides will transport the beam to the sample position at 29.6 m from the moderator. A new concept for double disk choppers will select the wavelengths and deal with frame overlap. CHESS will take full advantage of Repetition-Rate Multiplication (RRM) to analyze samples at multiple incident energies, maximizing the efficiency of the measurement. Finally, the detector tank will house a large array of curved 8-pack detector ^{3}He tubes giving a total solid angle coverage of 6.0 sr, and will incorporate Helmholtz coils for polarization analysis. Detailed Monte Carlo (MC) simulations of a real experiment on $K_2V_3O_8$ have been performed to optimize the instrument using McStas and MCViNE; these results were verified by running similar calculations on CNCS.

The Direct Geometry Instrument Suite for Inelastic Neutron Scattering at ORNL

Doug Abernathy, Arnab Banerjee, V. Ovi Garlea, Garrett Granroth, A. Sasha Kolesnikov, Daniel Pajerowski, Andrey Podlesnyak, Matt Stone, Barry Winn

Direct Geometry Team, Spectroscopy Group, Neutron Scattering Division, ORNL

The Direct Geometry Spectroscopy instruments at ORNL are ARCS, CNCS, HYSPEC and SEQUOIA. These four time-of-flight chopper spectrometers cover an extensive range of wave-vector and energy transfer space with varying degrees of neutron flux and resolution. The regions of reciprocal and energy space available to measure at these instruments are not exclusive and overlap significantly, allowing for better optimization of inelastic scattering experiments at the SNS. Brief overviews of the instruments will be presented, along with current scientific highlights, recent upgrades and some future plans for the Direct Geometry suite.

Chemical Spectroscopy: Indirect Geometry Suite of Neutron Scattering Instruments at ORNL

A. Timmy Ramirez Cuesta, Yongqiang Cheng, Luke Daemen, Niina Jalarvo, Eugene Mamontov,
Naresh Osti, *Barry Winn

Chemical Spectroscopy Team, Spectroscopy Group, Neutron Scattering Division, ORNL
*Direct Geometry Team, Spectroscopy Group, Neutron Scattering Division, ORNL

The Indirect Geometry Spectrometer instruments at ORNL are VISION and BASIS. Scientific highlights with both experimental and modeling results, and recent upgrades, are presented in this poster. In addition, future instruments such as ZEEMANS which also employ the indirect geometry spectroscopy technique will also be presented.

High resolution dynamics and structure measurements enabled by neutron Larmor labeling

Fankang Li[1, *], Jiazhou Shen[2], Lowell Crow[1], Steven R. Parnell[3], Masaaki Matsuda[1], Roger Pynn[1,2], Thomas Keller[4], Olivier Delaire[5] and Jaime A. Fernandez-Baca[1]

[1] Neutron Sciences Directorate, Oak Ridge National Laboratory, Oak Ridge, TN, 37830, USA

[2] Center for Exploration of Energy and Matter, Indiana University, Bloomington, IN, 47408, USA

[3] Faculty of Applied Sciences, Delft University of Technology, 2629JB Delft, The Netherlands

[4] Max-Planck-Institut Für Festkörperforschung, Heisenbergstrasse 1, 70569 Stuttgart, Germany

[5] Department of Physics, Duke University, Durham, NC 27708, USA,

*frankli@ornl.gov

To measure the crystal lattice distortion or the lifetime of weak interactions among quasiparticles, such as phonons, electrons and magnons, with high resolution, the key is to break the inverse relationship between the resolution and useable flux. By using the Larmor precession of the neutron spin inside a given magnetic field, its momentum or energy change during the interactions with sample can be measured with ultra-high resolution. Therefore, this unique property of neutron provides us with another approach to overcome some of the limitations of conventional neutron scattering instruments. Also, it can make the best use of all the available neutrons by allowing the use of large divergent beams. The progress on upgrading the HB-1 polarized triple axis spectrometer at the High Flux Isotope Reactor of ORNL with superconducting magnetic Wollaston prisms will be presented. For neutron diffraction, the achievable resolution of the absolute peak splitting and relative lattice distortion (Δd/d) can be 2×10^{-4} and 1×10^{-6} relatively. While for inelastic scattering, for example phonon linewidth measurements, the resolution can be <10μeV.

The Neutron Spin Echo Spectrometer at SNS (SNS-NSE)

Piotr A. Zolnierczuk, Laura R. Stingaciu, Wei-Ren Chen, Mary Odom

SANS/Spin Echo Team, Large Scale Structures Group, Neutron Scattering Division, ORNL

The SNS-NSE instrument is an ultrahigh resolution neutron spectrometer particularly suitable to investigate slow dynamical processes and unravel molecular motions at nanoscopic and mesoscopic scale in a variety of disciplines like: soft–matter and polymer science, biophysics, biochemistry, and nanotechnology. Due to a wavelength span of 2Å $< \lambda <$ 14Å using a simultaneous wavelength frame of 3 - 3.6Å high data collection efficiency is achieved allowing nearly gapless coverage of a broad wave-vector-time-range with only a few scattering angle settings. Typical applications include the molecular behavior of polymer melts, relaxation phenomena in networks and rubbers, interface fluctuations in complex fluids, transport processes in polymeric electrolytes and gel systems, the domain dynamics of proteins and enzyme's, lipid systems and biological membranes, disruptive effects of anti-inflammatory medication on membrane cell organization; transport process thru cell membranes and porous media. With proper adaptations the SNS-NSE instrument can also aid studies in condensed matter physics, materials science and magnetism.

The Suite of Small-Angle Neutron Scattering Instruments at ORNL

[2]Katherine Bailey, [1]Wei-Ren Chen, [1]Lisa DeBeer-Schmitt, [1]Changwoo Do, [2]Carrie Y. Gao, [1]Lilin He, [1]William T. Heller, [2]Luke Heroux, [1]Kenneth Littrell, [1]Sai Venkatesh Pingali, [1]Shuo Qian, [1]Volker S. Urban

[1]SANS/NSE Team, Large Scale Structures Group, [2]Scientific Associate Team 1, Beamline Support Group, Neutron Scattering Division, ORNL

The High Flux Isotope Reactor (HFIR) and the Spallation Neutron Source (SNS) of Oak Ridge National Laboratory are host to a diverse array of neutron scattering instruments. Among these instruments are four small-angle neutron scattering (SANS) instruments. The HFIR hosts the GP-SANS and Bio-SANS instruments, while the EQ-SANS and TOF-USANS instruments are located at the SNS. These instruments have complementary capabilities and serve diverse user communities. The GP-SANS and EQ-SANS have been built to be general purpose SANS instruments that serve broad user communities, while the Bio-SANS instrument of HFIR is specifically dedicated and optimized for biological materials and systems. The TOF-USANS instrument provides unique access to larger length scales –up to 20 μm– giving the capability of extending the q-range measurable on the other instruments by more than an order of magnitude with overlapping data. Here, we present an overview of the capabilities of these four instruments, sample environments that are available to the user communities, and future development plans across the suite of SANS instruments.

Magnetism Reflectometer BL 4A

Timothy Charlton, Valeria Lauter, Haile Ambaye, Mike Fitzsimmons

Reflectometry Team, Large Scale Structures Group, Neutron Scattering Division, ORNL

Scientific highlights and recent upgrades of the Magnetism Reflectometer at BL-4A at the Spallation Neutron Source are presented in this poster.

The Bio-Deuteration Laboratory at Oak Ridge National Laboratory

Kevin L. Weiss[1], Viswanathan Gurumoorthy[1], Sarah L. Lucas[1], Gwyndalyn Phillips[1], Swati Pant[1], Shuo Qian[1], Qiu Zhang[2], and Hugh O'Neill[1]

[1]Large Scale Structures Group, [2]Beamline Support Group, Neutron Scattering Division, ORNL

Abstract

Neutron scattering is a powerful, non-destructive method for obtaining unique information about the structure and dynamics of complex biological systems. The power of this method originates primarily from a sensitivity for hydrogen, which is one of the most abundant elements found in biology. Furthermore, the large neutron scattering length difference between hydrogen and deuterium can be exploited to selectively highlight different components of systems to obtain unique information regarding structure and dynamics. This makes the production of deuterium-labeled materials crucial for maximizing the utility of neutron scattering experiments for the biological sciences. To satisfy this critical need, the Center for Structural Molecular Biology operates the Bio-Deuteration Laboratory (BDL) as a centralized resource and training ground for the preparation of deuterium-labeled biomaterials in support of ORNL's neutron scattering facilities. Technical capabilities and recent developments of the BDL will be presented.

The Center for Structural Molecular Biology at ORNL

Sai Venkatesh Pingali[1], Shuo Qian[1], Qiu Zhang[2], Kevin Weiss[1], Luke Heroux[2], Volker Urban[1], Hugh O'Neill[1]

[1]Large Scale Structures Group, [2]Beamline Support Group, Neutron Scattering Division, ORNL

The Center for Structural Molecular Biology (CSMB) at Oak Ridge National Laboratory (ORNL) is a national user facility funded to support and develop the user access and science research program of the Biological Small-Angle Neutron Scattering (Bio-SANS) instrument at the High Flux Isotope Reactor (HFIR).

The Bio-SANS instrument at the HFIR is ideally suited for studies of biomacromolecules including proteins, DNA/RNA, lipid membranes and other hierarchical complexes. The Bio-SANS detectors now has a count rate capability of $>10^6$ Hz. Furthermore, the addition of the high-angle detector bank improved the accessible dynamic Q-range from a factor of 20 to 280 which translates to acquiring data simultaneously from $Q \sim 0.003$ to 0.85 Å^{-1}. This large dynamic Q-range is highly beneficial for time-resolved studies of hierarchical and large biological systems. We have also developed a series of new sample environment capabilities that open untapped opportunities for the studies of biological systems using neutrons. These include a pressure cell to monitor chemical reactions *in situ* such as biomass thermochemical pretreatment studies; a multi-position sample holder with rotational (tumbling) capability especially useful for studying colloidal suspensions; a humidity-controlled chamber critical for membrane studies; and a flow cell for systems that partition into multiple phases (e.g., microemulsions) with additional capability for flowing one or two phases during measurement. Furthermore, we can now perform grazing-incidence SANS in conjunction with a humidity chamber for studies of biomembranes.

The CSMB also operates a Bio-Deuteration Laboratory located at the Spallation Neutron Source (SNS) for deuterium labeling of biological macromolecules in support of the biology neutron scattering program. Key capabilities include parallel and preparative-scale bioreactor systems that allows high-density cell growth with precise control and monitoring of dissolved oxygen, pH, agitation, and feeding rate.

This resource complements capabilities at other Department of Energy (DOE) Office of Biological and Environmental Research (OBER) facilities for structural biology, and also supports studies of biomolecular complexes and biomass recalcitrance as part of the DOE Genomic Science Program. The CSMB supports a vibrant biological research community from academia, industry, and government laboratories. To broaden the impact of the CSMB and catalyze the synergy between OBER funded structural biology resources, we have established a collaborative program with the National Synchrotron Light Source II for joint access to SANS and small-angle X-ray scattering (SAXS) through both facilities.

The VENUS project at the Oak Ridge National Laboratory Spallation Neutron Source

Hassina Z. Bilheux[1], Kenneth W. Herwig[2], W. Scott Keener[2], George Q. Rennich[2], Jean C. Bilheux[1], Yuxuan Zhang[3], Matthew R. Pearson[2], Jiao Y. Y. Lin[1], Fahima F. Islam[1], C. Uli Wildgruber[2], Thomas Huegle[2], Irina I. Popova[2], Franz Gallmeier, Richard M. Ibberson[2], and Mike Herron[3]*
[1]Neutron Scattering Division, Oak Ridge National Laboratory, Oak Ridge TN, USA 37831
[2]Neutron Technologies Division, Oak Ridge National Laboratory, Oak Ridge TN, USA 37831
[3]SNS Upgrades Office, Oak Ridge National Laboratory, Oak Ridge TN, USA 37831

**bilheuxhn@ornl.gov (presenter)*

The VENUS project has officially started, and detailed engineering design is on its way to purchase the optical and beam delivery components of the beamline, such as the core vessel insert and the shutter insert. Located at the Spallation Neutron Source's First Target Station (beamline 10), the beamline is designed to utilize epithermal, thermal and cold neutrons from a 10 cm x 12 cm decoupled H_2 moderator. VENUS is optimized for both Bragg edge and epithermal imaging. Equipped with a T0 and four bandwidth choppers, it is optimized for two detector positions: (1) high flux, limited field-of-view (FOV) at 20 m; (2) lower flux, higher FOV and wavelength resolution at 25 m. Although not available at first at VENUS, the 20 m sample position is also designed to allow future magnification (using optical components) of an object onto the detector positioned at 25 m. The beamline specifications are described in Table 1. The collimation can vary from L/D 400 (the minimum L/D ratio that offers a full illumination of 20 cm x 20 cm at 25 m) to 2000, where *L* is the distance between the aperture of diameter, *D*, and the detector. With a cave of about ~ 90 m^2 (floor space), VENUS can accommodate large samples, sample environment, and equipment. This presentation gives the overall layout of the beamline, with the optimization of the optics and choppers. It also illustrates the future VENUS capabilities with example research experiments performed at the SNS SNAP and VULCAN beamlines.

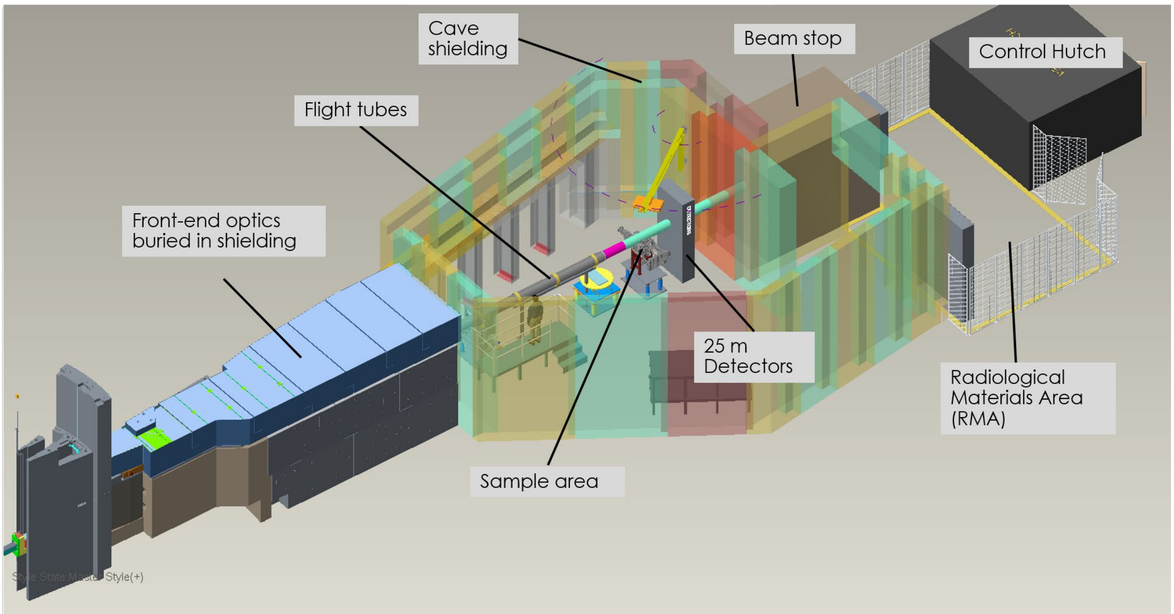

The VENUS instrument concept.

Acknowledgments

This research was sponsored by the Scientific User Facilities Division, Office of Basic Energy Sciences, U.S. DOE. This research used resources at the Spallation Neutron Source and the High Flux Isotope Reactor, U.S. Department of Energy (DOE) Office of Science User Facilities operated by the Oak Ridge National Laboratory. Some of this research was sponsored by the Laboratory Directed Research and Development Program of ORNL. Research at the Manufacturing Demonstration Facility (MDF) was sponsored by the U.S. DOE, Office of Energy Efficiency and Renewable Energy, Advanced Manufacturing Office, under contract DE-AC05-00OR22725 with UT-Battelle, LLC.

DEMAND, a Dimensional Extreme Magnetic Neutron Diffractometer at HFIR

H. B. Cao[1], B.C. Chakoumakos[1], K.M. Andrews[1], Y. Wu[1], R.A. Riedel[2], J. Hodges[2], W. Zhou[1], R. Gregory[2], B. Haberl[1], J. Molaison[1], and G.W. Lynn[1]

[1]Neutron Scattering Division, Oak Ridge National Laboratory
[2]Neutron Technologies Division, Oak Ridge National Laboratory

A two-dimensional (2D) Anger camera detector has been used at the HB-3A four-circle single-crystal neutron diffractometer at the High Flux Isotope Reactor (HFIR) since 2013. The 2D detector has enabled the capabilities of measuring sub-mm crystals and spin density maps, enhanced the efficiency of data collection and phase transition detection, and improved the signal-to-noise ratio [1]. Recently, the HB-3A four-circle diffractometer has been undergoing a detector upgrade towards a much larger area, magnetic-field-insensitive, Anger camera detector. The instrument will become capable of doing single-crystal neutron diffraction under ultra-low temperatures (50 mK), magnetic fields (up to 8 T), electric fields (up to 11 kV/mm), and hydrostatic high pressures (up to 45 GPa). Furthermore, half-polarized neutron diffraction is also available to measure weak ferromagnetism and local site magnetic susceptibilities. With the new high-resolution 2D detector, the four-circle diffractometer has become more powerful for studying magnetic materials under extreme sample environment conditions; hence, it has been given a new name: DEMAND [2]. DEMAND is fully suitable for studying material science, especially quantum materials, condensed matter physics, solid state chemistry, mineralogy, and other small molecular crystallography and magnetism.

1. Riedel, R.; Donahue, C.; Visscher, T.; Montcalm, C.; Cao, H.B. A High-Resolution Neutron Anger Camera Using Silicon Photo Multipliers (#2498). IEEE NSS&MIC 2017 N-24-5 Atlanta, USA. Available online: https://www.eventclass.org/contxt_ieee2017/online-program/session?s=N-24 (accessed on 20 December 2018).
2. Cao, H.B., B. C. Chakoumakos, Katie Andrews, Yan Wu, R. A. Riedel, Jason Hodges, Wenduo Zhou, Ray Gregory, Bianca Haberl, G. W. Lynn, DEMAND, a Dimensional Extreme Magnetic Neutron Diffractometer at the High Flux Isotope Reactor. *Crystals* 9, 5 (2019). https://doi.org/10.3390/cryst9010005

High **I**ntensity **D**iffractometer for **R**esidual Stress **A**nalysis (HIDRA)

Instrument Team: Jeff R. Bunn[1], Andrew E. Payzant[1], Chris M. Fancher[2], Paris Cornwell[3]
[1]Instrument Scientist, [2]Postdoctoral Research Associate, [3]Scientific Associate

Scientists and engineers use the 2nd generation Neutron Residual Stress Mapping Facility (NRSF2) to study residual stresses in a variety of structural materials and additively manufacture parts. NRSF2 is optimized to non-destructively investigated residual stresses by determining elastic strains for three-orthogonal scattering vectors by measuring the interplanar atomic spacing. This instrument is designed to use the high- penetration power of neutrons to map the spatially varying strain resulting from residual or applied stresses in bulk materials. Recently, the NRSF2 went through a major upgrade from an array of seven linear position sensitive detectors to a 30x30cm^2 2-dimensionsal detector and has been renamed the high intensity Diffractometer for residual stress analysis (HIDRA). This poster will detail the progress of the instrument upgrade and provide examples of users using NRSF2 for non-destructive analysis.

Single-Crystal Neutron Diffraction Instrument Suite at ORNL

H. B. Cao, B. C. Chakoumakos, L. Coates, M. D. Frontzek, C. Hoffmann, A. Y. Kovalevsky, Y. Liu, F. Meilleur, A. M. dos Santos, D. A. A. Myles, X. P. Wang, F. Ye
Neutron Scattering Division, Single-Crystal Team, Diffraction Group, Neutron Scattering Division, ORNL

The single-crystal diffraction instruments at ORNL are CORELLI, TOPAZ, and MaNDi at SNS and DEMAND, $WAND^2$ and IMAGINE at HFIR. SNAP at SNS is also being developed for some single-crystal diffraction. This nascent and unparalleled suite of diffractometers offers the potential to re-assert single-crystal diffraction using neutrons as a significant tool to study nuclear and magnetic structures of small unit cell crystals, nuclear structures of macromolecules, and diffuse scattering [1]. The signature applications and featured aspects of single-crystal neutron diffraction include high resolution nuclear structure analysis, magnetic structure and spin density determinations, contrast variation (particularly D_2O/H_2O) for nuclear structural studies, lack of radiation damage when using crystals of biological molecules such as proteins, and the fidelity to measure nuclear and magnetic diffuse scattering with elastic discrimination. Scientific highlights and current instrument status are presented.

[1] Coates, L., Cao, H.B., Chakoumakos, B.C., Frontzek, M. D., Hoffmann, C., Kovalevskyi, A. Y., Liu, Y., Meilleur, F., dos Santos, A.M., Myles, D.A.A., Wang, X., Ye, F., A Suite-level Review of the Neutron Single-Crystal Diffraction Instruments at Oak Ridge National Laboratory. *Review of Scientific Instruments* 89, 092802 (2018). DOI: https://doi.org/10.1063/1.5030896

Powder Diffraction Suite of Neutron Scattering Instruments at ORNL

Stuart Calder, Clarina Dela Cruz, Matthias Frontzek, Cheng Li, Jue Liu, Joerg Neuefeind, Katharine Page, Thomas Proffen, Qiang Zhang

Powder Diffraction Team, Diffraction Group, Neutron Scattering Division, ORNL

The powder diffraction instruments at ORNL are NOMAD, POWDER (HB-2A), POWGEN and WAND^2. This world-class suite utilizes the unique and complimentary capabilities of SNS and HFIR to enable measurements over an unparalleled regime at a single laboratory. This allows the instruments to tackle forefront scientific challenges through full crystal and magnetic structure refinements over large Q ranges, total scattering methods, fast measurements under changing in-situ conditions, and measurements in a wide array of sample environments [1]. Scientific highlights and recent upgrades are presented in this poster.

[1] S. Calder, K. An , R. Boehler, C. R. Dela Cruz, M. D. Frontzek , M. Guthrie, B. Haberl , A. Huq, S. A. J. Kimber, J. Liu, J. J. Molaison, J. Neuefeind , K. Page , A. M. dos Santos, K. M. Taddei, C. Tulk, and M. G. Tucker, "A suite-level review of the neutron powder diffraction instruments at Oak Ridge National Laboratory", Rev. Sci. Instrum. 89, 092701 (2018); https://doi.org/10.1063/1.5033906

PARALLEL SESSION

ABSTRACTS

Covalent functionalization of surface-modified metaloxide nanoparticles in experimental adhesive resins

Fernando L. Esteban Florez[1], Shuo Qian[2], Adam J. Rondinone[2], Sharukh S. Khajotia[1]

[1]University of Oklahoma Health Sciences Center, U.S.A, [2]Oak Ridge National Laboratory, U.S.A.

Objectives: Simple nanoparticles incorporation into polymers results in materials with inadequate surface properties. Consequently, nanoparticles' surface-modification and functionalization are required to enhance the tooth-adhesive-composite resin interface. The objective was to modify the surfaces of metaloxide nanoparticles with silanes and proteins, and characterize the nanoparticles-polymer matrix interfaces using cutting-edge scientific technologies.

Methods: Nitrogen-doped (N_TiO$_2$) and nitrogen-fluorine co-doped titanium dioxide nanoparticles (N_F_TiO$_2$) were synthesized using solvothermal reactions. N_TiO$_2$ (6-15nm) was then subjected to surface modification with either sodium hydroxide (NaOH, 15M), NaOH+(3-Aminopropyl) triethoxysilane (APTES, 85.5mM) or NaOH+APTES+albumin. Surface-modified nanoparticles suspended in deuterium oxide (D_2O, 10mg/mL) containing either NaCl (0.1 or 1.0M) or HCl (0.1M) were characterized using Small-Angle X-Ray Spectroscopy (SAXS) to determine nanoparticles' agglomeration levels. Experimental adhesive resins were synthesized by incorporating 20% (v/v) of either TiO_2, N_TiO$_2$ or N_F_TiO$_2$ (as-synthesized or surface-modified) into OptiBond Solo Plus (OPTB, Kerr Corp., USA). Specimens (n=8/group; d=6.0 mm, t=0.5mm) of unaltered (OPTB) and experimental adhesive resins were characterized with regard to nanoparticles' functionalization using Time-of-Flight Secondary Ion Mass Spectroscopy (ToF-SIMS), 2-D ToF-SIMS chemical mapping, Dual Focused Ion-Beam Nano-tomography (Dual-FIBNT) and Small-Angle Neutron Scattering (SANS).

Results: SAXS results indicated that surface-modified nanoparticles displayed higher X-Ray scattering intensities in a particle-size dependent manner. ToF-SIMS results demonstrated that nanoparticles incorporation did not adversely impact the polymer structure. 2-D ToF-SIMS chemical mapping determined the Ti^+ distribution and nitrogen-doping levels. Dual-FIBNT results demonstrated the 3-dimensional distribution of filler particles, nanoparticles and pores within the organic matrix of both unaltered and experimental adhesives. SANS results not only confirmed the nanoparticles' functionalization levels but also determined the types of nanoparticles-polymer matrix interfaces.

Conclusions: As-synthesized and surface-modified metaloxide nanoparticles were successfully fabricated. Nanoparticles were incorporated and covalently functionalized in a commercial dental adhesive resin, thereby holding the promise of materials with superior chemical, physical, mechanical and biological properties.

Funding: This project was supported by the Oklahoma Center for the Advancement of Science and Technology (HR16-131). A portion of this research was conducted at the Center for Nanophase Materials Sciences, which is a DOE Office of Science User Facility (CNMS18-034).

Spin Dynamics of the Elemental Quantum Spin Liquid β-Mn

Joseph Paddison, Junior Research Fellows
University of Cambridge, UK

Abstract:

Pure β-Mn is the only elemental metal that shows quantum spin-liquid-like behavior [1]. Its magnetic Mn atoms occupy a frustrated three-dimensional network of corner-sharing triangles. Unlike all other transition metals, β-Mn does not show long-range magnetic order to the lowest measured temperatures (~0.3 K). Instead, its magnetic response is dominated by strong antiferromagnetic spin fluctuations that persist up to room temperature and exhibit non-Fermi-liquid scaling [2].

I will present neutron-scattering measurements of the spin dynamics of β-Mn over a wide range of momentum transfer, energy transfer, and temperature. Our measurements reveal the temperature dependence of the on-site magnetic moment and the magnetic correlations. Our results shed new light on the unusual magnetic behavior of this remarkable element and demonstrate a data-driven approach to parameterizing magnetic correlations in metals.

[1] H. Nakamura et al., J. Phys. Condens. Matter 9, 4701 (1997).
[2] J. R. Stewart et al., Phys. Rev. Lett. 89, 186403 (2002).

Hybrid Skyrmions in Gd/Fe Multilayers

Dustin Gilbert, UT Researcher

University of Tennessee Knoxville

Abstract:

Magnetic skyrmions are chiral spin textures, initially presented as a novelty due to their topological character and formation mechanics, but subsequently have been presented as a potential game-changer for magnetic logic and data technologies. One barrier to skyrmion spintronics has been their stability – which tends to exist only in a narrow parameter space in temperature and magnetic fields, and virtually never at zero field. In this work, we present hybrid skyrmions with combined Bloch-Neel character, which are stable from <10 K to >320 K, over a field range of -60 mT to 200 mT, conveniently overlapping with 'ambient' conditions. Using small-angle neutron scattering (SANS) we have developed a mechanism to precipitate ordered lattices of these high-stable skyrmions. In ongoing studies on these GdFe skyrmions we have also demonstrated the ability to observe gigahertz-frequency dynamics in the skyrmions with SANS, opening the opportunity for in-situ high-frequency investigations with neutron scattering.

Extract Potential Hamiltonian from Neutron Scattering Data using a Machine Learning Assisted Approach

Anjana Samarakoon, Postdoctoral Research Associate
Direct Geometric Team, Oak Ridge National Laboratory

Abstract:

Precise modeling of a material is a key to understand its underlying interactions and physics but also revealing the competing phases in the nearby interaction space. Highly frustrated systems are important due to the richness in physics and diversity of phases including spin liquids with exotic topological states they display. Here, we present a machine learning workflow to fit multi-experimental data sets to find an optimal Hamiltonian while undertaking phase classification and extracting information about the topography around the region of interest. Experimental data from a spin-ice material, Dy2Ti2O7 including diffuse neutron scattering, heat capacity and susceptibility are utilized. This approach is shown to provide the best model in an efficient and effective way but also is powerful at planning the best experimental strategies.

New artificial magnetic honeycomb lattice for emergent physics and spintronics application

Deepak K. Singh
Department of Physics and Astronomy, University of Missouri, Columbia, MO

Two-dimensional magnetic nanostructured geometry, such as an artificial magnetic honeycomb lattice, provides facile platform to explore many novel properties of magnetic materials in one system. Originally envisaged to explore the physics of effective magnetic monopoles and magnetic field-induced avalanche of Dirac string, artificial magnetic honeycomb lattice has emerged as a key playground to discover new and exotic magnetic phases, such as magnetic charge ordered state and the spin solid state, in disorder free environment. We have created a new artificial permalloy honeycomb lattice of ultra-small connected element, with a typical length of ~ 12 nm, in this pursuit. Using neutron scattering and complementary measurements on the newly created honeycomb lattice, we have investigated emergent phenomena of short-range quasi-spin ice and long range spin solid order.[i] Additionally, two new properties of Wigner crystal type state of magnetic charges and magnetic diode-type rectification are discovered in the newly created artificial honeycomb lattice.[ii,iii] The new findings create a new vista for the next generation design of spintronics devices in this two-dimensional frustrated geometry. Research at MU is supported by the U.S. Department of Energy, Office of Basic Energy Sciences under Grant No. DE-SC0014461.

---

[i] A. Glavic, B. Summers, A. Dahal, J. Kline, W. Van Herck, A. Sukhov, A. Ernst and D. K. Singh, “Spin solid versus magnetic charge ordered state in artificial honeycomb lattice of connected elements”, *Advanced Science* **2018**, 1700856 (DOI: 10.1002/advs.201700856).

[ii] Y. Chen, B. Summers, A. Dahal, V. Lauter, G. Vignale and D. K. Singh, “Field and current control of the electrical conductivity of an artificial two-dimensional honeycomb lattice”, *Advanced Materials* **2019,** 201808298 (DOI: 10.1002/adma.201808298)

[iii] B. Summers, A. Dahal and D. K. Singh, “Magnetic diode behavior at room temperature in two-dimensional honeycomb”, *Advanced Electronic Materials* **2018**, 1700500 (DOI:10.1002/aelm.201700500).

POSTER ABSTRACTS

Theoretical Framework for Connecting the Nonlinear Rheology of Deforming Colloids to Their Microstructure from The Anisotropic Scattering Signature

Guan-Rong Huang[1], Yangyang Wang[2] and Wei-Ren Chen[1]

[1]Neutron Scattering Division, Oak Ridge National Laboratory [2]Center for Nanophase Materials Sciences, Oak Ridge National Laboratory

Abstract:

The flow of colloidal suspensions is ubiquitous in nature and industry. Colloidal suspensions exhibit a wide range of rheological behavior, which should be closely related to the microscopic structure of the systems. With in situ small-angle neutron scattering complemented by rheological measurements, we investigated the deformation behavior of a charge-stabilized colloidal glass at particle level undergoing steady shear. A short-lived, localized elastic response at particle level, termed as the transient elasticity zone (TEZ), was identified from the neutron spectra. The existence of the TEZ, which could be promoted by the electrostatic interparticle potential, is a signature of deformation heterogeneity: the body of fluids under shear behaves like an elastic solid within the spatial range of the TEZ but like fluid outside the TEZ. The size of the TEZ shrinks as the shear rate increases in the shear thinning region, which shows that the shear thinning is accompanied by a diminishing deformation heterogeneity. More interestingly, the TEZ is found to be the structural unit that provides the resistance to the imposed shear, as evidenced by the quantitative agreement between the local elastic stress sustained by the TEZ and the macroscopic stress from rheological measurements at low and moderate shear rates. Our findings provide an understanding on the nonlinear rheology of interacting colloidal glasses from a micro-mechanical view.

Exploring the topochemical reactions of organic crystals under high pressure using in situ neutron diffraction

Kuo Li*, Haiyan Zheng, Peijie Zhang

Center for High Pressure Science and Technology Advanced Research (HPSTAR)

It is always a mystery that how the chemical reactions happen under extreme conditions and what materials and compounds we can obtain. For materials composed of heavy elements, synchrotron X-ray techniques are always the best method for investigation, however, for the organic materials and compounds, X-ray is not a sensitive technique, neither the diffraction, nor the inelastic scattering. Neutron works much better for the C, H, O, N elements. Using in situ neutron diffraction under high pressure, we determined many crystal structures of unsaturated molecules, including the intermolecular distances between the unsaturated functional groups. From such kind of information, we concluded that most of the reactions are topochemical reactions.

Acetylene is the simplest unsaturated organic molecule. Under high pressure it crystalizes into a cubic structure and then transforms into an orthorhombic structure. When further compressed, it polymerizes along a specific direction to form cis-polyacetylene, which is directed by the crystal structure and hence is topochemical. By theoretical simulation we predicted that following such a route graphane will be produced, and by experimental investigation we obtained short-range ordered graphane and hence evidenced the mechanism. The intermolecular distance between the unsaturated carbon is 3.0-3.1Å, which is a crictical bar for the pressure-induced reaction.

To synthesize materials with improved ordering, we introduced functional groups to replace the hydrogen and hinder the random vibration and diffusion. By in situ neutron diffraction and synchrotron X-ray diffraction, we investigated the crystal structure of 2-butyne, diphenylbutadiyne (DPB), 2-butydioic acid, etc. For the direct bonding between the triple bonds of neighbored molecules, the intermolecular distance between the bonding atoms are always around 3.0-3.1Å.

We also find that for bigger molecules like DPB and the molecules with stronger intermolecular interactions like 2-butydioic acid, the phase transitions of restacking are not likely to happen. Hydrogen bond is the strongest intermolecular interaction and should be used to restrict the random diffusion and vibration. Other reaction besides the polymerization may also happen, including the hydrogen transfer, elimination, and condensation polymerization. Hydrogen plays a very important role in the reaction. Its location and movement under high pressure should be highly focused, and in situ neutron diffraction and inelastic scattering will be the key techniques.

SANS Study of Structures and Deuterium Incorporation into Vegetative Leaf Stalks of Deuterated Kale (*Brassica oleracea*)

Zhi Yang[1], Sam Bhagia[3], Hugh O'Neill[1], Barbara R. Evans[2], Arthur Ragauskas[4], Brian H. Davison[3] and Sai Venkatesh Pingali[1]

[1.] Neutron Scattering Division, [2.] Chemical Sciences Division, [3.] Biosciences Division, Oak Ridge National Laboratory, Oak Ridge Tennessee 37831; [4.] Department of Chemical and Biomolecular Engineering, University of Tennessee, Knoxville, Tennessee 37996.

The unique capabilities of small angle neutron scattering (SANS) assisted by NMR and FTIR have been applied to reveal the detailed molecular structure of both natural lignocellulosic biomass and model cellulosic composites. In this study, these techniques are applied to examine the stem structure of a deuterated herbaceous dicotyledonous plant, kale, which exhibits a hierarchical structure that resembles that of wood in vascular architecture with. In this study, partial deuteration was achieved through cultivating the kale plant in deuterated media to enhance contrast between component plant biopolymers. Cellulose microfibrils that solely contributes to SANS data in high-*Q* region ($Q > 0.08$ Å^{-1}) is determined to scatter similar to 65% D_2O solvent (SLD ~ 3.94 E-06 Å^{-2}), indicating that approximately 50% of the available covalently bonded H atoms would be substituted by D atoms (Fig. 1). In the low-*Q* region, the features responsible for these power-law decay show a neutron sensitivity that matches a solvent of 48% D_2O (SLD ~ 2.77 E-06 Å^{-2}) (Fig.2). To result in an overall SLD that is lower than cellulose, the SLD of lignin and hemicellulose needs to be lower to off-set the high SLD of cellulose within cell wall. To confirm the deuterium incorporation in the cellulose component of deuterated kale stem, contrast variation SANS experiments has been carried out on extracted cellulose (Fig.1B). The results demonstrated that the contrast matching points exhibit a nearly constant value of ~ 70% D_2O over the whole *Q* range, which is comparable to 65% D_2O obtained for the cellulose component in the deuterated kale stem (Fig.2). Finally, this study revealed the hierarchical structures of deuterated kale stems and different deuterium incorporation is found at different cell wall component polymers.

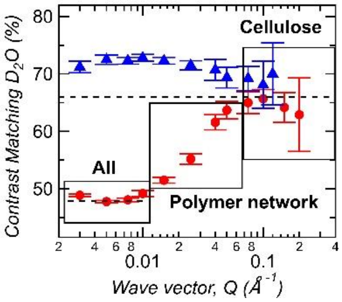

Figure 2. Contrast matching D_2O% as a function of wave vector *Q* for deuterated kale stem (red dot) and its cellulose extracts (blue triangle).

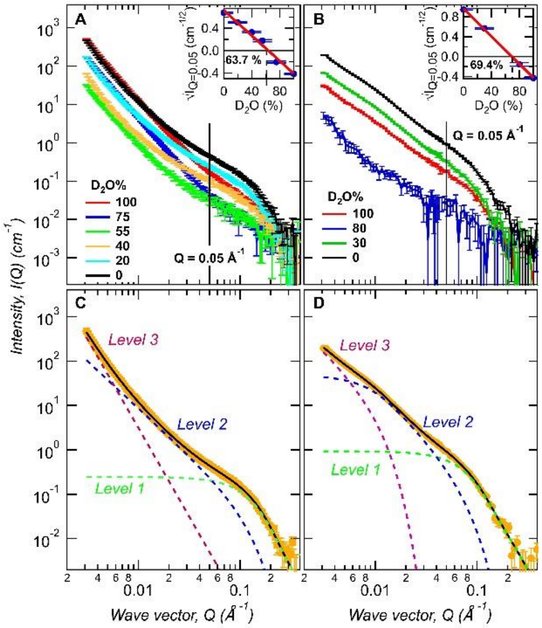

Figure 1. SANS profiles for contrast variation study of deuterated kale stems (A) and its cellulose extracts (B). Inset in (A) and (B) shows a plot of square-root of scattering intensity for a fixed *Q* (= 0.05 Å^{-1}) versus D_2O content of the solvent. A linear fit to the data shows zero contrast is obtained for 63.7% D_2O (A) and 69.4 % D_2O (B) for Q=0.05 Å^{-1}. (C, D) SANS profile of deuterated kale stem (C) and its cellulose extracts (D) in 0% D_2O. The Unified fit curves are shown as solid black lines in each figure. The three UF fit levels are shown as dashed green (Level 1), dashed blue (Level 2), and dashed magenta (Level 3).

Temperature-sensitive polymersomes for drug delivery probed by SANS

Veronika Kozlovskaya,[1] Yiming Yang,[1] Qian Shuo,[2] Volker Urban[2] and Eugenia Kharlampieva[1,3]

[1]Department of Chemistry, University of Alabama at Birmingham, Birmingham, Alabama 35294, United States

[2]Neutron Scattering Division, Neutron Sciences Directorate, Oak Ridge National Laboratory, Oak Ridge, Tennessee 37831, United States

[3]Center for Nanoscale Materials and Biointegration, University of Alabama at Birmingham, Birmingham, Alabama 35294, United States

Abstract

Polymeric vesicles, known as polymersomes, assembled from ABA triblock copolymers of poly(N-vinylcaprolactam)-poly(dimethylsiloxane)-poly(N-vinylcaprolactam) (PVCL-PDMS-PVCL) are a promising platform for biomedical applications, as the temperature-responsiveness of the PVCL blocks enables reversible vesicle shrinkage and permeability of the polymersome shell at elevated temperatures. We explored the effects of molecular weight, polymer block weight ratios, and temperature on the structure of these polymersomes via electron microscopy, dynamic light scattering, and small angle neutron scattering (SANS. We show that the shell structure and overall size of the polymersome can be tuned by varying the hydrophilic (PVCL) weight fraction of the polymer: at room temperature, polymers of smaller hydrophilic ratios form larger vesicles that have thinner shells, whereas polymers with higher PVCL content exhibit interchain aggregation of PVCL blocks within the polymersome shell above 50 °C. Model fitting and model-free analysis of the SANS data reveals that increasing the mass ratio of PVCL to the total copolymer weight from 0.3 to 0.56 reduces the temperature-induced change in vesicle diameter by a factor of 3 while simultaneously increasing the change in shell thickness by a factor of 1.5. Finally, by analysis of the shell structures and overall size of polymersomes with various PVCL weight ratios and those without temperature-dependent polymer components, we bring into focus the mechanism of temperature-triggered drug release. This work provides new fundamental perspectives on temperature-responsive polymersomes and elucidates important structure-property relationships of their constituent polymers.

Effects of Solvent Polarity on Segmental Dynamics in Sulfonated Polystryrene Networks: Quasi Elastic Neutron Scattering Study

Supun S. Mohottalalage[1], Sidath Wijesinghe[1], Manjula Senanayake[1], Chathurika Kosgallana[1], Naresh Osti[2] and Dvora Perahia[3]

[1]Department of Chemistry, Clemson University, Clemson, SC, United States. [2]Oak Ridge National Laboratory, Oak Ridge, TN, United States. [3]Department of Chemistry/Department of Physics, Clemson University, Clemson, SC, United States.

Incorporating ionic groups into a polymer changes dynamics in a significant way. These ionic groups serve as cross links and form clusters which unlocks different pathways. Here, the effects of solvent dielectrics on segmental dynamics of slightly sulfonated (3mol%) polystyrene (PSS) networks formed in non-polar environment were studied by quasi elastic neutron scattering (QENS) technique. Solvent dielectrics were tuned by addition of ethanol to 10%(w/w) PSS in cyclohexane. QENS experiment was carried out for q range 0.3 $Å^{-1}$ to 1.3 $Å^{-1}$ which captures the dynamics of 21 Å–5 Å in length scale. QENS scattering patterns were analyzed by Kohlrausch-Williams-Watts (KWW) to extract characteristic relaxation times. We find that PSS dynamics in cyclohexane is constrained at larger dimensions. Addition of small amount of ethanol (5% v/v) release the constrains. Surprisingly however, further addition of ethanol decreases segmental motion. This reduction could be attributed to overall plasticization of the polymer in presence of ethanol.

Observation of a mesoscopic magnetic modulation in chiral $Mn_{1/3}NbS_2$

Sunil K. Karna[1], F. N. Womack[1], R. Chapai[1], D. P. Young[1], M. Marshall[2], Weiwei Xie[2], D. Graf[3], Yan Wu[4], Huibo Cao[4], L. DeBeer-Schmitt[4], P. W. Adams[1], R. Jin[1], and J. F. DiTusa[1]

[1]Department of Physics and Astronomy, Louisiana State University, Baton Rouge, Louisiana 70803, USA
[2]Department of Chemistry, Louisiana State University, Baton Rouge, Louisiana 70803, USA
[3]National High Magnetic Field Laboratory, Florida State University, Tallahassee, Florida 32310, USA
[4]Neutron Scattering Division, Oak Ridge National Laboratory, Oak Ridge, TN 37831, USA

Abstract

We have investigated the structural, magnetic, thermodynamic, and charge transport properties of $Mn_{1/3}NbS_2$ single crystals through x-ray and neutron diffraction, magnetization, specific heat, magnetoresistance, and Hall effect measurements. $Mn_{1/3}NbS_2$ displays a magnetic transition at T_C ~ 45 K with highly anisotropic behavior expected for a hexagonal structured material. Below T_C, neutron diffraction reveals increased scattering near the structural Bragg peaks having a wider Q-dependence along the c-axis than the nuclear Bragg peaks. This indicates helimagnetism with a long pitch length of ~250 nm (or a wavevector q~0.0025 Å^{-1}) along the c-axis. This q is substantially smaller than that found for the helimagnetic state in isostructural $Cr_{1/3}NbS_2$ (0.015 Å^{-1}). Specific heat capacity measurements confirm a second order magnetic phase transition with a substantial magnetic contribution that persists to low temperature. The large low-temperature specific heat capacity is consistent with a large density of low-lying magnetic excitations that are likely associated with topologically interesting magnetic modes. Changes to the magnetoresistance, the magnetization, and the magnetic neutron diffraction, which become more apparent below 20 K, imply a modification in the character of the magnetic ordering corresponding to the magnetic contribution to the specific heat capacity. These observations signify a more complex magnetic structure both at zero and finite fields for $Mn_{1/3}NbS_2$ than for the well-investigated $Cr_{1/3}NbS_2$.

Neutron and X-ray Reflectivity Studies of Styrene Maleic Acid Polymer Interactions with Thylakoid Lipid Monolayers

O. Korotych[1], N. Brady[1], M. Phan[2], S. Satija[3], J. Ankner[2], and B. D. Bruce[1]

[1]*Biochemistry & Cellular and Molecular Biology Dept., University of Tennessee, Knoxville, TN 37966*
[2]*Neutron Scattering Division, Oak Ridge National Laboratory, Oak Ridge, TN 37830*
[3]*Center for Neutron Research, National Institute of Standards and Technology, Gaithersburg, MD 20899*

Derivatives of styrene-co-maleic acid (SMA) polymers have gained increasing interest for their use in the isolation and characterization of membrane proteins. These copolymers have been shown to extract membrane protein complexes, forming so-called styrene maleic acid lipid particles (SMALPs) – nanosized, polymer-encapsulated discs that can be utilized for structural, functional, and biophysical characterization of membrane proteins. This novel approach represents a cost-effective alternative to detergent isolation of membrane proteins and it also allows preserving native boundary lipids, which have been suggested to provide both structural and functional stability to membrane proteins. To date, no correlation between the physical properties of the SMA copolymers (styrene-to-maleic acid ratio or copolymer molecular weight), can be directly attributed to extraction efficiency of membrane proteins. Additionally, complex interfacial processes and polymer dynamics remain poorly understood, although they play a crucial role in lipid/protein solubilization. Thus, to better understand interactions between polymers and membranes, we are going to perform a systematic study of SMA interactions with well-defined, synthetic and native lipid monolayers and bilayers.

In this study we utilized *in situ* X-ray reflectometry (XRR) and neutron reflectometry (NR) at the liquid/air interface to capture the changes in the structure of lipid monolayers and the distribution of SMA within the lipid membrane during polymer adsorption. Using binary lipid mixtures composed of 80 mol% 1,2-dipalmitoyl-sn-glycero-3-phosphocholine (DPPC) and 20 mol% monogalactosyldiacylglycerol (MGDG), digalactosyldiacylglycerol (DGDG), sulfoquinovosyldiacylglycerol (SQDG), or 1,2-dipalmitoyl-sn-glycero-3-phosphorylglycerol (DPPG), this work aims to determine the contribution of individual thylakoid lipids on adsorption activity of SMA® 1440 – the most efficient polymer for solubilization of thylakoid membranes as determined in our previous study [1].

XRR results show drastic interruption of membrane structure upon SMA adsorption for the binary mixtures of DPPC with DGDG, MGDG, and SQDG. NR data reveals that lipid compostion regulates the polymer conformation during initial association and possibly membrane insertion. This work will be further extended to study 3-component lipid mixtures and natural membrane mimetics with various SMA copolymers to reveal a fundamental mechanism of interactions between SMA copolymers and membranes, facilitating SMALP formation.

[1] O. Korotych, J. Mondal, K. M. Gattás-Asfura, J. Hendricks, and B. D. Bruce. Evaluation of commercially available styrene-co-maleic acid polymers for the extraction of membrane proteins from spinach chloroplast thylakoids. *Eur. Polym. J.* **114**, 485–500 (2019).

A Novel 1m×1m Thermal Neutron Imager for SANS Operating in Ionization Mode with Pad Readout

Jack Fried, George Mahler, Neil Schaknowski, Graham Smith, Bo Yu

Instrumentation Division, Brookhaven National Laboratory, Upton, NY, USA

We have developed a ^{3}He based thermal neutron imager with an active area of 1m×1m for the small-angle neutron scattering (SANS) beamline QUOKKA at the Australian Nuclear Science and Technology Organization (ANSTO). This new detector, which was installed in November of 2018 as a replacement for an existing MWPC based detector, operates in ionization mode without any electron multiplication in the gas. The electrons created by the neutron - ^{3}He interaction are collected by discrete anode pads, each connected to an input channel of an ASIC directly mounted on the back of the anode pad plane. The custom, 64 channel ASICs and their readout boards can process up to 25k/s per channel.

Our group has been developing ^{3}He filled MWPCs for position sensitive thermal neutron detection, but these instruments incur dead-time losses as counting rate exceeds 10^5 cps. As the neutron flux reaches higher rates, the avalanche gain may become unstable and wire aging issues can occur. To achieve the ultimate parallelism and to avoid issues associated with the electron multiplication process, we are now focusing on developing ^{3}He based imaging detectors operating in ionization mode with anode pad readout [1,2]. This technique is made possible by the low noise custom ASIC developed specifically for this mode of operation [3].

The heart of this detector is a 4×4 array of 16 anode pad boards. Each 64 channel ASIC covers 8×8 pads, and there are 36 ASICs on each board. Each anode pad is 5mm×5mm resulting in an active area of 24cm×24cm per pad board. Each Pad board is coupled to a readout board which has a flexible ribbon cable for power and data communication to the outside of the pressure vessel. The 16 board pairs are mounted on a rigid aluminum frame with a gap of 0.5mm between pads of adjacent boards resulting in a seamless collection area. Overall, the total active area of the detector is 960mm×960mm, with 36,864 pads. The 16 anode pad boards and readout board pairs reside inside a common pressure vessel. An aluminized Mylar film is bonded to the inside of the entrance window and biased at about -1.5kV. A set of field shaping electrodes encloses the volume between the window electrode and the pad plane to ensure a uniform drift field to the edges of the active volume. The active gas depth between the window and the pad plane is 4cm. The pressure vessel is filled with a mixture of ^{3}He and CF_4 resulting in 90% efficiency for 4Å neutrons.

At ANSTO, this instrument is installed inside a large vacuum tank to reduce the neutron scattering with air. A total of 200W of power is dissipated inside the pressure vessel. A sealed enclosure is attached to the back of the detector housing the power supplies and gas circulation system. This chamber is connected to the atmosphere outside of the vacuum tank through hoses which supply forced ambient air cooling. The temperature of the in-detector electronics equalized at 40º C.

The most unique features of this detector are its counting rate, efficiency and long-term stability. The detector can process up to 2.5×10^4 cps per pad, and 2×10^7 cps per pad board (2304 pads). Limited by the data throughput of the Gigabit Ethernet interface, the overall rate limit of the 16-pad board detector is about 3×10^8 cps.

[1] N.A. Schaknowski, G.C. Smith, B. Yu and A. Doumas, “Two- dimensional ^{3}He Neutron Detectors with Pad Readout for High Rates”. 2005 IEEE NSS/MIC Conference Record, 1201-1204.

[2] B. Yu; N. A. Schaknowski; 1G. C. Smith; G. De Geronimo; E. O. Vernon; L. G. Clonts; C L. Britton; S. S. Frank “Thermal neutron detectors with discrete anode pad readout”, 2008 IEEE Nuclear Science Symposium Conference Record, 1878 – 1881.

[3] G. De Geronimo, J. Fried, G.C. Smith, B. Yu, E. Vernon, W.L. Brian, C.L. Britton, L.C. Clonts and S.S. Frank, “ASIC for Small Angle Neutron Scattering Experiments at the SNS”, IEEE Trans. Nucl. Sci. NS-54, 541-548 (2007).

Optimization of Particle Energy and Arrival Time Determination using GPUs for the Nab Experiment*

David Perryman
Department of Physics and Astronomy, The University of Tennessee at Knoxville

Measurements of neutron beta decay correlation parameters yield a ratio of axial and vector weak couplings as well as test physics beyond the Standard Model. The Nab (Neutron a b) experiment will extract these parameters by coincidence detection of beta decay's protons and electrons, which includes energy and time of flight determination. Because of the experiment's expected high data throughput in the form of digitized waveforms from pixelated silicon detectors, it is important to extract energies and times quickly and reliably. This poster will present results from timing and statistical studies using graphics processor based energy and time extraction.

*The Titan X used for this research was donated by the NVIDIA Corporation.

Power of new 2D-PSD of WAND^2

Koji Kaneko[1], Matthias D. Frontzek[2], S. Ikeda[3], M. Kakihana[4], M. Hedo[5], T. Nakama[5], Y. Onuki[5]

[1]Materials Sciences Research Center, Japan Atomic Energy Agency
[2]Neutron Scattering Division, Oak Ridge National Laboratory
[3]Graduate School of Material Science, University of Hyogo
[4]Graduate School of Engineering and Science, University of the Ryukyus
[5]Faculty of Science, University of the Ryukyus

Recent successive upgrades of the Wide Angle Neutron Diffractometer Squared (WAND^2)[1], located at the HB-2C beam port in HFIR, open unique capabilities in scattering researches. The original WAND was built in collaboration between Oak Ridge National Laboratory and Japan Atomic Energy Agency under US/Japan Cooperative Program on Neutron Scattering Research in 1980s. The WAND was equipped with the one-dimensional ^{3}He position sensitive detector (PSD) covering 125° in 2θ with moderate angular resolution of 0.25°. Latest upgrade was to replace the one-dimensional PSD by the two-dimensional one with high efficiency and better angular resolution. The new 2D-PSD covers scattering angles 120° in horizontal and ±7.5° in vertical. This allows efficient scans over wide reciprocal space. Namely, this is suitable to hunt for unknown magnetic peaks, to reveal diffuse scattering, and so on.

In commissioning, usefulness of WAND^2 was tested by looking at magnetic peaks in Eu intermetallic compounds. Despite strong neutron absorption of Eu, a relatively short incident wavelength of WAND^2 and its high efficiency lead to successful observations of magnetic peaks for small single crystals with a typical size of a few mm^3. In case for a cubic chiral magnet EuPtSi, which undergoes an antiferromagnetic transition at T_N=4.0 K, single crystal diffraction experiments on WAND^2 succeeded to reveal its unique ordering vector in the ground state of $\boldsymbol{q}_1$ = (0.2, 0.3, 0) and its cyclic permutations [2]. Additional first-order magnetic transition from $\boldsymbol{q}_1$ to a complex ordering vector $\boldsymbol{q}_1^*$ = (0.2, 0.3, $\pm\delta$) at $T^*\sim$ 2.5 K was also detected successfully. Furthermore, the magnetic-field induced order with the quite characteristic ordering vector of $\boldsymbol{q}_A$ = (±0.09, ±0.20, -(±0.28)) was unveiled as well. This finding was a key to identify that EuPtSi is the first compound to form a magnetic skyrmion lattice in a *f*-electron magnet.

Another success was achieved for another Eu divalent system Eu*T*In$_4$ (*T*=Ni, Pd and Pt), which crystallizes in the orthorhombic structure. Among these isoelectronic compounds, magnetic anisotropy changes drastically, unexpected for isotropic spin moment of Eu^{2+}. In WAND, we found a hint that this change of anisotropy arises from a slight modification in the ordering vector. However, 1D-PSD was insufficient to resolve how it is modified. The new 2D-PSD of WAND^2 allows to identify the accurate ordering vector across the series, owing to its high resolution and vertical access.

These successful observations in the very first stage of commissioning demonstrates powerfulness of WAND^2 for efficient survey of 3D reciprocal space. This will open new capabilities by neutron diffraction technique.

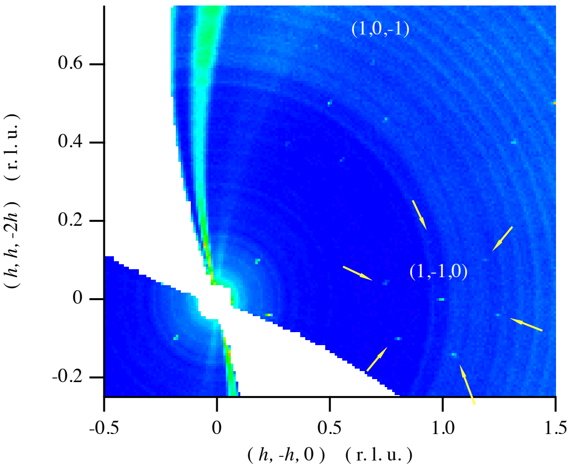

Figure 1 A part of the neutron scattering intensity map in the horizontal scattering plane defined by (1, -1, 0) and (1, 1, -2) in the field-induced ordered phase of EuPtSi recorded on WAND^2. Yellow arrows indicate the magnetic peaks around (1, -1, 0), which stems from the triple-$\boldsymbol{q}$ magnetic structure with $\boldsymbol{q}_A$. Vertical strong intensity region across the origin corresponds to the dark angle of the magnet.

[1] M. D. Frontzek *et al.*, WAND^2 -A versatile wide angle neutron powder/single crystal diffractometer. Rev. Sci. Instrum. **89**, 092801 (2018).

[2] K. Kaneko *et al.*, Unique Helical Magnetic Order and Field-Induced Phase in Trillium Lattice Antiferromagnet EuPtSi. J. Phys. Soc. Jpn. **88**, 013702 (2019).

A Helimagnetic Structure in $MnBi_2Se_4$

Judy Roth (1), Chongin Pak (1), Huibo Cao (2), Michael Shatruk (1)
1. Department of Chemistry and Biochemistry, Florida State University, Tallahassee, FL 32306, USA
2. Neutron Scattering Division, Oak Ridge National Laboratory, Oak Ridge, TN 37831, USA

$MnBi_2Se_4$ have been reported to show antiferromagnetic (AFM) ordering at T_N = 15 K. Based on the crystal structure of this material, which contains chains of edge-sharing $MnSe_6$ octahedra, it has been suggested that the magnetic structure should contain AFM-coupled spins oriented perpendicular to the chain direction. We noted, however, that inter-chain magnetic interactions should also be important and might even introduce some spin frustration due to the displacement of neighboring chains with respect to one another. Such interactions might lead to a more complex magnetic structure. Further support to our hypothesis came from the evaluation of the spin frustration factor ($f_{fr} = \left|\frac{\theta}{T_N}\right|$) from the Curie-Weiss law, which gave $f = 4.8$ measured with the magnetic field applied perpendicular to the chain propagation direction. In order to determine the magnetic structure of $MnBi_2Se_4$, large single crystals were grown by chemical vapor transport, using a mixture of the ternary compound and MnSe as precursors. The single-crystal neutron diffraction experiment was carried out on the HB-3A instrument at the Oak Ridge National Laboratory. The magnetic structure determination revealed that $MnBi_2Se_4$ forms an incommensurate helimagnetic structure, thus confirming our hypothesis of the non-trivial spin texture in this material. The details of the magnetic structure and its correlation to the crystal structure of $MnBi_2Se_4$ will be discussed.

Selective Alkyne Hydrogenation over CeO_2 Investigated by *in situ* vibrational spectroscopy studies

J. Moon, Y. Cheng, L. Daemen, M. Li, F. Polo-Garzon, A. J. Ramirez-Cuesta, and Z. Wu

Chemical Science Division and Chemical & Neutron Scattering Division, Oak Ridge National Laboratory, Oak Ridge, TN

Selective hydrogenation of alkynes is a key catalytic reaction applied industrially at different scale to purify olefin streams for preparation of high-added-value fine chemicals. Studies have been conducted for last decades to develop efficient catalyst and the substantial scientific literatures emphasize the dominance of palladium-based catalysts due to its high activity at moderate temperature and pressure, but it often suffers over hydrogenation and oligomerization. In recent years, Ceria is used as a catalyst in alkene hydrogenation, mainly as a support and often used as a promoter or a stabilizer, but it has been studied that CeO_2 itself exhibits outstanding catalytic performance for selective hydrogenation of propylene and acetylene[1]. Although it showed superior reactivity, the reaction mechanism still remains unclear. Here, we discuss our progress to understand its selective hydrogenation mechanism using *in situ* vibrational spectroscopy including inelastic neutron scattering (INS) and infrared spectroscopy (IR).

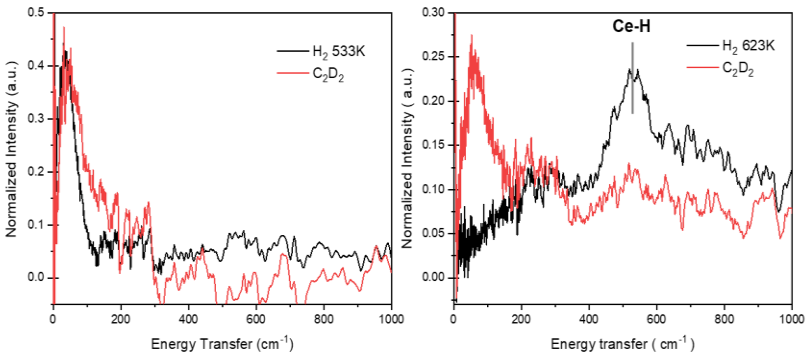

Figure 1. INS spectra of CeO_2 collected at 5K after H_2 treatment at 533K (left, black) and sequential C_2D_2 reaction at 423K (left, red), and after H_2 treatment at 623K (right, black) and sequential C_2D_2 reaction at 423 K (right, red)

Using *in situ* INS we observe the formation of hydride through hydrogen treatment step over 623 K and the consumption of the hydride after sequential reaction with acetylene (Fig. 1). This result suggests that Ce-H reacts with acetylene to form hydrogenation products, but to make it clear, we also report an *in situ* diffuse reflectance infrared Fourier transformed spectroscopy (DRIFT) study of CeO_2 under similar condition with INS measurement. The results clearly demonstrated the formation of chemisorbed C_2H_3 and C_2H_4 species during the acetylene hydrogenation after hydrogen treatment. For low temperature hydrogen treatment (533 K), OH site is first consumed in catalyzing the C_2H_2 selective hydrogenation, but for high temperature hydrogen treatment (>623 K), it showed that initially C_2H_2 reacted with hydride from Ce site causing the formation of C_2H_3 on Ce site and then form oligomers including vinylidene and methine groups in the structure[2]. This can be inferred that the Ce-H is more active than OH site in catalyzing C_2H_2 hydrogenation and cause oligomerization. The finding of this work gives insight to understand the mechanism of acetylene selective hydrogenation over CeO_2 and optimize the operation condition of selective hydrogenation over CeO_2.

1. G. Vile, et al., Ceira hydrogenation catalysis: High selectivity in the Conversion of Alkene to Olefins, J. Angrew. Chem., Int. Ed., **51**, 8620-8623 (2012)

2. T. Cao, et al., An in situ DRIFT mechanistic study of CeO2-catalyzed acetylene semihydrogenation reaction. Phys. Chem. Chem. Phys., **20**, 9659-9670 (2018)

Ammonia Synthesis Catalyzed by Electride-Supported Ruthenium Nanoparticles

J. Kammert, J. Moon, K. Page, Y. Cheng, A. Ramirez-Cuesta, J. Tong, Z. Wu

Chemical Sciences Division & Neutron Scattering Division, Oak Ridge National Laboratory, Tennessee
Department of Materials Science and Engineering, Clemson University

Ammonia synthesis has played a critical role in feeding the world through the latter half of the 20th century. Without the technology to fix nitrogen at an industrial scale, it would be impossible to feed approximately half of the global population. Ammonia also has potential applications as a liquid fuel that can be converted to hydrogen or perhaps even burned directly for energy. Recent studies have shown that metallic Ru nanoparticles supported on electrides such as $[Ca_{24}Al_{28}O_{64}]^{4+}(e^-)^4$ (also known as C12A7:e$^-$) and Ca_2N:e$^-$ demonstrate an order of magnitude higher activity for ammonia synthesis from N_2 and H_2 than other state-of-the-art materials such as Cs-promoted Ru supported on MgO.(1) An electride is a material that consists of a cationic structure capable of stabilizing anionic solvated electrons. It has been hypothesized that donation of electron density from the electride support to the Ru particles facilitates the N≡N dissociation step, which is widely agreed to be the rate-limiting step in this reaction. However, previous work in this area also suggests that donating electron density to supported Ru particles increases the competitive adsorption of strongly-bound H to the Ru active sites for N_2 dissociation.(*2*) This effect is not observed in the electride-supported Ru, so we have focused our study on understanding the nature of hydride species present in the active catalysts using *in situ* neutron scattering techniques, reaction kinetic studies, and electron microscopy.

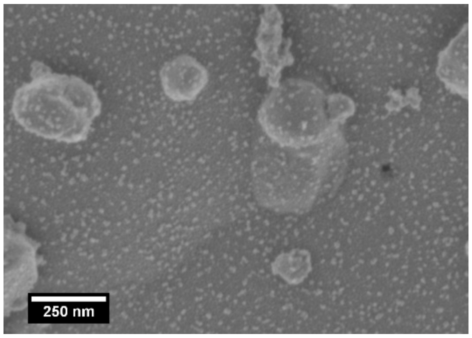

Figure 2: Scanning electron micrograph of 1 wt % Ru/C12A7:e$^-$ exemplifying dispersed Ru particles.

Recent studies suggest that the rate of ammonia synthesis over Ru/C12A7:e$^-$ per Ru atom is strongly dependent on particle size. Ammonia synthesis rates varied by over an order of magnitude based on the dispersion estimated by CO chemisorption.(*3*) We have synthesized Ru/C12A7:e$^-$ over a range of Ru loadings, and characterized particles of various levels of dispersion using probe molecule chemisorption. A scanning electron micrograph of 1 wt % Ru/C12A7:e$^-$ is shown in Figure 1, where dispersed Ru particles are clearly visible on the C12A7:e$^-$ support. Reaction testing indicates these catalysts are highly active for the ammonia synthesis reaction.

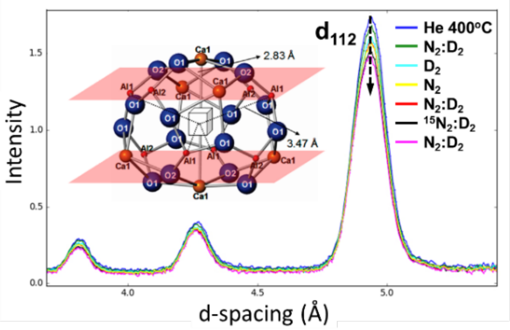

Figure 1: Evolution of the d_{112} feature in C12A7:e$^-$ during ammonia synthesis, observed by neutron diffraction.

In situ neutron diffraction indicates a transformation of the C12A7:e$^-$ framework during ammonia production, as illustrated in Figure 2. The influence of framework-encaged N- and H- species that could be generated under reaction conditions is being investigated using theoretical modeling approaches. Further study using quasi-elastic and inelastic neutron scattering is expected to yield insights into the nature of these species and the dynamics of their incorporation into the framework.

1. M. Kitano *et al.*, Essential role of hydride ion in ruthenium-based ammonia synthesis catalysts. *Chem Sci* **7**, 4036-4043 (2016).
2. S. E. Siporin, R. J. Davis, Isotopic transient analysis of ammonia synthesis over Ru/MgO catalysts promoted by cesium, barium, or lanthanum. *Journal of Catalysis* **222**, 315-322 (2004).
3. Y. Inoue *et al.*, Highly Dispersed Ru on Electride [Ca24Al28O64]4+(e–)4 as a Catalyst for Ammonia Synthesis. *ACS Catalysis* **4**, 674-680 (2014).

A Novel Automated Optimized, 3-D Printed Collimator Design for High Pressure Scattering

Fahima Islam[1], Jiao Y. Y. Lin[2], Bianca Haberl[3], Ian Lumsden[4], David Anderson[5] and Garrett E. Granroth[6]

[1] Neutron Scattering Division, Oak Ridge National Laboratory, Oak Ridge, TN 37831,islamff@ornl.gov
[2] Neutron Scattering Division, Oak Ridge National Laboratory, Oak Ridge, TN 37831,linjiao@ornl.gov
[3] Neutron Scattering Division, Oak Ridge National Laboratory, Oak Ridge, TN 37831,haberlb@ornl.gov
[4] Neutron Scattering Division, Oak Ridge National Laboratory, Oak Ridge, TN 37831, lumsdenI@ornl.gov
[5] Neutron Technology Division, Oak Ridge National Laboratory, Oak Ridge, TN 37831,andersondc@ornl.gov
[6]Neutron Scattering Division, Oak Ridge National Laboratory, Oak Ridge, TN 37831, granrothge@ornl.gov

Many current neutron scattering experiments require use complex sample environments which invariably contribute significant background to the experimental data. Generally, collimators which are part of the instrument have been used to improve the sample to cell signal ratio. Particularly for high pressure, however, collimation should be customized for different pressure environments since different pressure environments produce different results. For example, in high pressure diffraction, the Bragg peaks move and change with pressure. Furthermore, no unobstructed view of the sample is inherently possible if pressure is to be applied. It is thus crucial to separate the sample signal from the background signal generated by the high pressure cell.

Here we show a new avenue for custom-made collimators to overcome this challenge. Specifically, portable 3D-printed collimators can be tailored to a particular pressure cell and thus are a step further in background reduction. An automated work-flow has been developed to design a custom collimator, optimized for a given pressure environment and manufacturing constraints. The end result is a file ready for 3D printing. The collimator is conical in shape with tightly spaced neutron absorbing blades which are stacked in vertical and horizontal directions to provide transmitting channels. The optimization parameters include number of blades, blade-size, materials and the length of the collimator. A Monte-Carlo neutron ray-tracing simulation model based on MCViNE was developed to evaluate the performance of the collimator. An optimized collimator will maximize the sample signal to background ratio without sacrificing too much neutron flux. Thus, the optimization must strike a balance between improving relative sample signals and minimizing the loss of intensities, and at the same time account for engineering constraints imposed by the 3D printing techniques.

A clamp cell was chosen as a first example. It consists of a cylindrical sample of ~ 4 mm, enclosed in a cylindrical CuBe inner-sleeve and an Al outer-body with an overall outer diameter of ~30-50 mm. Note that there is significantly more cell materials than sample so the sample signal is very weak compared to the cell signal without a collimator. A collimator was designed, optimized, printed and tested on the SNAP neutron beam-line. The experimental results are then compared with the simulation results. The optimal collimator provides substantial improvement over the no collimator case. The developed computerized work flow for optimizing collimator will be readily extensible to novel integrated designs of the myriad sample environments required for any instrumentation.

Probing Heterogeneous Disorder in Complex Oxides

Eric O'Quinn[1], Jacob Shamblin[1], Igor Gussev[1], Will Cureton[1], Michelle Everett[2], Joerg Neuefeind[2], and Maik Lang[1]
[1]*Department of Nuclear Engineering, University of Tennessee*
[2]*Chemical and Engineering Materials Division, Spallation Neutron Source, Oak Ridge National Laboratory*

There has recently been an increased focus on understanding the structure-energetics-property relation of materials that can accommodate unconventional ordering (*e.g.,* glasses, quasicrystals, and materials with correlated disorder that is heterogeneous across different length-scales). In particular, compounds with the isometric pyrochlore ($A_2B_2O_7$) or spinel (AB_2O_4) structures can accommodate structural disorder which leads to excellent amorphization under energetic particle irradiation or high levels of oxygen conductivity. Thus, these materials find application as host materials for immobilizing actinides, such as plutonium, and fast ion conductors in solid oxide fuel cells. Despite the importance of the disordering process, there exists only a limited understanding of the role of local ordering on the energy landscape, mainly due to the use of techniques that can only characterize the average, long-range structure and are insensitive to disorder on the oxygen sublattice (*i.e.,* X-ray/electron diffraction). The innovative strategy of this research project is the application of combined pair distribution function (PDF) analysis from neutron total scattering. Our initial experiments revealed that a disordered, fluorite structure consists of a locally ordered, orthorhombic structural unit (Fig. 1) that is repeated by a pseudo-translational symmetry, such that orthorhombic and isometric arrays coexist at different length-scales (*1*). Further, when exposed to heavy ion irradiation, pyrochlores that exhibit differing material responses over long length scales (disorder *versus* amorphization) were shown to exhibit nearly identical local atomic arrangements (*2*). Such behavior has also been identified in isometric spinel (*3*). The results of this research provide much needed analysis of the sub-nanoscale regime of disordered complex oxides; such information will be important to accurately describe the behavior of materials in extreme environments, which is important for applications in advanced nuclear energy systems and solid oxide fuel cells.

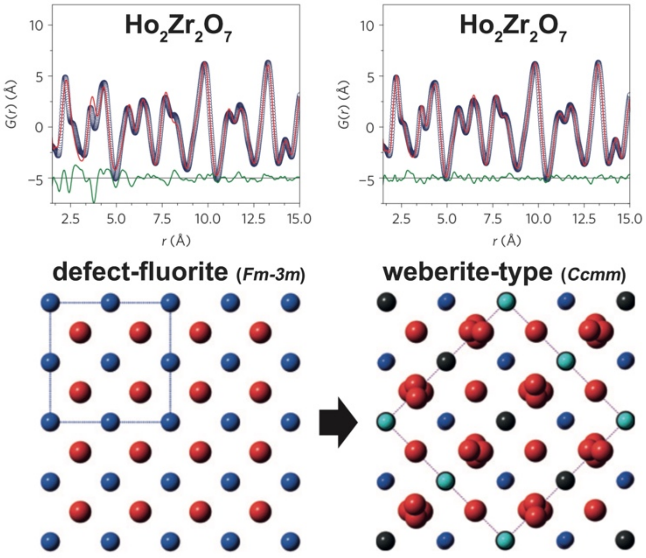

Figure 1: Neutron pair distribution function of disordered fluorite $Ho_2Zr_2O_7$ which is better modeled locally by the cation and vacancy ordered fluorite derivative weberite-type structure.

1. J. Shamblin *et al.*, Probing disorder in isometric pyrochlore and related complex oxides. *Nat. Mater.* **15**, 507–512 (2016).
2. J. Shamblin *et al.*, Similar local order in disordered fluorite and aperiodic pyrochlore structures. *Acta Mater.* **144**, 60–67 (2018).
3. E. C. O'Quinn *et al.*, Inversion in $Mg_{1-x}Ni_xAl_2O_4$ Spinel: New Insight into Local Structure. *J. Am. Chem. Soc.* **139**, 10395–10402 (2017).

Inelastic Neutron Scattering in Probing Molecular Magnetism

Duncan H. Moseley,[a] Zhiming Liu,[a] Shelby E. Stavretis,[a] Yongqiang Cheng,[b] Luke L. Daemen,[b] Antonio F. Moreira Dos Santos,[b] A. J. Ramirez-Cuesta,[b] and Zi-Ling Xue[a]

[a] *Department of Chemistry, University of Tennessee, Knoxville, Tennessee 37996, United States*

[b] *Neutron Scattering Division, Oak Ridge National Laboratory, Oak Ridge, Tennessee 37831, United States*

Neutron spectroscopy has proven invaluable in recent years for studying magnetic transitions in single-molecule magnets (SMMs). These methods, including both Inelastic Neutron Scattering (INS) and Quasielastic Neutron Scattering (QENS), are coupled with the use of temperature-, pressure-, and magnetic field-dependence to illuminate the nature of magnetic transitions and their relaxation via coupling with neighboring phonons. The use of variable temperature and magnetic fields has allowed for the assignment of magnetic transitions in SMMs. DFT phonon calculations using VASP and OClimax are also critical to understanding INS spectra, allowing the assignment of phonon modes, thus making clear magnetic peaks in SMMs.

Elucidation of lignin-acrylate hydrogel assembly using small-angle neutron scattering (Bio-SANS)

Kalavathy Rajan[1], Sai Venkatesh Pingali[2] and Stephen C. Chmely[1]

[1]Center for Renewable Carbon, University of Tennessee, Knoxville; [2]Oak Ridge National Laboratory, Oak Ridge, TN

Abstract

Lignin-based hydrogels are renewable, biocompatible and biodegradable, with a diverse range of applications including seed coatings and microencapsulation. Supramolecular networks, formed by crosslinking the many macro-monomer side-chains extending from the lignin nucleation sites, have been proposed to impart the superior material properties of copolymer hydrogels. However, previous reports have neither resolved the nano-scale assemblies of lignin-based hydrogels nor have elucidated their structure-function relationships. We therefore studied the poly-HEMA [poly-(2-hydroxyethyl methacrylate)] hydrogels, containing up to 40% (w/w) of methacrylated lignin, using small-angle neutron scattering (Bio-SANS). Contrast variation study with SANS, which employed 0, 31, 46, 75 and 100% volumetric ratios of D_2O (in H_2O), was used to resolve the structural features of lignin and HEMA at their respective match points. We were able to determine the shape, size (R_g) and number of pores of the hydrogel network. Lignin was observed to form a random coiled structure of approximately 80 Å in diameter, whereas the HEMA polymer network contained smooth pores of about 14 Å in diameter. Thus, understanding lignin-polymer interactions, and how these affect the internal morphology of the copolymer hydrogels, is critical to predict physical and chemical properties and to develop advanced materials for specific applications.

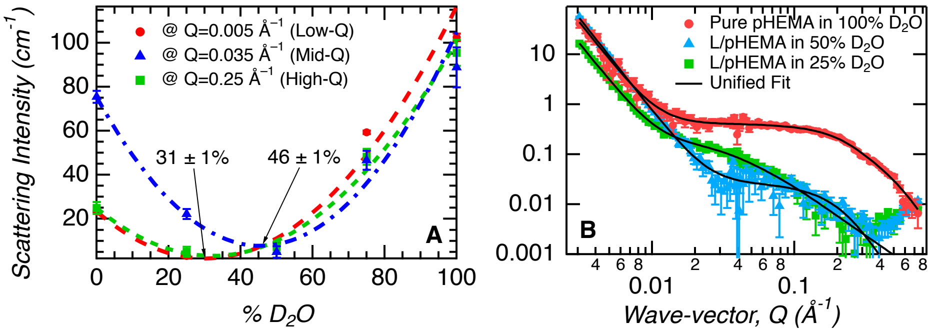

Figure 1. (A) Contrast variation of OSL-HEMA copolymer hydrogel showing two contrast matching SLD- 31% D_2O for poly-HEMA and 46% D_2O for lignin. (B) SANS profiles of pure poly-HEMA and OSL-HEMA at component contrast match points.

BEST STUDENT POSTER ABSTRACTS

Local Structural Study of Novel Mott-Insulating Cousins of the Iron Pnictides

B. Karki[1], A. Alfailakawi[1], B. A. Frandsen[2], J. C. Neuefeind[3], M. Everett[3] and B. Freelon[1]

[1] Department of Physics and Astronomy, University of Louisville, Louisville, KY 40208, USA
[2] Department of Physics and Astronomy, Brigham Young University, Provo, UT 84602, USA
[3] Oak Ridge National Laboratory, Oak Ridge, TN 37831, U.S.A.

ABSTRACT:

There has been significant interest in mixed anion materials since the discovery of high transition temperature (T_c) superconductivity in layered iron pnictides system. Electron-electron interaction leads to the emergence of fascinating collective electronic behavior, including novel magnetism, electronic nematic order and superconductivity. All of these properties are closely related in iron-based superconductors. The interplay between these orders can be understood by studying their co-evolution across the phase diagram through the chemical substitution. An important question in iron-based superconductivity has been whether superconductivity could emerge from materials that are in the Mott insulating region of the electronic phase diagram as is the case for cuprate high- T_c superconductors. In an effort to find such materials, the mixed-anion iron-oxychalcogenides have been explored.

Iron oxy-chalcogenides, $\mathrm{La_2O_2Fe_2O}M_2$ (M = S, Se), is the layered materials formed from stacking layered units of $\mathrm{La_2O_2}$ and $\mathrm{Fe_2O}M_2$ (M = S, Se). They are structurally reminiscent of the cuprates while possessing the Fe-chalcogen planes that are similar to the Fe-pnictides. This work describes the structural properties of , $\mathrm{La_2O_2Fe_2O}M_2$ (M = S, Se) which are closely related to the superconductivity because they are on the verge of a metal insulator transition. By exchanging S and Se it is possible to tune the electron correlation value from insulating to the metallic phase. Unlike the Fe-pnictides these materials do not show long range structural phase transition. However, both materials M = S, Se undergo magnetic phase transitions from paramagnetic antiferromagnetic phase at a Neel temperature 107 K and 90 K, respectively.

Neutron total scattering experiments on $\mathrm{La_2O_2Fe_2O}M_2$ (M = S, Se) were performed on Nanoscale Ordered Materials Diffractometer (NOMAD) beamline at Oak Ridge National Laboratory (ORNL) in order to collect Pair distribution function (PDF) data. PDF analysis involves Fourier transforming the measured total scattering intensity in order to obtain a real space representation of inter-atomic correlations. This technique is used to study local, short range structural correlations that deviate from the average structure. Our results for M = S, Se possess short-scale structural distortions however, neutron powder diffraction (NPD) provides clear evidence that the average, long-range structure remains tetragonal throughout the high and low temperature regimes. Local crystal structure was studied by investigating deviations in atomic positions and orthorhombicity. By tracking the orthorhombicity parameter we observe local scale distortions between the tetragonal and orthorhombic structure in a typical range of 1-2 nm as shown in **Figure 1**. These spatially limited distortions represent fluctuating nematic order which suggests the ubiquity of nematic fluctuations in iron-based superconductors and related materials. In addition, we found the discontinuity in c-lattice which may arise due to the buckling of $\mathrm{Fe_2O}$ plane. We anticipate that this buckling might be due to the change in octahedral height or tilting of the octahedral structure. Overall, these results suggest that structural distortion may play a role in absence of superconductivity in these materials.

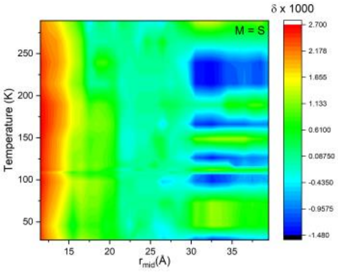

Fig 1. False color plots of the refined orthorhombicity determined from neutron PDF analysis of samples of M = S. Negative values of orthorhombicity indicate that the lattice parameter b is larger than a.

High-Throughput Phonon Calculations Using the Real-Space Multigrid Method (RMG)

Jiayong Zhang[1], Wenchang Lu[1], Emil Briggs[1], Y.Q. Cheng[2], A.J. Ramirez-Cuesta[2], Jerzy Bernholc[1]

1. Department of Physics, North Carolina State University,
2. Neutron Scattering Division, Oak Ridge National Laboratory

The RMG code(www.rmg.org), is a real-space multigrid method based code for electronic-structure calculations within the framework of Density Functional Theory (DFT), which is highly parallel with excellent scalability to thousands of nodes and GPUs. It has accurate forces and is very suitable for high-throughput, large-scale ab initio molecular dynamics (AIMD), which makes it a perfect backend driver for large scale phonon calculations combined with Finite Displacement Method (FDM) or AIMD.

Employing the FDM with assumption of harmonic approximation, we build supercells with small perturbations from atoms' equilibrium positions and perform self-consistent calculations to obtain interatomic forces in real space, which are transformed to reciprocal space to form dynamical matrices at arbitrary q values. Alternatively, the AIMD results can be used to extract force constants that include anharmonic and finite temperature effects, and thus to compute phonon band structures and spectra that include these effects. We have performed phonon calculations for a number of different systems, including silicon, ZrH_2, Carbazole and ZIF-8.

The inelastic neutron scattering spectra (INS) is further used to validate the reliability of the RMG code by comparing the calculated results with INS measured by the VISION instrument at the Spallation Neutron Source at ORNL.

The Influence of Side-chain Length on Backbone Rigidity for Conjugated Polymers

Zhiqiang Cao [a], Song Zhang [a], Luke Galuska [a], Tianyu Li [b], Kunlun Hong [b], and Xiaodan Gu [a]

[a] School of Polymer Science and Engineering, The University of Southern Mississippi, Hattiesburg

[b] Center for Nanophase Materials Sciences, Oak Ridge National Laboratory, Oak Ridge

Although huge progress has been made to optimize the optical and electronic properties of conjugated polymers (CPs), fully elucidating the origin of the increase in optical and electronic properties of CPs is still much-needed. Notably, the backbone rigidity of these CPs—which determines the delocalized electron cloud from its pi-conjugation—is critical for the materials' property. However, it remains a challenge to experimentally characterize conjugated backbone rigidity and relate these to the fundamental optical and electronic properties (electronic coupling, charge transport, etc.). To fill this underexplored area, we utilized chemical deuteration and neutron scattering techniques to quantify the chain rigidity then elucidate the role of the chain rigidity plays for CPs.

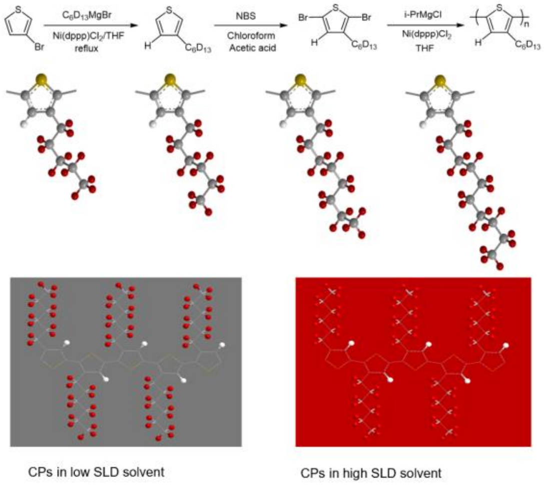

Figure 1: Two key techniques used to probe the backbone rigidity: (a) synthesis of P3ATs with deuterated side-chains, and (b) use of contrast matching technique to conceal the sidechain in deuterated solvents as illustrated by the same red color between solvents and sidechains in the cartoon.

The length of the conjugated polymer side chain plays an important role in the ultimate performance of conjugated polymeric devices, considering that longer side chains can contribute significant steric effects on the dihedral potentials, allowing kinks to happen in the backbone, thus reduce the persistence length. In order to study the effect length of the alkyl sidechain on the backbone rigidity for Poly(3-alkylthiophenes) (P3ATs), we synthesized deuterated polythiophene with various length of side-chains to understand the influence the sidechain length on the polymer backbone conformation as shown in **Figure 1**. Selective deuteration of polymeric side chains and contrast matching with solvents provides a unique way to hide the scattering signal from the long alkyl side-chains and probe only the scattering from the backbone. As shown in **Figure 1**, upon deuteration, the local scattering length density for the side chains increases, which can be matched by a deuterated solvent mixture. The neutron scattering will be performed on empty banjo quartz cell, mixture solvents in sample cell, the CPs dissolved in solvent in sample cells. The scattering will be performed at several sample to detector distance to cover a large enough scattering vector for easier data fitting. A typical Q range we would like to achieve is around 0.002 A^{-1} to 0.3A^{-1}. Through modelling the scattering data using various models (Worm-like chain model or Debye chain model[1,2]), the "naked" backbone rigidity can be extracted by comparing radius of gyration (R_g) and the molecular weight. The resultant persistence length (L_p) for CPs with various sidechains will be rationalized with respect to various sidechains.

(1) McCulloch, B. et. al. Polymer Chain Shape of Poly(3-Alkylthiophenes) in Solution Using Small-Angle Neutron Scattering. *Macromolecules* **2013**, *46* (5), 1899–1907.

(2) Chen, W.-R. et. al. Incorporating Intermicellar Interactions in the Fitting of SANS Data from Cationic Wormlike Micelles. *Langmuir* **2006**, *22* (15), 6539–6548.

Probing texture evolutions during friction stir processing of a Mg alloy: in-situ, real-time neutron diffraction study

Yuan Li[1], Ke An[2], Zhili Feng[3], and Hahn Choo[1]
1. Materials Science and Engineering, University of Tennessee, Knoxville, TN, 37996, USA
2. Neutron Scattering Division, Oak Ridge National Laboratory, Oak Ridge, TN, 37831, USA
3. Materials Science & Technology Division, Oak Ridge National Laboratory, Oak Ridge, TN, 37831, USA

The friction stir welding/processing (FSW/FSP), that uses the unique principles of the severe plastic deformation method, has a great potential as a novel method for the fabrication of bulk ultrafine-grained Mg alloys. Furthermore, there is a great potential to enhance the formability of Mg alloys significantly by using the FSP technique. For example, recent studies show that the FSP can be used for texture manipulation in Mg alloys resulting in significant improvements in mechanical behavior [1-3]. However, most of the studies are focused on the final texture after FSP.

In this study, in-situ texture evolution during friction stir processing (FSP) of AZ31B Mg alloy plates was studied using neutron diffraction. The ranges of the FSP parameters used are: 1-5 mm/sec traveling speed and 200-1,500 rpm clockwise FSP tool rotating speed which allows the thermo-mechanical input (in terms of Zener-Hollomon parameter, Z) by more than two orders of magnitude covering both low Z (slip dominant) and high Z (twin prevalent) regimes identified in previous constitutive studies. The variations in the onset and extent of characteristic grain rotations during FSP as a function of time from the tool pin and the Zener-Hollomon parameter (low Z vs. high Z) will be presented. Fig. 1 is the comparison of (0002) measured along ND (normal direction) and $(10\bar{1}1)$ intensity measured along PD (processing direction) between low Z (LZ) and high Z (HZ) processed. In addition, pole figures as a function of time will be reconstructed.

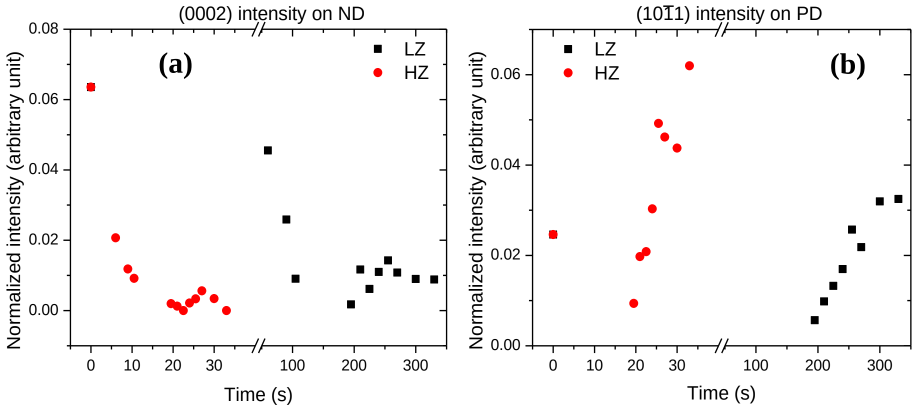

Fig. 1 (a) Evolution of (0002) intensity measured along ND and (b) evolution of $(10\bar{1}1)$ intensity measured along PD (RD) as a function of time during FSP at LZ and HZ conditions

[1] J.Q. Su, T.W. Nelson, C.J. Sterling, Scripta Materialia 52(2) (2005) 135-140.
[2] Z.Z. Yu, H. Choo, Z.L. Feng, S.C. Vogel, Scripta Materialia 63(11) (2010) 1112-1115.
[3] W. Woo, H. Choo, D.W. Brown, P.K. Liaw, Z. Feng, Scripta Materialia 54(11) (2006) 1859-1864.

Description of the Correlated Dynamics in D_2O in Real-Space and Time

Y. Sarathchandran[1], Y. Shinohara[2], T. Iwashita[3], W. Dmowski[1], D. Abernathy[2], and T. Egami[1,2]
[1]University of Tennessee Knoxville, USA, [2]Oak Ridge National Laboratory, USA,
[3]Oita University, Japan

The anomalous properties of water have their origins in the strong hydrogen bond network present in water. Even after decades of research on the structure and dynamics of water, the nature of the microscopic atomic dynamics leading to these properties remains unclear. This is partly because researchers use separate techniques to probe structure (diffraction) and dynamics (spectroscopy), thereby making a direct connection between spatial and temporal correlations impossible. This is where a time dependent pair correlation function, such as the Van Hove function, becomes valuable. Here we discuss our work in which we combined inelastic neutron scattering measurements with the Van Hove function, $g(r, t)$, to understand the spatial and temporal correlations in the hydrogen bond mediated dynamics of heavy water (D_2O).

The Van Hove function describes the temporal evolution of the structure of a system in real space and time, making it the ideal method to study dynamic systems. It is calculated by double-Fourier transforming the dynamic structure factor, S(Q, E), obtained from inelastic scattering experiments. To obtain high-quality Van Hove function free from termination errors, one would require the S(Q, E) to be measured up to high momentum (>9 $Å^{-1}$) and energy transfers (> 10 meV). This used to be a time-consuming process until the arrival of synchrotron and spallation scattering facilities.

Our previous work on water dynamics using x-ray scattering experiments [1][2] has demonstrated the feasibility of the above method. The obtained oxygen-oxygen Van Hove function has given valuable dynamical information on the inter-molecular dynamics in water. Neutron scattering measurements are ideal to observe the dynamics of hydrogen atoms due to their high scattering cross-section for neutrons. By seeing the temporal evolution of the correlations involving hydrogen atoms, the hydrogen bond mediated dynamics could be better understood.

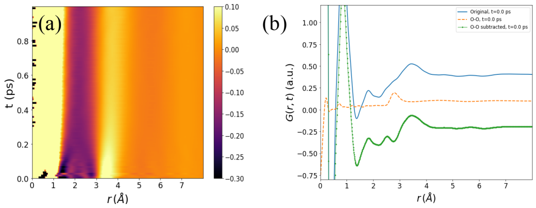

Figure 1. (a) $g(r, t)$ of D_2O, (b) t=0 plots of original (blue), O-O (orange), and O-O subtracted (green) $g(r, t)$.

Using time-of-flight neutron spectroscopy at ARCS, SNS, S(Q,E) of heavy water was measured for three temperatures, 295K, 333K and 363K. The resulting Van Hove function of D_2O, as seen in Fig. 1a, is a combination of three atomic pair correlations, O-D, D-D and O-O. Among them the dominant contributors are D-D and O-D correlations. Previous inelastic x-ray scattering measurement of D_2O is used to subtract the O-O correlations (as shown in Fig. 1b) as x-rays do not detect hydrogen atoms due to their low electron density. The Van Hove function after the subtraction contains only D-D and O-D contributions. The relaxation behavior of these atomic correlations is studied directly from the Van Hove function by fitting the peak decay with a decay function. We observed a two-step relaxation process for these correlations involving caging motion and correlated dynamics of atoms. Classical MD simulations on water shows strong agreement with these experimental observations. This result highlights the effectiveness of combining the Van Hove function with neutron scattering experiments to explore dynamic systems.

References

1. Y. Shinohara, W. Dmowski, T. Iwashita, B. Wu, D. Ishikawa, A. Q. R. Baron, and T. Egami, *Phys. Rev. E* **98**, 022604 (2018).
2. T. Iwashita, W. Bin, W. -R. Chen, S. Tsutsui, A. Q. R. Baron, and T. Egami, *Sci. Adv.* **3**, e1603079 (2017).

Anharmonic effects on phonon eigenvectors and *S(Q,E)* in quantum parraelectric $SrTiO_3$

Xing He[1], Dipanshu Bansal[1] , Barry Winn[2], Songxue Chi[2], Lynn Boatner[2], Olivier Delaire[1]

[1] Department of Mechanical Engineering and Materials Science, Duke University

[2] Oak Ridge National Laboratory

The Hybrid Spectrometer (HYSPEC) and HB3 triple-axis spectrometer at Oak Ridge National Laboratory (ORNL) were used to track phonon intensities in the quantum paraelectric system $SrTiO_3$ over a wide temperature range and for a large volume in reciprocal space. Anomalous temperature-dependent phonon intensities are observed in multiple Brillouin zones (BZs) from these inelastic neutron scattering (INS) experiments. The $S(\boldsymbol{Q},E)$ data reveal a strong softening of the transverse optic (TO) mode, and simultaneously a strongly anomalous evolution of the intensity of transverse acoustic (TA) modes, which decreases dramatically on cooling. The experimentally observed trends are confirmed and rationalized using ab initio molecular dynamics (AIMD) and anharmonically renomralized phonon methods, which achieve quantitative agreement with the INS experiments. By analyzing the simulated T-dependent force constants and eigenvectors, it is found that the structure factors $|F|^2$ of TA and TO modes change dramatically with temperature, as a direct consequence of the strong anharmonicity in this system. Moreover, we identify that the changes of Ti and O eigenvectors are responsible for these striking observations. These results explain the long-standing phenomenon first observed in INS experiments by Yamada and Shirane [1]. Our results also systematically extend this observation to multiple BZs and other high symmetry directions ([1,0,0] and [1,1,0]). These results establish how striking T - dependencies of phonon intensities beyond the harmonic picture can be quantitatively measured through the INS mapping of $S(\boldsymbol{Q}, E)$ volumes, providing direct insights into the behavior of phonon eigenvectors, and also show how first-principles simulations including anharmonic effects can reproduce and rationalize such anharmonic effects. These findings are also valuable to understand other quantum ferroelectric/paraelectric perovskite materials such as $KTaO_3$ and related ferroelectricity and quantum effects [2, 3].

1. Yamada, Yasusada, and Gen Shirane. "Neutron scattering and nature of the soft optical phonon in $SrTiO_3$." Journal of the Physical Society of Japan 26.2 (1969): 396-403.

2. Rowley, S. E., et al. "Ferroelectric quantum criticality." Nature Physics 10.5 (2014): 367.

3. Taniguchi, Hiroki, Mitsuru Itoh, and Toshirou Yagi. "Ideal soft mode-type quantum phase transition and phase coexistence at quantum critical point in O^{18} -exchanged $SrTiO_3$." Physical Review Letters 99.1 (2007): 017602.

Mosaic of Frustrated Magnets

Xiaojian Bai[1], Zhiling Dun[1], Joseph A.M. Paddison[1,2], Martin Mourigal[1]

[1]School of Physics, Georgia Institute of Technology
[2] Churchill College, University of Cambridge

Magnetism is a frontier of the basic science and constant source of technological innovation. One of fundamental scientific quests is to understand the novel phases of matter realized in magnetic materials at low temperatures. Microscopic competing interactions due to underconstrained geometry can greatly facilitate the formation of new quantum phases. The materials with such characteristic are dubbed frustrated magnets. Typical frustrated geometries include *pyrochlore lattice*[1], *kagome lattice*[2] *and triangular lattice*. We present in-depth studies on three materials hosting magnetic lattices with these geometries and demonstrate a rich physical landscape of interesting phenomena from resolution of cluster loop scattering (Fig. 1a and 1b) to emergent charge ordering (Fig. 1c and 1d). The primary experimental tool that we use to probe these systems is neutron scattering. Neutron carries magnetic moment and can scatter off target materials through magnetic interactions. The scattering can be either elastic or inelastic, capable of probing both static spin structure and excitations in materials. With modern time-of-flight instruments at Oakridge national lab, we are able to map out the entire 4-dimensional dynamical magnetic response of the materials. Theoretical modelling is crucial to unpack the enormous amount of information in the data and form an intuitive understanding of the physics. Our works add new discoveries and scientific advance to the old realm of magnetism.

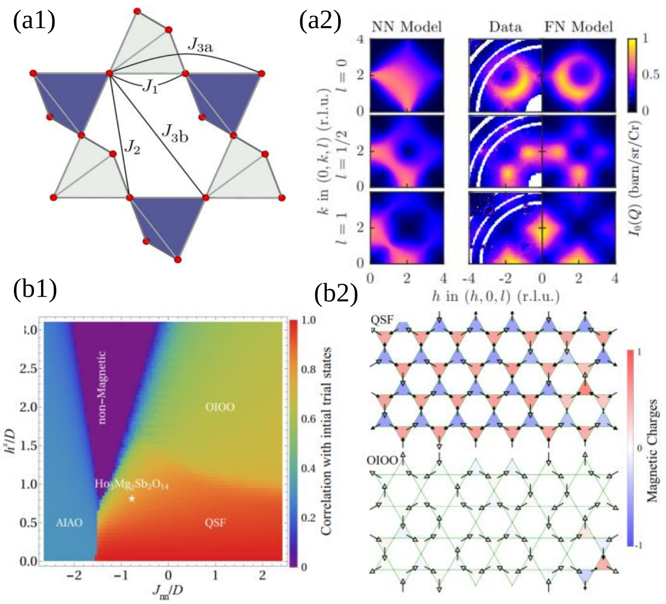

Figure 1: (a1) The pyrochlore lattice of Cr^{3+} ions (red spheres) in $MgCr_2O_4$ and definition of exchange interactions up to third neighbors. (a2) Selected slices across the instantaneous structure factor for constant momentum transfer along the (0, 0, l) and comparison between NN and FN models. (b1) Mean-field phase diagram of Kagome ice system with transverse field and long-range dipolar interactions. (b2) Spin configurations in the quantum spin fragmented phase (QSF) and the one-in-one-out phase (OIOO). The color indicates the effective magnetic charges defined as the sum of the spins on each triangle.

1. Bai, Xiaojian, et al. "Magnetic Excitations of the Classical Spin Liquid MgCr2O4." *Physical Review Letters* 122.9 (2019): 097201.
2. Dun, Zhiling, et al. "Quantum Spin Fragmentation in Kagome Ice Ho3Mg2Sb3O14." arXiv preprint arXiv:1806.04081 (2018).

Lattice dynamics across the temperature- or pressure-induced structural phase transition in SnSe and SnS

Tyson Lanigan, Jennifer Niedziela, Shan Yang, Dipanshu Bansal, Andrew May, Tao Hong,
Daniel Pajerowski, Georg Ehlers, Olivier Delaire
Duke University
Oak Ridge National Laboratory

SnSe and SnS are two promising thermoelectric materials, which have demonstrated outstanding figure-of-merits, but whose transport properties exhibit strong anisotropies tied to their layered crystal structure. At high temperature or high pressure, they undergo a continuous structural phase transition between a low-symmetry Pnma phase and a higher-symmetry Cmcm phase (SnSe: Tc ~ 805K and Pc ~10GPa, SnS: Tc~880K). In order to rationalize the strong anharmonicity and anisotropy in thermal conductivity, we have used time-of-flight (TOF) and triple-axis inelastic neutron scattering (INS) to map the phonon dispersions and density of states (DOS) of both compounds at high temperature across the phase transition. Our results show a striking, extended softening and broadening of phonon excitations with temperature and the soft mode character of this transition is clearly revealed. We extracted the phonon scattering rates by deconvoluting instrumental resolution effects, for both time-of-flight and triple-axis measurements. Scattering rates calculated from the two methods agree remarkably well. We performed systematic first-principles simulations of the temperature-dependent phonon dynamical structure factor, $S(\mathbf{Q},E)$, and scattering rates, which we compare with our experimental results. Furthermore, we have used TOF neutron diffraction, inelastic X-ray scattering and Raman spectroscopy to track the transition as a function of pressure finding good agreement with the previously reported transition pressure of ~10GPa. The projected DOS is tracked with pressure in order to follow the anisotropy of the lattice dynamics with pressure. We contrast some of the behaviors observed in our measurements and simulations with rocksalt chalcogenides (SnTe, PbTe, PbSe).

Funding from US-DOE/BES/MSED, Office of Science Early-Career-Award, and as part of the S3TEC-EFRC.

Interaction of Zinc Oxide Nanoparticles with Water

Takat B. Rawal,[1,2] Ali Ozcan,[6,8] Shih-Hsein Liu,[2,3] Sai Venkatesh Pingali,[4] Oguz Akbilgic,[5] Laurene Tetard,[6,7] Hugh O'Neill,[4] Swadeshmukul Santra,[6,8,9] Loukas Petridis[1,2*]

[1]Department of Biochemistry and Cellular and Molecular Biology, University of Tennessee, Knoxville, TN, 37996

[2]UT/ORNL Center for Molecular Biophysics, Oak Ridge National Laboratory, Oak Ridge, TN, 37830

[3]Center for Renewable Carbon, University of Tennessee, Knoxville, TN, 37996

[4]Neutron Scattering Division, Oak Ridge National Laboratory, Oak Ridge, TN, 37830

[5]University of Tennessee Health Science Center-Oak Ridge National Laboratory Center for Biomedical Informatics, Memphis, TN, 38163

[6]Nanoscience Technology Center, University of Central Florida, Orlando, FL, 32826

[7]Department of Physics, University of Central Florida, Orlando, FL, 32816

[8]Department of Chemistry, University of Central Florida, Orlando, FL, 32816

[9]Department of Materials Science and Engineering and Burnett School of Biomedical Sciences, University of Central Florida, Orlando, FL, 32816

ABSTRACT

Novel technological applications in catalysis and bactericidal formulation have emerged for zinc oxide (ZnO) nanoparticles owing to their ability to generate reactive oxygen species by fostering H_2O dissociation. Rational improvement of those properties requires a mechanistic understanding of ZnO nanoparticle reactivity, which is currently lacking. Here, we study the structural and electronic properties of nanometer-sized ZnO, determine the binding energetics of H_2O adsorption and compare to an extended macroscopic surface. We show that the electronic density of states of ZnO nanoparticles is size-dependent, exhibiting a decreasing bandgap with the increase of nanoparticle diameter. The electronic states near the Fermi energy dominantly arise from O 2p states, which are spatially localized on "reactive" surface O atoms on the nanoparticle edges. The "reactive" O atoms are doubly coordinated, whereas most other surface O atoms are three-coordinated and bulk O atoms are four-coordinated. The lower coordination induces a spontaneous dissociation of H_2O at the nanoparticle surface edges. The surface Zn and O atoms have inhomogeneous electronic and geometrical/topological properties, thus providing non-equivalent sites for molecular and dissociative H_2O adsorption. The binding energy of H_2O to the nanoparticle is found to be site-dependent and correlated with the Bader charge of surface Zn atom. The free energy of H_2O binding is dominated by the electronic DFT interaction energy. Entropy is found to stabilize the unbound form, because the increase in vibrational contribution is greater than the decrease in translational and rotational contribution, whereas solvation stabilizes the unbound state. The absence of rough edges and "reactive" sites on the extended macroscopic ZnO surface prevents spontaneous dissociation of single H_2O molecule. This study underlies the importance of coupling geometrical and electronic properties for determining the reactivity of nanoparticles and provides a simple elucidation of the superior catalytic activity of ZnO nanoparticles compared to ZnO in macroscopic forms. In addition, our approach of employing small-angle neutron scattering and first-principles simulations of anti-microbial ZnO nanoparticles in the present study provides an illustration of integrating experimental and theoretical techniques to unravel the structures of ZnO nanoparticles and their interaction with H_2O.

Accessing ligand-induced dynamics in maltose binding proteins using neutron scattering and computational methods

Shantanu Shukla[*¥], Laura Stingaciu[¥], Jose Borreguero Calvo[¥], Christopher Stanley[§], Matthew Cuneo[£], Dean Myles[¥]

[*]Graduate Program in Genome Sciences and Technology, University of Tennessee, Knoxville, TN; [¥]Neutron Science Directorate, Oak Ridge National Laboratory, Oak Ridge, TN; [§]Computing and Computational Science Directorate, Oak Ridge National Laboratory, Oak Ridge, TN; [£]Department of Structural Biology, Saint Jude Children's Hospital, Memphis, TN

ATP-dependent transport is energetically expensive, and its evolutionary cost likely shapes the specificity and affinity profiles of ABC transporter systems, especially of their periplasmic binding proteins (PBPs). PBPs have a conserved αβ-fold in which two hinged globular domains provide a binding pocket that undergoes large ligand induced conformational changes. To characterize differential ligand binding in structurally related isoforms, we determined the atomistic structures of three maltose binding protein (MBP) isoforms from *Thermotoga maritima* (tmMBP1, tmMBP2 and tmMBP3) using X-ray crystallography. We then used small-angle X-ray scattering to quantify the conformational ensembles sampled by the three isoforms in solution, both in the presence and absence of their cognate ligands. The scattering data was fitted against the trajectories generated by computational molecular dynamics (MD) simulations. These studies show that the three MBP isoforms exhibit a strong size-selective preference for substrates, with tmMBP1 and tmMBP2 binding tri- and tetra-saccharides and tmMBP3 binding only the disaccharide. In addition, the MD simulations revealed motions in surface loops remote from the binding pocket that were suppressed upon substrate binding, suggesting possible correlated motions and/or conformational substates that may help regulate substrate binding. We have used neutron spin echo spectroscopy and small angle neutron scattering to examine the total internal dynamics of these proteins, independent of either diffusion or tumbling motions in solution. We will present our results and discuss how this may help decipher possible allosteric control of the ABC transporters by the associated PBPs.

Thermo-Mechanical Fatigue of Additively Manufactured Ti-6Al-4V

Sabina Kumar, Rakesh Kamath, Suresh Babu, Chen Yan
University of Tennessee, Knoxville; Manufacturing Demonstration Facility, ORNL; SNS, ORNL

Metal Additive Manufacturing (AM) is a complex technology wherein a part is fabricated by the layer by layer deposition of metal powders with a heat source. Research in Metal AM has shown that steady state conditions assumed during traditional manufacturing cannot be necessarily assumed in AM, because of the rapid changes in energy deposition during the build. For instance, the area which has a shorter scan path will have a shallow temperature distribution across the scanned area, thereby, the thermal gradients at those regions will be low. Whereas the areas that have a longer scan path, will have a vast temperature distribution across the scanned area thereby having larger thermal gradients. If we magnify one voxel of the transient temperature distribution of an Inconel 718 build, we can notice that the interface stabilities of the two phases are dictated by both the thermal and mechanical gradients. Therefore, it is evident that in AM, these macro scale gradients can modify sub-micron level thermo-mechanical gradients.

To further understand the role of these thermo-mechanical gradients on an AM part, we use the Gleeble Thermo-Mechanical Simulator to conduct experiments, in which we can apply a temperature and mechanical loads simultaneously. We chose Ti-6Al-4V for our study as this is a commonly used alloy in Metal AM. Preliminary thermo-mechanical fatigue (TMF) testing showed a softening behavior, with the softening more significant on the compressive side. In order to see for any phase transformations that could have occurred on thermo-mechanical fatiguing, we exploit the benefits of the neutron beam.

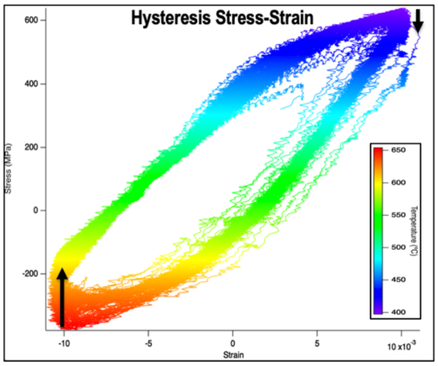

Ti-6Al-4V is a two-phase alloy with an HCP α phase and a BCC β phase. At room temperature Ti-6Al-4V has about 90 – 95 % α phase. We hypothesized that on thermo-mechanical cycling we will have a phase transformation. For a preliminary test, we placed a thermo-mechanically fatigued sample in the path of the beam. In Ti-6Al-4V, the [110] β peak is a peak that almost always clings onto the [101] α peak. At the end of TMF, we do notice a very prominent [110] β peak stand out. On further peak analysis using the Reitveld Refinement method, we find that the beta phase fraction increases on thermo-mechanical cycling. To further study this behavior, we did in-situ thermo-mechanical tests at the VULCAN beamline that is equipped with the MTS load frame. With minor alterations to the experimental setup, we were able to apply thermal and mechanical loads simultaneously with the beam on. We notice two interesting things. AM builds are highly textured because of the way they are fabricated. On TMF, we do notice a texture change at the end of the cycling. With respect to the phase transformation, we do see an increase in the β phase fraction from Bank 2, with an increase in lattice parameter, whereas the Bank 1 remains constant. Therefore, this experiment gives us an insight on the interface stability of the two-phase alloy on thermo-mechanical cyclic loading conditions.

		Experimental Alpha Phase Fraction	Alpha Lattice Parameter (Å)	Experimental Beta Phase Fraction	Beta Lattice Parameter (Å)	χ^2 (Goodness of fit)
Bank 1	*Initial d_0*	**94.6 %**	a_0 = 2.92, c = 4.66 c/a = 1.595	**5.39 %**	a_0 = 3.19	2.546
	After 70 cycles	**94.5 %**	a_0 = 2.95, c = 4.73 c/a = 1.603	**5.43 %**	a_0 = 3.23	4.136
Bank 2	*Initial d_0*	**97.3 %**	a_0 = 2.92, c = 4.66 c/a = 1.595	**2.65 %** ↑	a_0 = 3.19	1.833
	After 70 cycles	**93.47 %** ↓	a_0 = 2.93, c = 4.66 c/a = 1.590	**6.1 %**	a_0 = 3.21	2.342

Nanocarbon Dimensionality Controls Mesoscopic Structure of an All-Aromatic Polyetherimide

Ryan J. Fox[1], Maruti Hegde[1], William T. Heller[3], Amar S. Kumbhar[1,2], Daniel P. Cole[4], Theo J. Dingemans[1]

[1]Department of Applied Physical Sciences and [2]Chapel Hill Analytical and Nanofabrication Laboratory, University of North Carolina at Chapel Hill, 121 South Road, Chapel Hill, NC 27599-3050, USA.
[3]Neutron Scattering Division, Oak Ridge National Laboratory, Oak Ridge, 37831, Tennessee, USA
[4]U.S Army Research Laboratory, Aberdeen Proving Ground, MD, 21005, USA

Nanocarbons, i.e. fullerene (C60), nanotubes, and graphene, are known to induce crystallization in polymers, which can increase the polymer stiffness and improve the thermo-mechanical performance. Here, we elucidate the influence of nanocarbon dimensionality on the thermo-mechanical properties by preparing nanocomposites from 0-D (C60) and 1-D (single walled carbon nanotubes, SWCNTs) with an amorphous high-performance polyetherimide (ODPA-P3). Nanocomposites containing either C60 or SWCNT induced crystallization of ODPA-P3, but only SWCNTs improve the thermomechanical performance. Through optical, electron, and atomic force microscopy, wide- and small-angle X-ray scattering (W/SAXS), and small-angle neutron scattering (SANS), we show that the mesoscopic crystalline structure and orientation of the polymer is controlled by the nanocarbon dimensionality. We find that SWCNTs template the formation of highly anisotropic and in-plane aligned crystalline ODPA-P3, while C60 induces pseudo-homeotropic alignment of spherulitic crystal domains. Through time-resolved SANS, we investigate the kinetics of polymer crystallization during in-situ imidization and conclude that interfacial solvent is key in nanocarbon-induced crystallization. Our results show that anisotropic nanocarbons modulate the mesoscopic polymer structure in a way that is key for improvement of the thermo-mechanical performance of polymers.

In situ tracking of the cyclic deformation behavior of a high-entropy alloy

Rui Feng[1], Xie Xie[1], Dunji Yu[2], Yan Chen[2], Ke An[2], Tamas Ungar[3, 4], and Peter. K. Liaw[1]

[1] Department of Materials Science and Engineering, The University of Tennessee, Knoxville, TN 37996, USA;
[2] Neutron Scattering Division, Oak Ridge National Laboratory, Oak Ridge, TN 37831, USA;
[3] Department of Materials Physics, Eötvös University Budapest, PO Box 32, H-1518, Hungary;
[4] School of Materials, The University of Manchester, M13 9PL, UK.

Abstract

Recently, high-entropy alloys (HEAs) attract worldwide attention due to their outstanding properties, showing a huge potential as engineering structural materials. In practical engineering applications, materials are usually subjected to cyclic loading during service, leading to fatigue fracture. However, few low-cycle fatigue (LCF) studies have been reported on HEAs so far. In this study, the LCF behavior of a multiphase HEA, are systematically studied by integrated experiments and fatigue-life prediction models. Real-time in-situ neutron diffraction was employed to dynamically monitor the cyclic deformation behavior of this HEA (Fig. 1). Advanced microcopy techniques, such as transmission-electron microscopy (TEM), electron-backscattered diffraction (EBSD), and scanning-electron microscopy (SEM), were used to characterize the microstructural evolution during LCF. The in situ tracking of the cyclic deformation behavior of this HEA will pave the way to design innovative HEAs with outstanding fatigue resistance.

Acknowledgement: We appreciate the support of the U.S. Army Research Office project (W911NF-13-1-0438) and National Science Foundation (DMR-1611180) with the program directors, Drs. M. P. Bakas, S. N. Mathaudhu, D. M. Stepp, G. Shiflet, and D. Farkas.

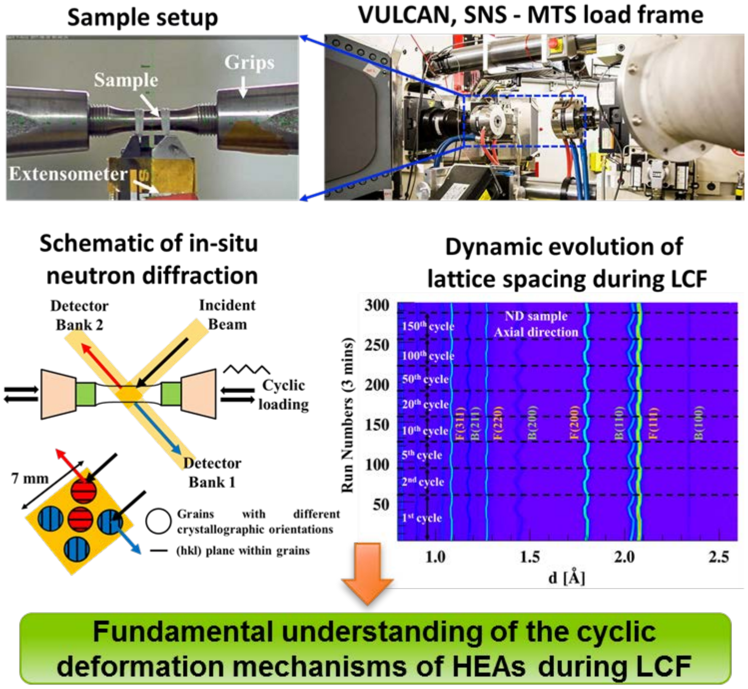

Fig. 1 Schematic of in-situ neutron-diffraction study of the LCF behavior of HEAs.

In-situ Mechanical Neutron Diffraction Loading Characteristics of GRCop-84 Fabricated by SLM

R. Minneci, C. Rawn, D. Ellis, Z. Jones, J. Bunn, K. An, Y. Chen,

University of Tennessee, Knoxville, NASA GRC, NASA MSFC, Oak Ridge National Laboratory

GRCop-84 or Cu-8 Cr-4 Nb At% is an alloy developed by NASA in the 80's that has seen a renewed interest due largely to new fabrication techniques. This alloy consists primarily of two phases of relatively pure Cu matrix and fine intermetallic dispersion of a mechanically and thermodynamically stable intermetallic Cr_2Nb (cubic Laves phase C15) that improves the mechanical stability at high (700 – 900 K) temperatures while preserving most of its thermal conductivity[1]. GRCop-84 has some of the best available properties, but its high cost has limited its practical application in industry. However, it has shown potential with additive manufacturing (AM) where it can be produced significantly faster, more inexpensively, with better than or equal to properties, and significantly improved geometry control compared to traditionally fabricated, wrought hardware[2]. However before AM parts can be used in service they must go through thorough evaluation due to AM's intrinsic porosity, thermal residual stresses, and reproducibility concerns.

Previously, we have conducted a series of neutron residual stress measurements on bulk powder bed selective laser melted (SLM) samples fabricated by NASA Marshall Space Flight Center on HFIR's HB-2B beamline using Cu's 311 peak to help characterize thermal residual strain under various conditions. However, various unknowns have limited the analysis to qualitative results when more quantitative are desired. GRCop-84 has various unknowns such as an accurate elastic modulus and Poisson's ratio for calculating stress from planar strain accurately and general understanding of phase and planar stress partitioning. If strain is not distributed evenly between planes or is not distributed as predicted between the phases, then our assessments on a single Cu peak will be limited. Furthermore better understanding dislocation density, texture, preferred orientation, phase-specific load sharing, and evolution of lattice strain supports both previous diffraction experiments and further development of the alloy. In order to address these concerns, an in-situ mechanical test was devised to leverage the MTS load frame, time-of-flight diffraction, and axial and transverse detector banks of SNS's VULCAN beamline.

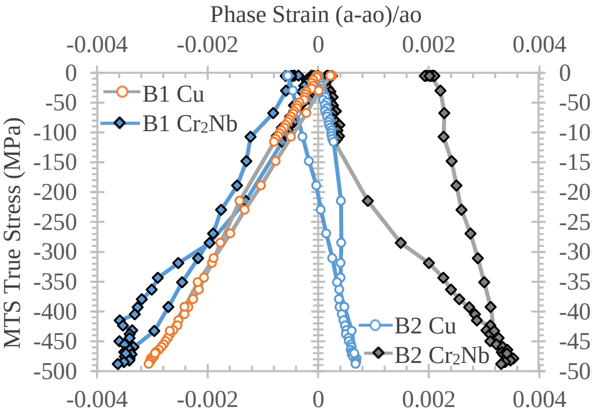

Figure 1 – Calculated phase strain of Cu and Cr_2Nb in 'xy' HIP sample for both B1 (axial) and B2 (transverse) directions.

The in-situ mechanical experiments were conducted with SLM samples (from the same batch as those measured on HB-2B) of GRCop-84 on VULCAN with compression samples. Compression samples were electron discharge machined (EDM) from large 20 mm cubes into 8 mm diameter compression cylinders. The cylinders were machined parallel and perpendicular to the build direction ('z' and 'xy', respectively) and were in an as-built (directly removed from the build plate after AM) or HIPed condition. The samples were compressed to roughly 10% strain and slowly relieved to measure the elastic modulus in unloading as the elastic loading region was not linear. Cu's (111), (200), (220), (311), and (222) diffraction peaks and Cr_2Nb's (333), (422), and (440) peaks were designated for analysis. The phase strain has been measured, shown in Fig. 1, from lattice parameters calculated by sequential Rietveld refinements, the individual lattice strains have been measured, the intergranular strain generated in loading has been measured, and the phases' Poisson ratios, preferred orientation, and texture have been approximated for the samples measured.

1. Anderson, K.R., et al., *Microstructural evolution and thermal stability of precipitation-strengthened Cu 8Cr 4Nb alloy.* Materials Science and Engineering: A, 1993. **169**(1-2): p. 167-175.
2. Gradl, P.R., et al. *Development and Hot-fire Testing of Additively Manufactured Copper Combustion Chambers for Liquid Rocket Engine Applications*. in *53rd AIAA/SAE/ASEE Joint Propulsion Conference*. 2017.

Structural insights into low and high recalcitrant natural poplars with neutron and X-ray scattering:

Authors: Riddhi Shah1,2; Samarthya Bhagia2; Sai Venkatesh Pingali2; Arthur Ragauskas1,2; Brian Davison1,2 and Hugh O'Neill1,2

1 Bredesen Center for Interdisciplinary Research, University of Tennessee, Knoxville 2 Oak Ridge National Laboratory

Structural changes leading to biomass recalcitrance is crucial to study for the future development of biofuels and bioproducts. A genome wide association study identified two naturally occurring poplars, BESC-316 and GW-11012, that had 22% and 18% lignin content, respectively. The lower lignin content genotype showed greater sugar release before and after hot water pretreatment compared to the lower lignin counterpart. We used small-angle neutron scattering (SANS) and wide-angle x-ray scattering (WAXS) to investigate the structural changes in the BESC-316 and GW-11012 genotypes that were subjected to hot water pretreatment (160˚C 70min, 180˚C 18min and 180˚C 45min) to obtain information about cellulose microfibril organization, the lignin and hemicellulose network, and overall morphology of the plant cell walls. Both poplars were cut longitudinally in a similar growth ring region and wood chips of size 1cm x 1cm x 1mm were made. Cellulose microfibril arrangement in GW-11012 is consistent with aggregated microfibrils and differed significantly from the well-ordered cellulose microfibrils in BESC-316 before pretreatment (Figure 1). Post-pretreatment, little change was seen in cellulose arrangement for GW-11012 whereas BESC-316 showed aggregation of microfibrils. SANS showed that GW-11012 had increased scattering intensity in the mid Q region compared to BESC-316 which may be due to pores. After pretreatment, both genotypes have very similar scattering patterns indicative of similar structural changes occurring in the pretreated cell walls. Cellulose accessibility measured using the modified Simons' stain before and post pretreatment was similar for GW-11012 and BESC-316. No significant difference in the amount of 5-hydroxymethyl furfural, furfural and acetic acid for BESC-316 and GW-11012 was observed in the pretreatment liquor. We will discuss differences in sugar release of the native and pretreated BESC-316 and GW-11012 due to the variations in the cellulose microfibril arrangement, fibrillar orientation, porosity, and lignin content.

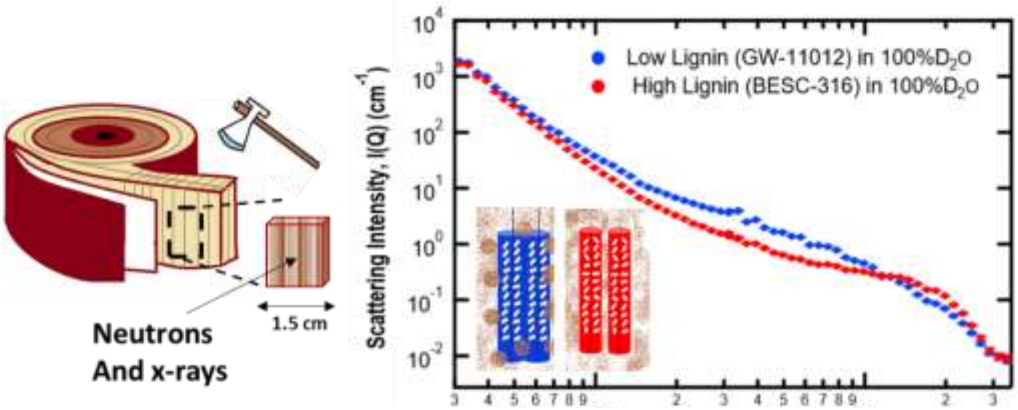

Figure 1 Both poplars used in this study were 4 years old and wood sections were cut from the outer most growth ring in a longitudinal manner in order to not disrupt the cellulose microfibrillar arrangement. The small angle neutron scattering curves were obtained by azimuthally averaging the 2D scattering pattern. The red curve is for high lignin containing poplar while the blue curve is for low lignin containing poplar. Schematic (insertion in the I(Q) vs Q plot) shows the interpretation of the SANS curves

Pressure-induced quantum phase transition in an S=1/2 quantum antiferromagnet $C_9D_{18}N_2CuBr_4$

Qing Huang[1] and Tao Hong[2]
1. Department of Physics and Astronomy, University of Tennessee
2. Neutron Scattering Division, Oak Ridge National Laboratory

Quantum phase transitions [1] are a novel type of phase transition, manifesting changes of the entire system from one quantum state to another in the extreme quantum limit at T=0 K. In actual experiments, the control parameter can be chemical doping, or external magnetic field or hydrostatic pressure, etc. While the quantum critical point (QCP) exists at T=0 K, the so-called quantum critical regime where the behavior of the system is strongly influenced by the critical point extends outward to finite temperatures. Understanding quantum phase transitions holds the promise of the description of the universal aspects of critical states where the physical properties can be described by a set of critical exponents and scaling functions depending only on the symmetry and dimensionality but not on the microscopic details of the Hamiltonian.

An S=1/2 organic-metallic compound bis(cyclopentylammonium)tetrabromocuprate(II) ($C_9D_{18}N_2CuBr_4$, DLCB for short) has been revealed recently [2]. Based on the view of the crystal structure (Fig. 1a), it is suggested to be a coupled two-leg spin ladder. The specific heat measurement at ambient pressure shows a sharp anomaly at T_N~2.0 K, suggesting that the inter-ladder coupling is sufficiently strong to drive the system to the long-range magnetically ordered phase [3]. The magnetic order wavevector was found as (1/2 1/2 1/2) from the neutron diffraction measurements with a reduced moment size ~0.4 μ_B. Importantly, the analysis of the spin Hamiltonian suggests that DLCB is close to the QCP in two dimensions at ambient pressure [3].

We carried out a single-crystal neutron diffraction study about the effect of the hydrostatic pressure on the magnetic order in DLCB using the cold-neutron triple-axis spectrometer (CTAX), HFIR. We find that the scattering intensity of the magnetic Bragg peak at **q**= (1/2 1/2 -1/2) becomes continuously diminished with the increase of pressure (Fig. 1b). At and above a critical pressure P_c~1.0 GPa, there is no evidence of magnetic Bragg peak at least down to 0.3 K. The determined pressure dependence of the staggered moment size and ordering temperature is summarized in Fig. 1c, indicative of a quantum phase transition at P_c. Therefore, it provides us great opportunities for a test of the predicted quantum critical scaling [4] and study of fractional excitations at the deconfined QCP by means of inelastic neutron scattering [5].

[1] S. Sachdev, Quantum Phase Transition, Cambridge University Press (1999).
[2] F. Awwadi *et al.*, Inorg. Chem. **47**, 9327 (2008).
[3] T. Hong *et al.*, Phys. Rev. B 89, 174432 (2014) and Nat. Phys. **13**, 638 (2017).
[4] S. Sachdev, T. Senthil and R. Shankar, Phys. Rev. B **50**, 258 (1994).
[5] T. Senthil *et al.*, Science 303, 1490 (2004); Phys. Rev. B **70**, 144407 (2004).

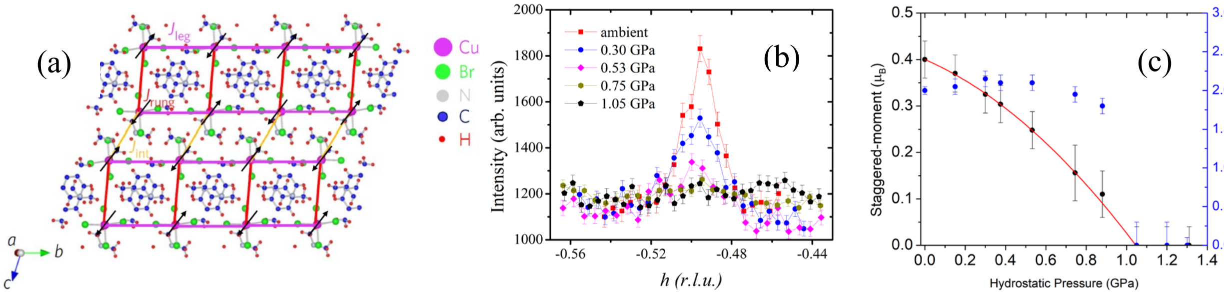

Figure 1: (a) The crystal and magnetic structure of DLCB at ambient pressure. (b) The typical θ/2θ scans at different pressures and T=0.3 K. (c) The measured pressure dependence of the ordered moment size and ordering temperature.

Crystallographic texture measurement at Oak Ridge National Laboratory

Nathan Peterson[1], Chris Fancher[2], Jeff Bunn[2], Andrew Payzant[2], Sean Agnew[1]
[1]University of Virginia, [2]Oak Ridge National Laboratory

Nearly all single crystals are anisotropic, where the properties depend on the crystallographic direction. According to Neumann's principle, the point group of the crystal determines the minimum symmetry present in a given physical property (e.g. stiffness tensor). Thus, both the symmetry and the orientation of the single crystal dictate the anisotropy of the crystal. Most engineering materials are polycrystalline and exhibit preferred crystallographic orientations, and as such their properties can be anisotropic as well. The type and degree of anisotropy depends upon the intrinsic anisotropy of the single crystal and the strength of the preferred orientation. The complete description of the preferred orientation is often referred to as "texture" and is quantified as an orientation distribution (OD), which represents the probability of finding a given orientation in a given volume. Thus, having the ability to characterize the OD, in polycrystalline materials is crucial for process and component design engineers, for a wide variety of use cases, ranging from structural to functional materials.

Due to the unfortunate demise of the general user program at the Lujan Center at Los Alamos National Laboratory, access to the **HI**gh **P**ressure **P**referred **O**rientation beamline is no longer an option for users wishing to readily measure and analyze the crystallographic texture of their samples. This gap in capability leaves an opportunity for growth at both the Spallation Neutron Source (SNS) and High Flux Isotope Reactor (HFIR) at ORNL. Due to the wide variety of sample environments and instrument configurations, no one instrument is suitable for all situations, however many situations could be accommodated with multiple instruments. The instruments highlighted will be: TOPAZ, VULCAN, NOMAD and POWGEN at SNS, and WAND and NRSF2 at HFIR. Specific attention will be drawn to the experimental requirements for measuring crystallographic texture at the various instruments.

Photoexcitation Tunable Magnetization at Hybrid Perovskite/ Ferromagnet Interface

Miaosheng Wang[a], Hengxing Xu[a], Valeria Lauter[b,*], Bin Hu[a,*]

[a] Department of Materials Science and Engineering, University of Tennessee, Knoxville, Tennessee 37996, United States

[b] Neutron Scattering Division, Neutron Sciences Directorate, Oak Ridge National Laboratory, Oak Ridge, Tennessee 37831, United States

Hybrid lead halide perovskites are emerging semiconductors which have demonstrated extraordinary performance on photovoltaic and light-emitting devices. Meanwhile, the potential of perovskites for spin-related optoelectronics has just begun to raise up due to the strong spin-orbital coupling (SOC) for efficient spin manipulation by using optical methods and relatively long spin coherence lifetime for spin-related optoelectronic properties to occur. [1] However, traditional investigations on spintronic devices based on semiconductor/ferromagnet heterojunctions mainly focus on the spin injection and spin transport. The understanding of the magnetism properties at the perovskite/ferromagnet interface remains unclear. Our recent studies have found the intrinsic magneto-electric coupling at hybrid perovskite and ferromagnetic Cobalt interface based on magneto-dielectric measurements. Specifically, we experimentally demonstrated that the spin on ferromagnetic Co surface can effectively interact with the electrical polarization from asymmetric orbitals on the perovskite surface and consequently generate a magneto-dielectric phenomenon at room temperature. [2] Here, we discuss our recent progress on exploring magnetism properties at semiconducting hybrid perovskite/ferromagnetic Co interface by using Magnetism Reflectometer with *laser* photoexcitation at BL-4A in SNS, ORNL.

---

[1] J. Wang, D. Sun*, Z. Vardeny*, *Nat. Commun.* **10**, 129 (2019).

[2] M. Li, B. Hu*, *Adv. Mater.* **29** (2016).

Revisiting St. Venant’s Principles

Mehmet Haza Seren, Columbia University

Saint Venant’s principle enables engineers to replace complex stress distributions in materials with the ones that are easier to understand and solve. The principle is named after Adhémar Jean Claude Barré de Saint-Venant, a French mechanician and mathematician who published it in 1855 without any mathematical proof. It states that the difference between the effects of two different, but statically equivalent loads becomes very small at sufficiently large distances from the load. A more common definition asserts that the effect of edges, stress concentrators and inhomogeneities become negligible at distances two to four characteristic lengths or more from these features. This informal statement is well known among structural and mechanical engineers and is widely used in practice. Since it was generalized from experience and it was accepted as purely empirical, there are many recent articles using applied mathematics to define its theoretical foundation. Most of these articles do not agree with each other and yield different characteristic lengths.

In our research, we investigated the application of St. Venant’s principle to quasi-homogeneous composite solids consisting of homogeneous phases. We used both analytical and numerical approaches to describe the characteristic length in such systems and compared our results with previous work. We found that four characteristic lengths are sufficient to eliminate stress disturbances. Beyond this length the material is stress-free. We are now using St. Venant’s principle to compute optimal probe sizes for x-ray and neutron diffraction experiments. In such systems.

Mehmet Hazar Seren
Columbia University

SANS as a tool to study the effects of solvent polarity on assembly of ionic block polymers in solutions

Manjula Senanayake[1], Supun Samindra[1], Lilin He[2], Dvora Perahia[1]

[1]Department of Chemistry, Clemson University, Clemson, SC, 29631

[2]HFIR, Oak Ridge National Laboratory, Oak Ridge, TN, 37831

Ionic block copolymers find broad uses in transport-controlled applications such as drug delivery, clean energy and separation science. Ion transport capability of ionic segment is the key which opens the door for their use in those applications. Polymers in this class have a relatively higher glass transition temperature (Tg), therefore, polymer solutions are often used for processing. Tuning ionic clusters formed in solutions that can propagate into membranes offers a path to tailor performance. Here, micellar structures of a symmetric ABCBA co-polymer, where C is a randomly sulfonated polystyrene, B is hydrogenated polyisoprene, and A is poly (t-butyl styrene), resolved by SANS. The polarity of the solvent is changed by adding propanol ($f_{\text{pro}} = 0.1$ to 1) to cyclohexane. Core-shell aggregates dominate the solutions of the pure solvents with the ionic blocks residing in the core of the micelle. The packing of the ionizable segments is significantly tighter in a hydrophobic environment than in a hydrophilic one. The corona however is more compact in the hydrophilic environment. A transitional region is observed as the fully miscible solvents are mixed with elongated structures dominating the solution.

Superionic diffusion and anharmonic lattice dynamics in $AgCrSe_2$

J. Ding,[1] J. L. Niedziela,[2] D. Bansal,[3] A. F. May[2], G. Ehlers[2], D. Abernathy[2], Y. Ren[4], A. Alatas[4], A. Said[4], and O. Delaire[1,5]

[1] Department of Mechanical Engineering and Materials Science, Duke University, Durham, North Carolina 27708, USA

[2] Oak Ridge National Laboratory, Oak Ridge, TN 37830, USA

[3] Department of Mechanical Engineering, Indian Institute of Technology Bombay, Mumbai, Maharashtra 400076, India

[4] Advanced Photon Source, Argonne National Laboratory, Argonne IL 60439, USA

[5] Department of Physics, Duke University, Durham, North Carolina 27708, USA

Superionic conductors exhibit promising thermoelectric properties due to their ultralow thermal conductivity. By analogy with the liquid state, in which shear modes vanish, it was previously proposed that the transverse acoustic (TA) phonons would break down in the superionic phase[1]. In contrast, our study shows the TA modes persist in the superionic phase, but they are strongly scattered by both anharmonicity and disorder on the Ag sublattice, especially at shorter wavelengths.[2] We report on neutron/x-ray scattering and first-principles studies of the lattice dynamics and ionic diffusion of $AgCrSe_2$. A low frequency mode around 3.5 meV dramatically broadens and softens across the superionic transition, as observed in the phonon density of states from neutron powder scattering. We show how this mode is related to the stochastic diffusion of Ag atoms occurring in the superionic state, which is probed via quasi-elastic neutron scattering. At low temperature in the normal state, the Ag atoms are weakly bonded with Cr-Se layer but still undergo phonon-like large-amplitude anharmonic in-plane vibrations. In the superionic phase at high temperature, our momentum-resolved inelastic x-ray scattering measurements on single-crystals clearly establish the persistence of long-wavelength TA phonons, whereas the shorter wavelength, non-dispersive portions of the TA branches severely broaden reflecting a breakdown of these quasiparticles. Further, we observe the diffusion of Ag atoms in *ab initio* molecular dynamics and a strong repulsion between Ag neighbors, affecting the diffusion mechanism. Pair distribution functions from x-ray measurements and simulations also agree pretty well. Our studies of atomic dynamics and diffusion help rationalize the emergence of ultralow thermal conductivity for thermoelectrics and will facilitate the design of high-performance solid-state electrolytes.

INS/IXS measurements supported by the S3TEC EFRC, DOE BES Award #DESC0001299. First-principles modeling supported by the US DOE BES Early Career Award #DESC0016166. Sample synthesis supported by the US DOE BES, Materials Sciences and Engineering Division.

1. Li, B., et al. "Liquid-like thermal conduction in intercalated layered crystalline solids." *Nature materials* 17.3: 226 (2018).
2. Niedziela, J. L., et al. "Selective breakdown of phonon quasiparticles across superionic transition in CuCrSe2." *Nature Physics* 15.1: 73 (2019).

Neutron Scattering and Microscopy Studies of Water Near Hydrophilic CuO Nanostructures

J. Torres[1], Z. N. Buck[1], H. Kaiser[1], X. He[1], T. White[1], R. A. Winholtz[1], K. W. Herwig[2], M. Kidder[2], E. Mamontov[2], L. Daemen[2], H. Bilheux[2], M. Tyagi[3], F. Y. Hansen[4], and H. Taub[1].

[1]University of Missouri (MU) and Research Reactor (MURR), [2]Oak Ridge National Laboratory,
[3]National Institute of Standards and Technology, [4]Technical University of Denmark

Oscillating heat pipes (OHPs) offer a promising heat transfer device for a variety of applications, including the cooling of electronic devices. Recently, it has been shown that the performance of a copper-OHP operating with water as the working fluid can be enhanced by coating its internal surface with hydrophilic "grass-like" cupric oxide nanostructures (**Fig. 1a**) [1]. To investigate the microscopic origin of enhanced OHP thermal performance, we used neutron scattering and electron microscopy methods at ORNL, NIST, and MU to characterize the structure, phase transitions, and dynamics of water at the CuO/water interface, which span a wide range of length and time scales.

First, we demonstrated the superhydrophilicity of the CuO coating by imaging *in situ* the wetting of micron-sized liquid water droplets to CuO nanostructures in a scanning electron microscope (SEM) during condensation (**Fig. 1b**). Further evidence of a strong hydrophilic interaction came from our high-energy-resolution elastic neutron scattering measurements in which the water undergoes continuous freezing over 200-280 K, which strongly contrasts the abrupt freezing transition of water near bare copper [2]. Furthermore, the elastic scans suggest the presence of at least two distinct water types, differing in their freezing behavior and their location within the nanostructures. Our quasielastic neutron scattering (QENS) spectra supported this interpretation by providing evidence of diffusion on three different time scales: near the surface, 1) bounded translational motion on a ns timescale (**Fig. 1d**), 2) rotational motion that is about 10 times faster, and, further from the substrate, 3) translational motion close to the rate of bulk supercooled water.

Our neutron diffraction measurements at MURR indicate that, at low hydration levels, the interfacial water freezes into an amorphous solid – a similar behavior to 'nonfreezing' water in nanoporous silica materials. At higher hydration, hexagonal ice begins to form small (~30 nm) crystallites. Vibrational spectra obtained by inelastic neutron scattering show evidence of both amorphous and crystalline phases, consistent with our previous elastic scans and neutron diffraction measurements. Work is currently underway to study water dynamics in a CuO-treated OHP using time-resolved neutron imaging at HFIR.

1. F. Z. Zhang *et al*., *J. Heat Transfer* **138**, 062901 (2016).
2. J. Torres *et al*., *J. Appl. Phys*. **125**, 025302 (2019).

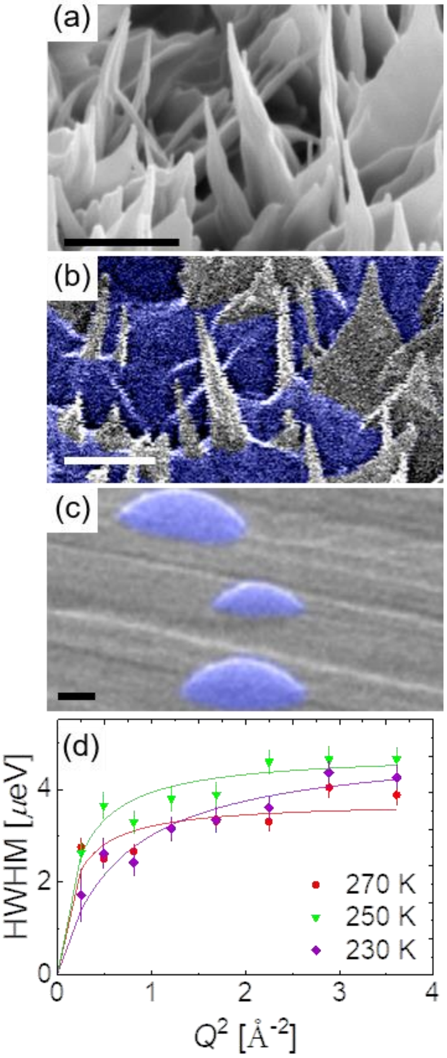

Figure 1. (false-colored) SEM images of (a-b) CuO nanostructures and (c) bare copper foil captured (a) before and (b-c) during water condensation. Scale bars are 0.5 μm. (d) Half-width at half-max vs. Q^2 of the Lorentzian function used fit to QENS spectra obtained on BASIS and which describes bounded diffusion of water on the CuO blades. Curves are drawn as guides to the eye.

Neutron total scattering analysis of radiation effects in pyrochlores and related structures

Igor Gussev[1], Eric C. O'Quinn[1], Will Cureton[1], Roman Sherrod[1], Joerg Neuefeind[2], and Maik Lang[1]

1 Department of Nuclear Engineering, University of Tennessee, Knoxville, TN, USA

2 Chemical and Engineering Materials Division, Spallation Neutron Source, Oak Ridge National Laboratory, Oak Ridge, TN, USA

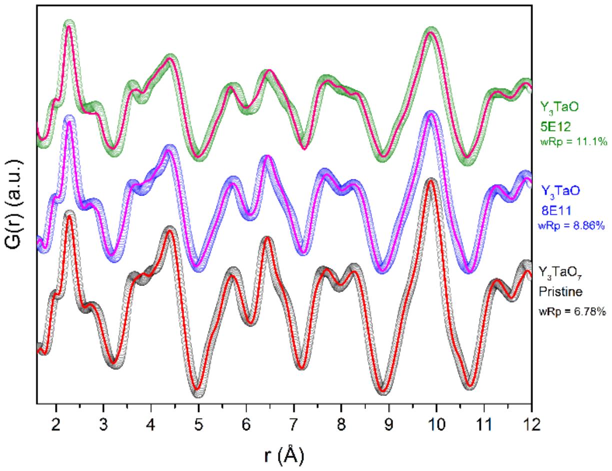

Figure 1: Neutron pair distribution function of Y_3TaO_7 weberite prior and after irradiation with 2.2 GeV Au ions.

Advances in the development of nuclear technology in recent decades require newly engineered materials that maintain structural stability in harsh working conditions, such as extreme radiation fields and extreme heat fluxes. Complex oxide ceramics are promising candidates for a number of energy-related applications, such as nuclear waste-containing matrices and solid electrolyte fuel cells, where a material's structural order and disorder play a key role in its performance. Recent neutron total scattering experiments have revealed that irradiation-induced structural disorder in pyrochlore oxides ($A_2B_2O_7$) is heterogeneous [1] across different length scales and much more complex than previously thought. Select compositions undergo disorder or amorphization over long lengths scales, yet substantially change their local symmetry which is best described by a transformation from an ordered cubic pyrochlore phase to an orthorhombic weberite-type phase [2]. This contribution shows neutron total scattering results on structurally and compositionally related weberite-type (A_3BO_7) and "stuffed pyrochlore" (A_2BO_5) oxides. Irradiation experiments were performed using 2.2 GeV Au ions at the X0 beamline of the GSI (Darmstadt, Germany). Samples were analyzed by means of neutron total scattering at the Nanoscale-Ordered Materials (NOMAD) beamline at the Spallation Neutron Source of Oak Ridge National Laboratory. It is shown that the starting structure has a profound influence on the radiation resistance of the material. Orthorhombic Dy_2TiO_5 is much more susceptible to ion-beam induced amorphization compared with $Dy_2Ti_2O_7$ pyrochlore. However, a comprehensive description of radiation damage must include effects across all length scales. "Stuffed" pyrochlore oxides (Dy_2TiO_5) that are much less stable over the long-length scales may exhibit a significantly enhanced stability at the short-range structure. This behavior can be understood in terms of local atomic arrangements and associated structural constraints. The weberite-type Y_3TaO_7 has orthorhombic weberite symmetry at both short- and long-ranges prior to irradiation. Strikingly, this leads to an improved structural stability (**Fig. 1**) over all length scales compared with pyrochlore oxides under the same irradiation fluence as no major atomic rearrangements are occurring during ion irradiation.

[1] J. Shamblin *et al.*, "Similar local order in disordered fluorite and aperiodic pyrochlore structures," *Acta Mater.*, vol. 144, pp. 60–67, 2018.

[2] C. K. Chung *et al.*, "Thermodynamic and structural evolution of Dy2Ti2O7 pyrochlore after swift heavy ion irradiation," *Acta Mater.*, vol. 145, pp. 227–234, 2018.

Spin and Lattice Diffuse Scattering from High-Entropy Alloys

H. Wang[1], Z. Wang[1], W. Dmowski[1], F. Ye[2], H. Bei[2], T. Egami[1,2,3]

[1]Materials Science and Engineering Department, University of Tennessee, Knoxville
[2] Oak Ridge National Laboratory
[3]Joint Institute for neutron Sciences, University of Tennessee

High-entropy alloy (HEA) is a promising structural material due to exceptional mechanical properties and irradiation resistance. The high entropy of HEA leads to the phase stabilization of the alloy. The distinct mechanical behaviors of the HEA mainly results from the lattice distortions which induce high atomic-level stresses [1]. To demonstrate the existence of high atomic-level stresses and their interaction, the diffuse scattering which originate from the Eshelby field of atomic-level stresses were investigated for NiCoCr, NiCoFe, and NiCoFeCr single crystals using Corelli, SNS, ORNL.

Studies show that the Ni, Co, and Fe magnetic momentum are aligned with themselves and each other. While, the Cr magnetic momentum tends to oppositely align with itself and others [2]. Through the comparison of the diffuse scattering of each sample at low temperature, 6K, with sample at room temperature, the spin diffuse scattering was elucidated for these three HEAs concluding that the spins are not collinear and show spin-glass-like behavior. This study sheds light on the large spatial variation in local properties in HEAs.

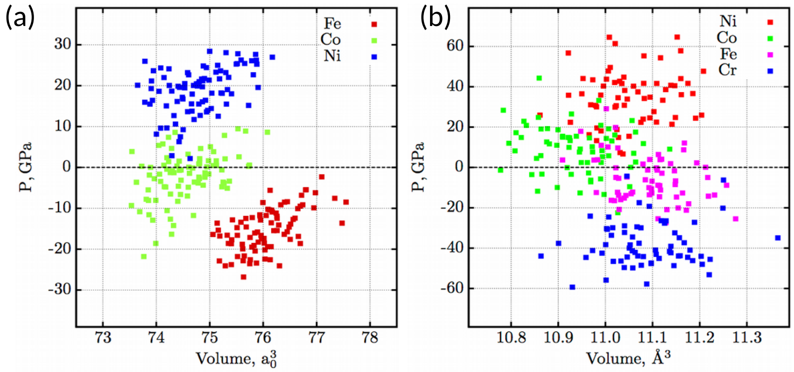

Figure. 1 Atomic-level pressure of each atom for (a) NiCoFe and (b) NiCoFeCr [3].

[1] T. Egami, W. Guo, P. D. Rack and T. Nagase, Met. Mat. Trans. A, 45 (2014): 180-183.
[2] Wu, M. C. Troparevsky, Y. F. Gao, J. R. Morris, G. M. Stocks, and H. Bei,Curr. Opin.Solid State Mater. Sci. 21 (2017) 267.
[3] T. Egami, M. Ojha, O. Khorgolkhuu, D. M. Nicholson, and G. M. Stocks, J. of Metals, 67 (2015): 2345-2349.

Tuning the magnetic properties of $NiBr_2$ with cobalt doping

H. Suriya Arachchige[1,2], Binod K. Rai[2], G. Pokharel[1,2], A. F. May[2], A. Aczel[3], T. J. Williams[3], M. Frontzek[3], M. Lumsden[3], C. D. Batista[1,4], D. G. Mandrus[1,2,5], A. D. Christianson[2]

[1] Department of Physics & Astronomy, University of Tennessee, Knoxville, TN 37996, USA
[2] Materials Science & Technology Division, Oak Ridge National Laboratory, Oak Ridge, TN 37831, USA
[3] Neutron Scattering Science Division, Oak Ridge National Laboratory, Oak Ridge, Tennessee 37831, USA
[4] Neutron Scattering Division and Shull-Wollan Center, Oak Ridge National Laboratory, Oak Ridge, TN 37831, USA
[5] Department of Materials Science and Engineering, University of Tennessee, Knoxville, Tennessee 37996, USA

$NiBr_2$ crystallizes in the trigonal space group $R\bar{3}m$ and exhibits both commensurate (T_N= 44 K) and incommensurate magnetic order (T_{IC}=22.8 K). The commensurate order is characterized by antiferromagnetic stacking of layers of ferromagnetically coupled Ni spins. The incommensurate order arises out of competition of the in-plane exchange interactions which results in a helical magnetic structure with a propagation vector $\vec{k} = \left[0.027, 0.027, \frac{3}{2}\right]$. The magnetic properties of $NiBr_2$ can be tuned with chemical substitution. Here we focus on the series $Ni_{1-x}Co_xBr_2$, where x = 0, 0.2, 0.25, 0.3, and 0.45. Neutron single crystal diffraction measurements show a decrease in T_N with doping while changes in T_{IC} are more subtle. Additionally, our neutron scattering studies reveal that the incommensurate magnetic Bragg peaks near (1 0 0.5) and equivalent wave vectors in $NiBr_2$ evolve into a ring of magnetic scattering with Co substitution which is recently predicted to be a signature of non-trivial spin textures.

Funding Acknowledgments

This work was supported by U.S. DOE, Office of Science, Basic Energy Sciences, Materials Sciences and Engineering Division and the Gordon and Betty Moore Foundation’s EPiQS Initiative.

Control of Structure and Metal-Oxide Phase In MOF-Derived Carbons Through Controlled Carbonization Environments

Gregory S. Day,[1] Jialuo Li,[1] Zachary Perry,[1] Matthew R. Ryder,[2] Katharine Page,[2] Hong-Cai Zhou[1]
[1]Department of Chemistry, Texas A&M University [2]Oak Ridge National Laboratory

Metal-organic frameworks (MOFs) have been well studied for their high surface area and porosity. However, there has been increasing interest in investigating MOF materials that have undergone a carbonization process. These MOF-derived carbons share several benefits with their as-synthesized counterparts, namely, highly disperse metal centers and permanent porosity. However, the porosity of these materials is typically decreased from that of their precursors as a consequence of the carbonization process. In order to investigate the structure of these materials under different carbonization conditions, we investigated the carbon materials that resulted from the carbonization of an iron-containing MOF, PCN-250, under different gas flow environments. The presence of different gas species, which can have different affinity levels towards the MOF structure, result in alterations in the resulting framework porosity and internal surface area. Additionally, it has been observed that the phase of iron-based nanoparticles generated during carbonization is strongly influenced by the gas environment. Carbonization under an inert atmosphere results in the formation of a reduced iron species that auto-ignites when exposed to air. Interestingly, performing the same calcination experiments with the isolated metal units of PCN-250, without the carbon scaffold of the MOF, results in the generation of different iron phases. Additionally, specific gas conditions can influence the generation of different iron oxide phases. By controlling the environment, we can selectively yield iron (II,III) oxide or iron (III) oxide. Neutron scattering pair distribution function (PDF) analysis, has been conducted on several of these MOF-derived carbons, showing both the distinct generation of iron phases, as well as altered carbon environments.

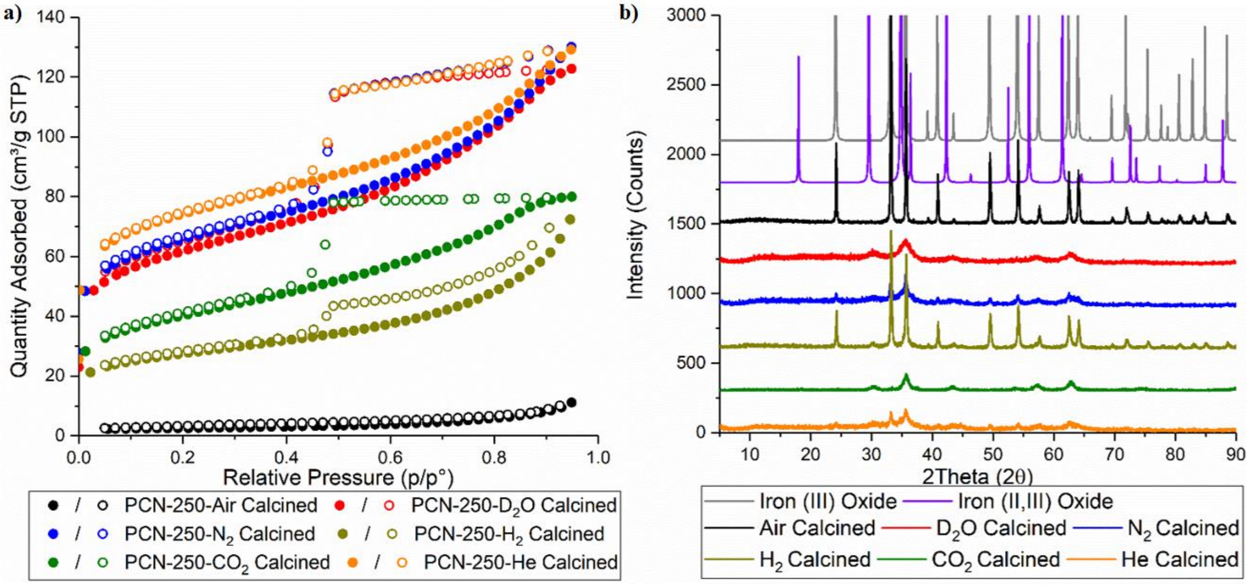

Figure 1: a) N_2 adsorption isotherms of PCN-250 after carbonization under different gas conditions. b) PXRD patterns of the PCN-250 carbonization products showing the different phases generated.

Neutron scattering study of breathing pyrochlore lattice material $LiGaCr_4S_8$

G. Pokharel[1,2], H. Suriya Arachchige[1,2], A. F. May[2], S. Calder[3], T. Hong[3], G. Sala[3], G. Ehlers[4],
R. S. Fishman[2], D. Mandrus[5, 2, 1], A. D. Christianson[2,1]

[1]Department of Physics and Astronomy, University of Tennessee, Knoxville, TN
[2]Materials Science and Technology Division, Oak Ridge national laboratory, Oak Ridge, TN
[3]Neutron Scattering Division, Oak Ridge national laboratory, Oak Ridge, TN
[4]Neutron Technologies Division, Oak Ridge national laboratory, Oak Ridge, TN
[5]Department of Materials Science and Engineering, University of Tennessee, Knoxville, TN

Abstract

We present a study of a breathing pyrochlore lattice material $LiGaCr_4S_8$ using neutron scattering measurements. Magnetoelastic coupling in $LiGaCr_4S_8$ drives negative thermal expansion in the temperature range 12-110 K. No long-range magnetic order is observed down to 1.5 K in neutron diffraction. However, short-range spin correlations are observed and persist to at least 100 K. The fitting of magnetic diffuse scattering to a Heisenberg model indicates that the spin-spin couplings are antiferromagnetic (J=0.584 meV) and ferromagnetic (J'=-1.622 meV) within the small and large Cr_4 tetrahedra respectively. Neutron diffraction also indicates the existence of additional short-range magnetic order below 12 K. Inelastic neutron scattering data shows two bands of spin excitations with maximum energy near 15 and 2 meV at 4 K. The intensity of the high energy inelastic signal weakens above 10 K though persists to nearly 100 K. The low energy part of the spectrum behaves as a damped harmonic oscillator that can be described by a single temperature dependent relaxation.

Framework Doping of Ni Enhances Pseudocapacitive Na-ion Storage of (Ni)MnO_2 Layered Birnessite

Xiaoqiang Shan,[†] Fenghua Guo,[†] Tongxin Zhou,[†] Katharine L. Page,[‡] Jorge C. Neuefeind,[‡] Bruce Ravel,[⊥]
Milinda Abeykoon,[§] Gihan Kwon,[§] Daniel Olds,[§] Dong Su,[//] Xiaowei Teng[†*]

[†]Department of Chemical Engineering, University of New Hampshire, Durham, New Hampshire 03824, USA
[‡]Chemical and Engineering Materials Division, Oak Ridge National Laboratory, Oak Ridge, Tennessee 37830, USA
[⊥] Synchrotron Science Group at NSLS-II, National Institute of Standards and Technology, Upton NY, 11973
[§]National Synchrotron Light Source II, Brookhaven National Laboratory, Upton, New York 11973, USA
[//]Center for Functional Nanomaterials, Brookhaven National Laboratory, Upton, New York 11973, USA

Layered MnO_2 birnessite are widely used materials for aqueous Na-ion electrochemical energy storage. However, its storage capacity is rather low due to limited redox activity. Although doping strategies could be used to tune the structure and electrochemical performance of birnessite, most of studies only involve the doping of guest ions into interlayer and the resulting performance is still unsatisfactory. Here, we reported a framework doping of Ni-ion into MnO_2 birnessite. Characterized by neutron total scattering and pair distribution function (PDF) analysis, the (Ni)MnO_2 birnessite was comprised of disordered [NiO_6] and ordered [MnO_6] octahedra, and showed enhanced specific capacity and cycle life in full-cells (63 mAh g^{-1} at 0.2 A g^{-1} after 2000 cycles). In situ XRD, in situ PDF, XANES and XPS provided strong evidences that homogenous [Ni/MnO_6] octahedra were both redox active and remained a highly stable and reversible long-range order and local structure during charge-discharge processes, while disordered [NiO_6] octahedra significantly improved pseudocapacitive redox charge storage.

Hydrogen Dynamics in Barium Hydride

Eric Novak, Luke Daemen, Takeshi Egami, Niina Jalarvo

Department of Materials Science and Engineering, University of Tennessee, Knoxville, TN

Neutron Sciences Directorate, Oak Ridge National Laboratory, Oak Ridge, TN

Jülich Centre for Neutron Science (JCNS), Forschungszentrum Jülich GmbH, Jülich, Germany

Department of Physics and Astronomy, University of Tennessee, Knoxville, TN

With the ever-increasing demand for renewable energy sources, the search for solid state hydrogen storage materials with fast hydrogen transport is becoming more important. Alkaline earth hydrides are a promising candidate due to their ability to store large amounts of hydrogen and some exhibit fast ionic transport of hydride ions. The ionic conductivity of barium hydride, BaH_2, has already surpassed the good oxide ion and proton conductors that are used in applications today, even after those materials have been enhanced by doping.[1] A temperature-induced structural phase transition occurs around T = 775 K, which leads to over a magnitude increase in the ionic conductivity. To optimize the uptake and release of hydrogen in these systems, understanding the nature of the hydrogen bonding and how the hydride ions diffuse through the lattice is crucial.

First, we employ X-ray (XRPD) and neutron powder diffraction (NPD), along with total neutron scattering, to fully characterize the structure of the material. XRPD and NPD examine the long range, time-averaged structure while total neutron scattering yields information about short range order, such as disorder and defects. These techniques form of a complete picture of the energy landscape, both locally and globally. Combining this with inelastic neutron scattering yields information about the bonding energies and vibrational (phonon) modes. The hydrogen in BaH_2 is located on two distinct crystallographic sites, with each site producing separate vibrational modes in the INS spectra. Following the temperature dependence of the vibrational modes can give insight into the hydrogen release mechanism. Our INS results suggest that both hydrogen sites are sufficiently mobile and are diffusing at temperatures above 600 K.

Second, we explore the diffusion of hydride ions in BaH_2 using quasielastic neutron scattering (QENS) and electrochemical impedance spectroscopy (EIS). QENS probes the microscopic diffusion mechanism on length scales < 40 Å. The diffusion of the hydride ions is well described by the Chudley-Elliott jump diffusion model. Jump distances, residence times, diffusion coefficients, and activation energies can be extracted to give insight into the diffusion pathways.

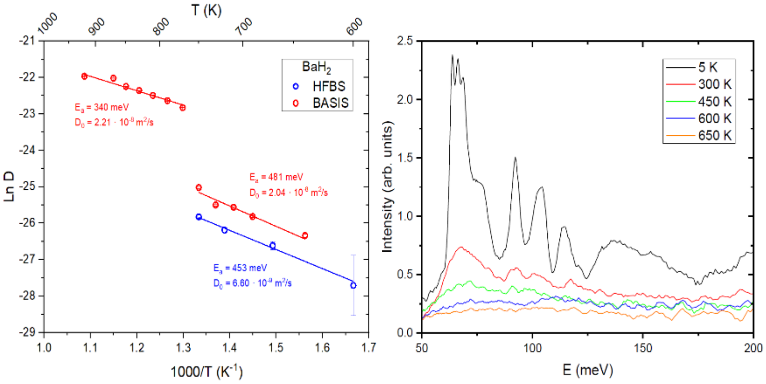

Fig. 1 (a) Arrhenius diagram for QENS measurements at BASIS and HFBS for BaH_2. (b) INS spectra measured at VISION

In addition to the temperature-induced phase transition at T = 775K, there is a pressure-induced phase transition that occurs around P = 2.3 GPa at RT. We have conducted high pressure NPD experiments on BaD_2 to characterize the crystal structure in both the low- and high-pressure phases. We plan to measure QENS at elevated pressures to understand how pressure effects the hydrogen dynamics.

[1] Verbraeken, M. C., Cheung, C., Suard, E. & Irvine, J. T. S. High H− ionic conductivity in barium hydride. *Nature Materials* **14**, 95, doi:10.1038 (2014).

In situ Low-temperature Pair Distribution Function (PDF) Analysis and Molecular Dynamics Simulations of CH$_4$ and CO$_2$ Hydrates

B.R. Cladek[1], S.M. Everett[2], M.T. McDonnell[3], M.G. Tucker[2], D.J. Keffer[1], C.J. Rawn[1]
[1]Material Science and Engineering- University of Tennessee, [2]Neutron Scattering Division, Oak Ridge National Laboratory, [3]Computer Science and Mathematics Division, Oak Ridge National Laboratory

Natural gas hydrates (NGH) form in ocean floor and sub-surface permafrost deposits in high-pressure, low temperature environments.[1] A driving convergence research focus on these deposits is their potential as a future energy source. Naturally occurring CH$_4$ hydrates primarily crystallize in the sI clathrate structure, Fig. 1(a). This lattice is composed of hydrogen bonded water cages (the host), each of which occlude one gas molecule (the guest), in Fig. 1(b,c). The sI framework can host other molecules, but this research focuses on CH$_4$-CO$_2$ hydrates to support current explorations in which CH$_4$ may be harvested from hydrate deposits via exchange with CO$_2$.[1-2] CO$_2$ replacement in the hydrate structure is energetically preferred, facilitating CO$_2$ byproduct sequestration while obtaining new fuel sources. Equilibrium models predict that a mixed hydrate solid solution in which CO$_2$ replaces some CH$_4$ is stable at higher temperature and lower pressure than pure CH$_4$ hydrate, and thermodynamic stability increases as the CO$_2$ fraction increases. The impact of varying the guest molecules and mixed guest systems is a relevant topic to study due to concerns about the stability of NGH under changing environmental conditions. A detailed understanding of the guest-host interactions in gas hydrates is necessary for the advancement of emerging technologies and processes which will utilize NGH deposits. The gas hydrate crystal has a high degree of disorder at all temperatures from the motion of the occluded gas molecules. Molecular dynamics (MD) simulations show that this disorder is not described by long-range crystallographic models. *In situ* neutron total scattering experiments and pair distribution function (PDF) analysis are used to characterize the short-range order in CH$_4$-CO$_2$ hydrates. Extraction of detailed information from PDF data of complex systems requires methods such as MD simulations combined with Reverse Monte Carlo (RMC) fitting. Preliminary MD models of CH$_4$-CO$_2$ hydrates demonstrate the benefit of neutron PDF experiments by providing simulated PDFs (Fig. 2), visualization of molecular motion, and analysis of thermodynamic interaction energies throughout the CH$_4$-CO$_2$ guest composition.[3] *In situ* variable temperature neutron PDF data of CH$_4$, CO$_2$, and mixed CH$_4$-CO$_2$ hydrate were collected at the NOMAD beamline at the Spallation Neutron Source (SNS), Oak Ridge National Laboratory. RMCProfile is used to fit the data to large box models produced with MD simulations. PDF experiments performed *in situ* provide structural characterization, while the variable temperature measurements lead to inferred dynamics. Dynamics will also be directly observed with complementary inelastic neutron scattering (INS) experiments on the VISION beamline for chemical bond analysis.

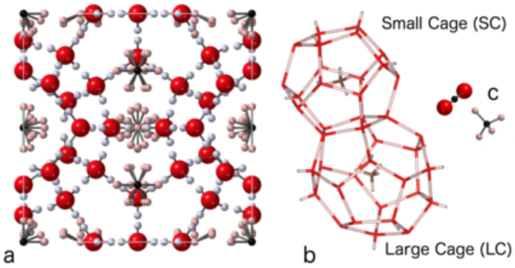

Figure 1: The sI unit cell (a) is made up of two small cages and six large cages (b). Both cages can each host one molecule, such as CH$_4$ or CO$_2$ (c).

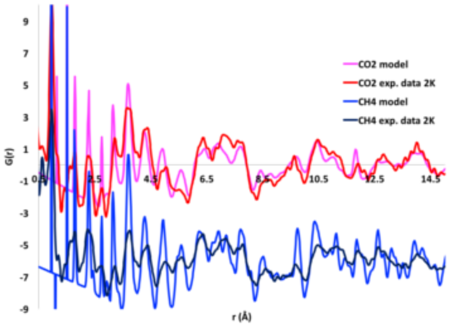

Figure 2: PDF data from CH$_4$ and CO$_2$ hydrates collected on NOMAD at 2 K compared with simulated PDFs from MD.

1. Koh, C., Sloan, E. , *Clathrate Hydrates of Natural Gases*. Third ed.; CRC Press: Boca Raton, 2007.
2. Boswell, R.; Schoderbek, D.; Collett, T. S.; Ohtsuki, S.; White, M. D.; Anderson, B. J., The Ignik Sikumi Field Experiments, Alaska: Design, Operations, and Implications for CO2-CH4 Exchange in Gas Hydrate Reserviors. *Energy & Fuels* 2016.
3. Cladek, B.R.; Everett, S. M.; McDonnell, M.T. ; Tucker, M.G. ; Keffer, D.J. ; Rawn, C.J., Guest-Host Interactions in Mixed CH$_4$ – CO$_2$ Hydrates: Insights from Molecular Dynamic Simulations. *The Journal of Physical Chemistry C* 2018.

Toward Elucidating the Mechanism of Lytic Polysaccharide Monooxygenases: Chemical Insights from X-ray and Neutron Crystallography

G. C. Schröder[1,2], W.B. O'Dell[1,2,3] and F. Meilleur[1,2]

[1] Department of Molecular and Structural Biochemistry, North Carolina State University
[2] Neutron Scattering Division, Oak Ridge National Laboratory
[3] Current affiliation: Institute for Bioscience and Biotechnology Research, National Institute of Standards and Technology and the University of Maryland

Lytic polysaccharide monooxygenases (LPMOs) are mononuclear copper oxidases that disrupt saccharide chains by oxidizing carbons involved in glycosidic bonds.[1] LPMOs are abundant in both bacteria and fungi and have been shown to be catalytically active on cellulose, chitin, hemicellulose, amylopectin and amylose.[2] LPMOs are responsible for the oxidative cleavage of crystalline cellulose, which makes them essential in biorefinery processes. Chain disruption of crystalline cellulose by LPMO increases the accessibility of the substrate to hydrolytic enzymes and cellulose-active LPMOs are already in use industrially. Fungal lytic polysaccharide monooxygenases (LPMOs) have been intensely studied since their first characterization in 2010 as a unique class of copper enzymes capable of oxidizing carbohydrates. The LPMO active site consists of a single copper ion coordinated in a conserved 'histidine-brace' motif. The amino and N_δ nitrogens of the N-terminal histidine along with N_ε of His84 provide three equatorial ligands in T-shaped coordination. Tyr168 provides one axial ligand to the copper ion. LPMOs require the input of two electrons and of one oxygen molecule (O_2 or H_2O_2) to achieve hydroxylation of one carbon in the glycosidic bond. To further understand the mechanism by which LPMOs oxidize the glycosidic bond, we combine high resolution X-ray and neutron protein crystallography to deliver precise, all atom structures of key reaction intermediates that can reveal i) the positions and interactions of all hydrogen atoms in the enzyme, ii) atomistic details of the active site without perturbing the metal oxidation state, and iii) the chemical nature of the activated dioxygen species coordinated to the active site copper. Previous work in our group has shown provided insight into the binding of oxygen at the LPMO active site as well as the role of His 157 protonation in catalysis. Oxygen pre-binds in an active site pocket containing His157 and it has been computationally shown that low pH conditions where His157 is doubly protonated, make oxygen binding energetically favorable. We have sought to gain further insight into the catalytic mechanism of LPMO using X-ray and neutron crystallographic structures. We have heterologously expressed *Nc*PMO-2 and grown crystals sufficiently large for neutron protein diffraction. To investigate the effect of His 157 protonation on oxygen binding and catalysis, crystals were soaked in low pH conditions and a complete neutron dataset at 2.1 Å was collected on MaNDi at the Spallation Neutron Source (SNS) at Oak Ridge National Laboratory. Additionally, to complement previous X-ray data collected on the reduced active form of LPMO at cryo-conditions, we collected a 2.5 Å cryo-neutron dataset at MaNDi at SNS on an ascorbate reduced LPMO crystal to determine the nature of the activated oxygen species at the LPMO active site.

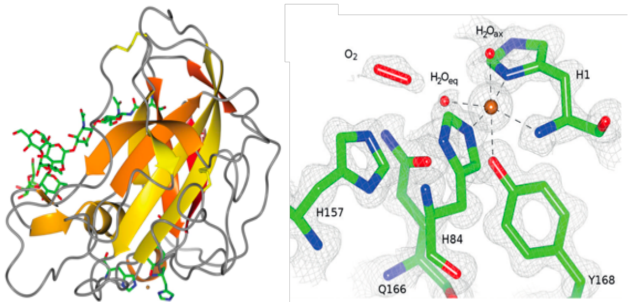

Figure 1 (A) The structure of LPMO showing the location of the active site. (B) LPMO active site illustrating the classic "histidine brace" coordinating the active site copper. *Figure from O'Dell et al.*[1]

1. O'Dell W.B., Agarwal P.K. & Meilleur F. (2017) Oxygen Activation at the Active Site of a Fungal Lytic Polysaccharide Monooxygenase. *Angew. Chemie - Int. Ed.* **56**, 767–770
2. Frandsen K.E.H., Simmons T.J., Dupree P., *et al.* (2016) The molecular basis of polysaccharide cleavage by lytic polysaccharide monooxygenases. *Nat. Chem. Biol.* **12**, 298–303

Mapping Conformational Space of the 70S *E. coli* Ribosome in Solution Using Small Angle Scattering and Molecular Modeling

Emily Armbruster[1,2], Kevin Weiss[2], Loukas Petridis[2], Jose Borreguero Calvo[2], Peter Cornish[1], Sai Venkatesh Pingali[2]

[1]Department of Biochemistry, University of Missouri, Columbia, MO
[2]Oak Ridge National Laboratory, Oak Ridge, TN

Proteins, the workhorse of a biological cell, are produced and distributed by a large, flexible, macromolecular machine called the ribosome. messenger RNA (mRNA) is translated by the ribosome to create a protein in a process that involves large scale molecular movements of the ribosome and determining the varied structural conformations involved can provide insight toward understanding ribosomal function. Currently, the field of functionally oriented structural biology emphasizes the importance of mapping conformational space. However, mapping the continuous structural variation of the ribosome is difficult due to low energetic barriers between ribosomal conformational states. These difficulties have interfered in characterizing the conformational distortions of the ribosome as it unwinds structured mRNA during translation, a phenomenon that impacts the production and diversity of proteins in the cell. This study combines experimental small-angle scattering methods with molecular modeling to elucidate the ensemble of structural conformations of 70S *E. coli* ribosome in solution. We will discuss the observed structural differences between a vacant ribosome, a ribosome as it translates linear mRNA, and a ribosome as it translates structured mRNA.

NADPH-Dependent Assimilatory Sulfite Reductase is a conformationally dynamic redox enzyme

Daniel T. Murray and M. Elizabeth Stroupe

Department of Biological Science and Institute of Molecular Biophysics, Florida State University

NADPH-dependent assimilatory sulfite reductase (SiR) is a dodecameric, 800 kDa metalloenzyme that is responsible for the reduction of sulfite (SO_3^{2-}) to sulfide (S^{2-}), a pivotal step in the biosynthesis of amino acids cysteine and methionine, vitamins thiamine and biotin, and the peptide antioxidant glutathione. SiR is composed of an octameric NADPH-binding flavoprotein (SiRFP) and four copies of a monomeric, siroheme-containing hemoprotein (SiRHP). SiR is responsible for carrying out one of the only six-electron reductions in nature, all without releasing any intermediate byproducts during the course of sulfur assimilation. I have preliminary X-ray diffraction data of the minimal dimer complex of a SiRFP fragment bound to SiRHP (SiRFP-HP) and am working to optimize crystal growth so that we may learn about the structural interface that is involved in dimerization. Cryo-electron microscopy (cryo-EM) is being applied to SiR, but a degree of troubleshooting exists due to damaging interactions of the protein with the air-water interface once applied to EM grids. I would like to use small angle neutron scattering (SANS) to answer how each subunit interacts during subunit assembly and what conformational changes are associated with catalysis in this multimeric redox engine that is analogous to SiRFP homologs cytochrome p450 reductase and mammalian nitric oxide synthase. SANS studies have shown that oxidized SiRFP takes an extended conformation in solution, confirming the recent crystallographic model and making it exceptional among diflavin reductases[1]. Now, SANS will be applied to analyzing the envelope structures of selectively deuterated subunits of SiR through two aims. The first aim endeavors to examine the structural interface of the SiRFP-HP dimer and observe the predicted disorder-to-order transition of SiRHP's N-terminus upon complex assembly[2]. In the second aim, we will observe subunit conformations and orientations with respect to each other in the dodecameric SiR holoenzyme. Combining the static technique of X-ray crystallography with the in-solution capabilities of SANS will elucidate details regarding how this dynamic oxidoreductase achieves its remarkable efficiency.

1. Tavolieri, A., Murray, D., Askenasy, I., Pennington, J., McGarry, L., Stanley, C., and Stroupe, M. NADPH-dependent sulfite reductase flavoprotein adopts an extended conformation unique to this diflavin reductase. *J Struct Biol*. **205** (2): 170-179 (2019).
2. Askenasy, I., Murray, D., Andrews, R., Uversky, V., He, H., and Stroupe, M. Structure-Function Relationships in the Oligomeric NADPH-Dependent Assimilatory Sulfite Reductase. *Biochem*. **57** (26): 3764-3772 (2018).

Disordered Structure and Structural Water Promote Aqueous Sodium-ion Energy Storage in $Na_{0.27}MnO_2$ Birnessite

Xiaoqiang Shan[a], Fenghua Guo[a], Daniel S. Charles[a], SaeWon Kim[a], Zachary Lebens-Higgins[b], Sara Mohamed[b], Jinpeng Wu[c], Wenqian Xu[d], Wanli Yang[c], Katharine L. Page[e], Joerg C. Neuefeind[e], Mikhail Feygenson[e, f], Louis Piper[b], and Xiaowei Teng[a]

[a] Department of Chemical Engineering, University of New Hampshire, Durham, New Hampshire 03824, USA
[b] Department of Physics, Applied Physics and Astronomy, Binghamton University, Binghamton, New York 13902, United States
[c] Advanced Light Source, Lawrence Berkeley National Laboratory, Berkeley, California 94720, USA
[d] Advanced Photon Source, Argonne National Laboratory, Argonne, Illinois 60439, USA
[e] Chemical and Engineering Materials Division, Spallation Neutron Source, Oak Ridge National Laboratory, Oak Ridge, Tennessee 37831, USA
[f] Juelich Centre for Neutron Science, Forschungszentrum Juelich GmbH, 52425 Juelich, Germany

Birnessite is a low-cost and environmentally friendly layered material for aqueous electrochemical energy storage; however, its storage capacity is poor, mainly due to its narrow potential window in an aqueous electrolyte and low redox activity. Herein we reported a Na-rich disordered birnessite structure ($Na_{0.27}MnO_2$) for aqueous Na-ion electrochemical storage with a much-enhanced storage capacity and cycling life (83 mAh g^{-1} after 5000 cycles in full-cell). Neutron total scattering and *in situ* X-ray diffraction measurements showed that both structural water and the Na-rich disordered structure attributed to the improved electrochemical performance of $Na_{0.27}MnO_{2.}$ Particularly, the co-deintercalation of the hydrated water and Na-ion during the high potential charging process resulted in the shrinkage of interlayer distance and thus stabilized the layered structure. Our results provide a genuine insight into how structural disordering and structural water improve Na-ion storage in a layered electrode and open up a new exciting direction for improving aqueous batteries.

Solvent Effects on the Structure of Sulfonated Polystyrene: A SANS Study

[1]Chathurika Kosgallana, [1]Sidath Wijesinghe, [1]Manjula Senanayake, [1]Supun Mohottalalage, [2]Lilin He, [1]Dvora Perahia

[1]Department of Chemistry, Clemson University, Clemson, SC, [2]Oak Ridge National Laboratory, Oak Ridge, TN

Ionomers form dynamic sparse networks, which are driven by ionic association, in solutions at extremely low ionic content. Here, we study the factors that affect the structure of slightly sulfonated polystyrene (PSS) networks formed in solutions, using small angle neutron scattering (SANS). SANS measurements were carried out in 0.25-10Wt% PSS in toluene/ethanol solutions, across a broad temperature range. In toluene, a good solvent for the PS, an upturn is observed at low q, which is a characteristic of a network formation. The SANS patterns consist of a broad signature at intermediate q, attributed here to an average network mesh size, determined by the distance between ionic physical crosslinks. With increasing concentration, R_g increases due to increasing cluster size and numbers. The long-range correlations were captured by the Beacuge model. The PS chains assume an overall prolate configuration around the ionic clusters. Surprisingly, while the long-range correlations diminish with addition of ethanol, the mesh size decreases. While the ionic clusters become less defined, the PS chains are concurrently affected, assuming a more constrained chain configuration.

Non-Destructive Characterization of Zircaloy-4 Using Neutron Radiography and Neutron Computed Tomography

Brianne Beers[1,2], Hassina Bilheux[2], Jean Bilheux[2], Jun-Li Lin[3], Brent Heuser[3]
[1]University of Tennessee – Knoxville, [2]Oak Ridge National Laboratory, [3]University of Illinois at Urbana-Champaign

Zirconium (Zr) alloys are used as nuclear fuel cladding in light water reactors (LWRs) because of their high corrosion resistance and low thermal neutron cross sections. Zircaloy-4 is one such Zr alloy used in pressurized water reactors (PWRs) – a type of LWR. Zircaloy-4 cladding experiences the uptake of H in an outer layer of corrosion during normal reactor operation. Once the critical solid solubility of H within the cladding is reached, Zr hydrides ($ZrH_{1.7}$) are formed. The presence of these hydrides causes material embrittlement. This work aims to quantify the hydrogen (H) concentration, which relates to hydride distribution, within prepared Zircaloy-4 samples through the use of neutron radiography (NR) and neutron computed tomography (NCT). NR and NCT are non-destructive characterization methods because there is no need to alter or damage the sample in any way prior to data collection. In addition, these neutron imaging techniques take advantage of the fact that the cold neutrons from the beamline are more likely to interact with the H than the surrounding Zr alloy. This is due to the fact that H is a large cross section to cold neutrons in comparison to Zr. In this project, Zircaloy-4 samples were hydrided in a vacuum environment before being imaged at the CG-1D beamline of the High Flux Isotope Reactor (HFIR). Images were collected using a charge-coupled device (CCD) with a $^{6}LiF/ZnS$ scintillator. The H concentration within the Zircaloy-4 samples is calculated by determining the linear attenuation coefficient value associated with each image pixel (the effective pixel size is approximately 36 μm). In addition to the NR and NCT, neutron diffraction and grating interferometry techniques will be used to find correlations between defects within the Zircaloy-4 samples and the location of H and hydrides. Neutron diffraction measurements were collected at the VULCAN beamline of the Spallation Neutron Source (SNS) at ORNL; the neutron beam was focused on the areas within the samples known to contain a hydride blister in order to identify crystalline changes that might indicate the presence of defects. The grating interferometry system, to be installed at CG-1D, will be used to collect defect information at the sub-micron level and in three dimensions (3-D).

Acknowledgments

This research used resources at the High Flux Isotope Reactor, a U.S. Department of Energy (DOE) Office of Science User Facility operated by the Oak Ridge National Laboratory.
This research was sponsored by the Scientific User Facilities Division, Office of Basic Energy Sciences, U.S. DOE.
This research was also supported by the US DOE NEUP ATF IRP under contract number IRP-12-4728 and by the US NSF under grant number DMR-1207102.
Brianne would like to acknowledge ORNL staff scientists Y. Yan for his assistance during early discussions, and M. Cinbiz for providing the samples.

Notice of Copyright

Local Structural Study of Novel Mott-Insulating Cousins of the Iron Pnictides

B. Karki[1], A. Alfailakawi[1], B. A. Frandsen[2], J. C. Neuefeind[3], M. Everett[3] and B. Freelon[1]

[1] Department of Physics and Astronomy, University of Louisville, Louisville, KY 40208, USA
[2] Department of Physics and Astronomy, Brigham Young University, Provo, UT 84602, USA
[3] Oak Ridge National Laboratory, Oak Ridge, TN 37831, U.S.A.

ABSTRACT:

There has been significant interest in mixed anion materials since the discovery of high transition temperature (T_c) superconductivity in layered iron pnictides system. Electron-electron interaction leads to the emergence of fascinating collective electronic behavior, including novel magnetism, electronic nematic order and superconductivity. All of these properties are closely related in iron-based superconductors. The interplay between these orders can be understood by studying their co-evolution across the phase diagram through the chemical substitution. An important question in iron-based superconductivity has been whether superconductivity could emerge from materials that are in the Mott insulating region of the electronic phase diagram as is the case for cuprate high- T_c superconductors. In an effort to find such materials, the mixed-anion iron-oxychalcogenides have been explored.

Iron oxy-chalcogenides, $La_2O_2Fe_2OM_2$ (M = S, Se), is the layered materials formed from stacking layered units of La_2O_2 and Fe_2OM_2 (M = S, Se). They are structurally reminiscent of the cuprates while possessing the Fe-chalcogen planes that are similar to the Fe-pnictides. This work describes the structural properties of , $La_2O_2Fe_2OM_2$ (M = S, Se) which are closely related to the superconductivity because they are on the verge of a metal insulator transition. By exchanging S and Se it is possible to tune the electron correlation value from insulating to the metallic phase. Unlike the Fe-pnictides these materials do not show long range structural phase transition. However, both materials M = S, Se undergo magnetic phase transitions from paramagnetic antiferromagnetic phase at a Neel temperature 107 K and 90 K, respectively.

Neutron total scattering experiments on $La_2O_2Fe_2OM_2$ (M = S, Se) were performed on Nanoscale Ordered Materials Diffractometer (NOMAD) beamline at Oak Ridge National Laboratory (ORNL) in order to collect Pair distribution function (PDF) data. PDF analysis involves Fourier transforming the measured total scattering intensity in order to obtain a real space representation of inter-atomic correlations. This technique is used to study local, short range structural correlations that deviate from the average structure. Our results for M = S, Se possess short-scale structural distortions however, neutron powder diffraction (NPD) provides clear evidence that the average, long-range structure remains tetragonal throughout the high and low temperature regimes. Local crystal structure was studied by investigating deviations in atomic positions and orthorhombicity. By tracking the orthorhombicity parameter we observe local scale distortions between the tetragonal and orthorhombic structure in a typical range of 1-2 nm as shown in **Figure 1**. These spatially limited distortions represent fluctuating nematic order which suggests the ubiquity of nematic fluctuations in iron-based superconductors and related materials. In addition, we found the discontinuity in c-lattice which may arise due to the buckling of Fe_2O plane. We anticipate that this buckling might be due to the change in octahedral height or tilting of the octahedral structure. Overall, these results suggest that structural distortion may play a role in absence of superconductivity in these materials.

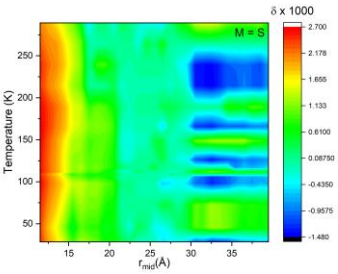

Fig 1. False color plots of the refined orthorhombicity determined from neutron PDF analysis of samples of M = S. Negative values of orthorhombicity indicate that the lattice parameter b is larger than a.

Charge-Order and Phonon Coupling in La1.67Sr0.33NiO4

A. M. Merritt, A. Christianson, A. Banerjee, D. Reznik
AMM and DR: Department of Physics, University of Colorado, Boulder CO, AC and AB: Oak Ridge National Laboratory, Oak Ridge TN

Charge order manifesting as stripes in the nickelates $La_{2-x}Sr_xNiO_4$ have been at the center of research on correlated electrons. Owing to the similar structures of La_2CuO_4 and La_2NiO_4, they are of interest for comparing lattice dynamics that possibly couple to electronic order with the cuprates. There is evidence from both the experimental and theoretical side that dynamic charge stripes should interact with the Ni-O bond-stretching optic phonon at higher energy. As the Ni-O bond-stretching mode naturally has a polar effect, it should couple to charge dynamics such as the charge order. The charge order, based on hole doping, will then couple to the hole segregation in the stripes. In previous measurements no significant anomalies were observed [1]. More recently, we discovered and characterized the dispersion of dynamic charge stripes and found that there is no measurable interaction between the dynamic charge stripes and low-energy phonons [2].

Our most recent work with $La_{1.67}Sr_{0.33}NiO_4$ on ARCS has proven fruitful; we have found clear anomalies at the stripe ordering wave vector in the longitudinal phonons (Fig. 1). The observed effects are consistent with a coupling of the dynamic charge order to the phonon producing a twin phonon peak. The stripes couple to the phonon through the localization of charge and to neighboring charge fluctuations through Coulombic mechanisms, but only in the direction of stripe propagation. As shown in Ref. [2], $La_{1.67}Sr_{0.33}NiO_4$ exhibits peak dynamic stripe intensity at 240K. Below this temperature, the stripes freeze and exhibit only static ordering. Our observations match this. The overdamped peak at 240K hardens and narrows upon cooling down to 190K, where most of the dynamic stripe intensity dissipates, and displays no change from 190K cooling down to 10K where the static stripe intensity builds. This clearly establishes the effect of the dynamic stripes versus the static stripes on the Ni-O bond stretching phonon of interest.

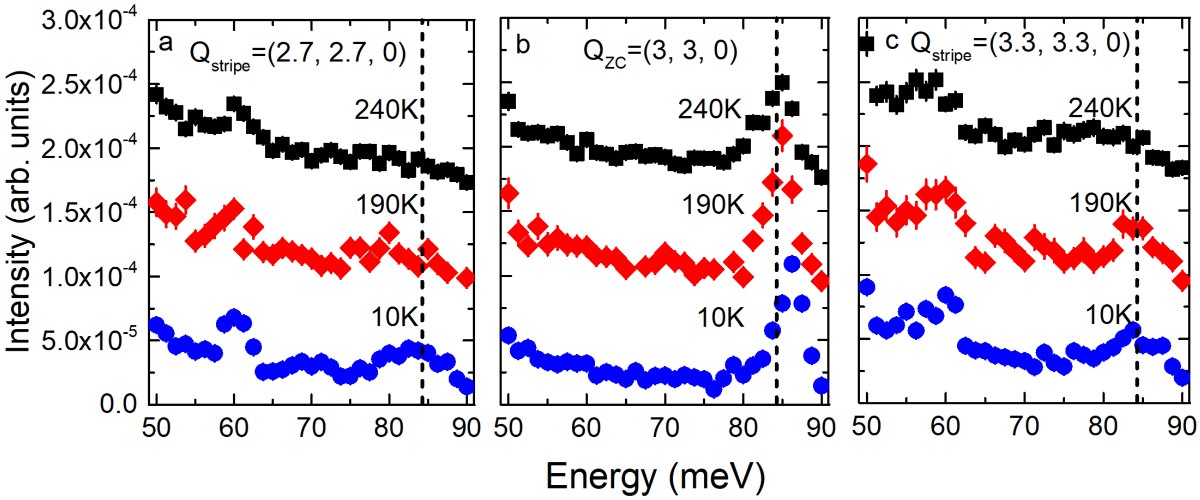

Figure 1. Neutron scattering measurements of phonons in $La_{1.67}Sr_{0.33}NiO_4$ at 240K, 190K and 10K. At 240K the stripes are purely dynamic. At 10K the stripes are purely static. At 190K the stripes exhibit some dynamic but mostly static order. Dashed lines indicate the ~85 meV phonon of interest. (a) Q=(2.7, 2.7, 0), the stripe-ordering wavevector. Note the large change with temperature in the phonon intensity around 85 meV. (b) Q=(3, 3, 0). (c) Q=(3.3, 3.3, 0), the stripe-ordering wavevector.

[1] J. M. Tranquada, *et al.*, Phys. Rev. Lett. **88**, 075505, (2002).
[2] S. Anissimova, *et al.*, Nat. Comm. **5**, 3467 (2014).

Ion Implantation Leading to Magnetism in Epitaxial Many-Layer Graphene

A. R. Mazza,[1] A. Miettinen,[2] T. R. Charlton,[3] T. Z. Ward,[4] X. He,[5] E. H. Conrad,[2] P. F. Miceli[1]
[1] *Department of Physics and Astronomy, University of Missouri, Columbia*
[2] *School of Physics, Georgia Institute of Technology*
[3] *Spallation Neutron Source, Oak Ridge National Laboratory*
[4] *Materials Science and Technology Division, Oak Ridge National Laboratory*
[5] *Electron Microscopy Core, University of Missouri, Columbia*

P-orbital magnetism observed in graphene is of interest both to fundamental physics and for its potential application in new classes of spintronic devices. One potential avenue to altering graphene is using defects to generate p-orbital magnetism. Indeed, atomic hydrogen creating sp^3 defects attached to the graphene surface as well as vacancies in graphene have been shown to induce magnetism, while high energy (MeV) proton irradiation has been shown to produce ferromagnetism at room-temperature in graphite. However, detailed investigations of these systems are absent so that little is known about the density and configuration of defects, the role of interfaces, or how these relate to magnetism.

We use *low-energy* (350-2000V) ion implantation to explore the role of defects in creating magnetism in epitaxial graphene. X-ray diffraction, measured *in situ* at MU, has been used to study the effect of implantation. We observe the graphene inter-planar spacing to *expand* as much as 5% due to the H dose. However, this expansion profile is highly dependent on the ion distribution. This difference is due to different types of structural changes which scale with ion range – when ions reach the graphene/SiC interface they create a high density of carbon interstitials in graphene which can create a larger interlayer expansion than in the case of ions remaining in graphene. The role of strain and carbon interstitials in the magnetism observed from magnetometry is investigated in multiple samples. It is believed that hydrogen passivates these carbon interstitials and exploratory measurements using neutron reflectometry were performed to investigate.

From measurements on BL-4A and we can see clear differences in SLD profiles between D/H implantation, allowing us to extract a density profile of implanted defects. For example, a sample having a dose of 0.38H/C revealed that all of the hydrogen remained, showing *for the first time* that proton implantation leads to the incorporation of hydrogen. This indicates that hydrogen is indeed chemisorbed between graphene sheets. SQUID magnetometry shows an implantation-induced magnetic moment that persists to room temperature and we investigate how the moment scales with defects/interstitial formation. Ongoing measurements will seek to understand the relationship of the magnetization and defect profiles in magnetic graphene samples.

Acknowledgement of Funding: NSF grant no. DGE-1069091, DOE SCGSR, ORNL GO! Program, portion of this work used resources at the Spallation Neutron Source, a DOE Office of Science User Facility operated by the Oak Ridge National Laboratory

Description of the Correlated Dynamics in D_2O in Real-Space and Time

Y. Sarathchandran[1], Y. Shinohara[2], T. Iwashita[3], W. Dmowski[1,] D. Abernathy[2], and T. Egami[1,2]
[1]University of Tennessee Knoxville, USA, [2]Oak Ridge National Laboratory, USA,
[3]Oita University, Japan

The anomalous properties of water have their origins in the strong hydrogen bond network present in water. Even after decades of research on the structure and dynamics of water, the nature of the microscopic atomic dynamics leading to these properties remains unclear. This is partly because researchers use separate techniques to probe structure (diffraction) and dynamics (spectroscopy), thereby making a direct connection between spatial and temporal correlations impossible. This is where a time dependent pair correlation function, such as the Van Hove function, becomes valuable. Here we discuss our work in which we combined inelastic neutron scattering measurements with the Van Hove function, *g(r, t)*, to understand the spatial and temporal correlations in the hydrogen bond mediated dynamics of heavy water (D_2O).

The Van Hove function describes the temporal evolution of the structure of a system in real space and time, making it the ideal method to study dynamic systems. It is calculated by double-Fourier transforming the dynamic structure factor, S(Q, E), obtained from inelastic scattering experiments. To obtain high-quality Van Hove function free from termination errors, one would require the S(Q, E) to be measured up to high momentum (>9 $Å^{-1}$) and energy transfers (> 10 meV). This used to be a time-consuming process until the arrival of synchrotron and spallation scattering facilities.

Our previous work on water dynamics using x-ray scattering experiments [1][2] has demonstrated the feasibility of the above method. The obtained oxygen-oxygen Van Hove function has given valuable dynamical information on the inter-molecular dynamics in water. Neutron scattering measurements are ideal to observe the dynamics of hydrogen atoms due to their high scattering cross-section for neutrons. By seeing the temporal evolution of the correlations involving hydrogen atoms, the hydrogen bond mediated dynamics could be better understood.

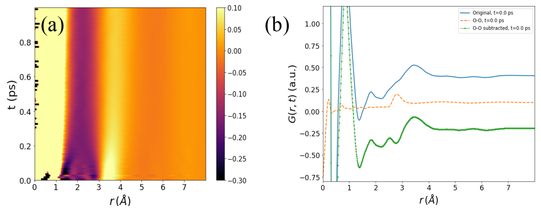

Figure 1. (a) *g(r, t)* of D_2O, (b) t=0 plots of original (blue), O-O (orange), and O-O subtracted (green) *g(r, t)*.

Using time-of-flight neutron spectroscopy at ARCS, SNS, S(Q,E) of heavy water was measured for three temperatures, 295K, 333K and 363K. The resulting Van Hove function of D_2O, as seen in Fig. 1a, is a combination of three atomic pair correlations, O-D, D-D and O-O. Among them the dominant contributors are D-D and O-D correlations. Previous inelastic x-ray scattering measurement of D_2O is used to subtract the O-O correlations (as shown in Fig. 1b) as x-rays do not detect hydrogen atoms due to their low electron density. The Van Hove function after the subtraction contains only D-D and O-D contributions. The relaxation behavior of these atomic correlations is studied directly from the Van Hove function by fitting the peak decay with a decay function. We observed a two-step relaxation process for these correlations involving caging motion and correlated dynamics of atoms. Classical MD simulations on water shows strong agreement with these experimental observations. This result highlights the effectiveness of combining the Van Hove function with neutron scattering experiments to explore dynamic systems.

References

1. Y. Shinohara, W. Dmowski, T. Iwashita, B. Wu, D. Ishikawa, A. Q. R. Baron, and T. Egami, *Phys. Rev. E* **98**, 022604 (2018).
2. T. Iwashita, W. Bin, W. -R. Chen, S. Tsutsui, A. Q. R. Baron, and T. Egami, *Sci. Adv.* **3**, e1603079 (2017).

Neutron scattering study of breathing pyrochlore lattice material $LiGaCr_4S_8$

G. Pokharel[1,2], H. Suriya Arachchige[1,2], A. F. May[2], S. Calder[3], T. Hong[3], G. Sala[3], G. Ehlers[4],
R. S. Fishman[2], D. Mandrus[5, 2, 1], A. D. Christianson[2,1]

[1]Department of Physics and Astronomy, University of Tennessee, Knoxville, TN
[2]Materials Science and Technology Division, Oak Ridge national laboratory, Oak Ridge, TN
[3]Neutron Scattering Division, Oak Ridge national laboratory, Oak Ridge, TN
[4]Neutron Technologies Division, Oak Ridge national laboratory, Oak Ridge, TN
[5]Department of Materials Science and Engineering, University of Tennessee, Knoxville, TN

Abstract

We present a study of a breathing pyrochlore lattice material $LiGaCr_4S_8$ using neutron scattering measurements. Magnetoelastic coupling in $LiGaCr_4S_8$ drives negative thermal expansion in the temperature range 12-110 K. No long-range magnetic order is observed down to 1.5 K in neutron diffraction. However, short-range spin correlations are observed and persist to at least 100 K. The fitting of magnetic diffuse scattering to a Heisenberg model indicates that the spin-spin couplings are antiferromagnetic (J=0.584 meV) and ferromagnetic (J'=-1.622 meV) within the small and large Cr_4 tetrahedra respectively. Neutron diffraction also indicates the existence of additional short-range magnetic order below 12 K. Inelastic neutron scattering data shows two bands of spin excitations with maximum energy near 15 and 2 meV at 4 K. The intensity of the high energy inelastic signal weakens above 10 K though persists to nearly 100 K. The low energy part of the spectrum behaves as a damped harmonic oscillator that can be described by a single temperature dependent relaxation.

Combined Inelastic Neutron Scattering (INS) and First-Principles Study of Metal-Hydrogen Systems

Pandey Anup, Oak Ridge National Laboratory

Metal-Hydrogen systems have a great potential as hydrogen-storage materials due to their ability to enter and leave the materials easily. Inelastic neutron scattering (INS) is a powerful technique to study the vibrational structure of metal-hydrogen systems. Using experimental INS spectra and *ab initio* calculations, we have shown the experimental evidence of the anomalous hydrogen-hydrogen distances in ZrV2:Hx systems, violating the so-called Switendick criterion. For alkali hydrides, for the first time, we measured the high pressure INS spectra of sodium hydride (NaH) at 1GPa and 2GPa and used it validate INS simulated from first-principles calculations. We also extended our calculations to the remaining alkali-hydrides and studied their thermodynamic properties.